DEVELOPMENTS IN WATER SCIENCE, 41

OTHER TITLES IN THIS SERIES

VOLUMES 1-3, 6, 9, 12, 15 AND 16 ARE OUT OF PRINT

4 J.J. FRIED
GROUNDWATER POLLUTION
5 N. RAJARATNAM
TURBULENT JETS
7 V. HÁLEK AND J. ŠVEC
GROUNDWATER HYDRAULICS
8 J. BALEK
HYDROLOGY AND WATER RESOURCES IN TROPICAL AFRICA
10 G. KOVÁCS
SEEPAGE HYDRAULICS
11 W.H. GRAF AND C.H. MORTIMER (EDITORS)
HYDRODYNAMICS OF LAKES: PROCEEDINGS OF A SYMPOSIUM
12-13 OCTOBER 1978, LAUSANNE, SWITZERLAND
13 M.A. MARIÑO AND J.N. LUTHIN
SEEPAGE AND GROUNDWATER
14 D. STEPHENSON
STORMWATER HYDROLOGY AND DRAINAGE
17 A.H. EL-SHAARAWI (EDITOR) IN COLLABORATION WITH S.R. ESTERBY
TIME SERIES METHODS IN HYDROSCIENCES
18 J. BALEK
HYDROLOGY AND WATER RESOURCES IN TROPICAL REGIONS
19 D. STEPHENSON
PIPEFLOW ANALYSIS
20 I. ZÁVOIANU
MORPHOMETRY OF DRAINAGE BASINS
21 M.M.A. SHAHIN
HYDROLOGY OF THE NILE BASIN
22 H.C. RIGGS
STREAMFLOW CHARACTERISTICS
23 M. NEGULESCU
MUNICIPAL WASTEWATER TREATMENT
24 L.G. EVERETT
GROUNDWATER MONITORING HANDBOOK FOR COAL AND OIL SHALE DEVELOPMENT
25 W. KINZELBACH
GROUNDWATER MODELLING: AN INTRODUCTION WITH SAMPLE PROGRAMS IN BASIC
26 D. STEPHENSON AND M.E. MEADOWS
KINEMATIC HYDROLOGY AND MODELLING
27 A.M. EL-SHAARAWI AND R.E. KWIATKOWSKI (EDITORS)
STATISTICAL ASPECTS OF WATER QUALITY MONITORING – PROCEEDINGS OF THE WORKSHOP HELD AT
THE CANADIAN CENTRE FOR INLAND WATERS, OCTOBER 1985
28 M.K. JERMAR
WATER RESOURCES AND WATER MANAGEMENT
29 G.W. ANNANDALE
RESEVOIR SEDIMENTATION
30 D. CLARKE
MICROCOMPUTER PROGRAMS FOR GROUNDWATER STUDIES
31 R.H. FRENCH
HYDRAULIC PROCESSES IN ALLUVIAL FANS
32 L. VOTRUBA, Z. KOS, K. NACHÁZEL, A. PATERA AND V. ZEMAN
ANALYSIS OF WATER RESOURCE SYSTEMS
33 L. VOTRUBA AND V. BROŽA
WATER MANAGEMENT IN RESERVOIRS
34 D. STEPHENSON
WATER AND WASTEAWATER SYSTEMS ANALYSIS
35 M.A. CELIA ET AL.
COMPUTATIONAL METHODS IN WATER RESOURCES, VOLUME 1 MODELING SURFACE AND SUB-SUR-
FACE FLOWS. PROCEEDINGS OF THE VII INTERNATIONAL CONFERENCE, MIT, USA, JUNE 1988
36 M.A. CELIA ET AL.
COMPUTATIONAL METHODS IN WATER RESOURCES, VOLUME 2 NUMERICAL METHODS FOR TRANS-
PORT AND HYDRAULIC PROCESSES. PROCEEDINGS OF THE VII INTERNATIONAL CONFERENCE, MIT, USA,
JUNE 1988
37 D. CLARKE
GROUNDWATER DISCHARGE TESTS: SIMULATION AND ANALYSIS
38. J. BALEK
GROUNDWATER RESOURCES ASSESSMENT
39. E. CUSTODIO AND A. GURGUÍ (EDITORS)
GROUNDWATER ECONOMICS
40 D. STEPHENSON
PIPELINE DESIGN FOR WATER ENGINEERS: THIRD REVISED AND UPDATED EDITION
41 D. STEPHENSON AND M.S. PETERSEN
WATER RESOURCES DEVELOPMENT IN DEVELOPMENT IN DEVELOPING COUNTRIES

APPLIED GEOPHYSICS IN HYDROGEOLOGICAL AND ENGINEERING PRACTICE

Edited by

WILLIAM E. KELLY

Department of Civil Engineering, University of Nebraska-Lincoln, W348 Nebraska Hall, Lincoln, NE 68508-0531, U.S.A.

STANISLAV MAREŠ

Charles University, Faculty of Science, Department of Applied Geophysics, Albertov 6, Prague 2, Czechoslovakia

Authors

Miloš Karous, William E. Kelly, Ivan Landa, Stanislav Mareš, Oldřich Mazáč, Karel Müller and Jarmila Müllerová

ELSEVIER

Amsterdam — London — New York — Tokyo 1993

ELSEVIER SCIENCE PUBLISHERS B.V.
Sara Burgerhartstraat 25
P.O. Box 211, 1000 AE Amsterdam, The Netherlands

ISBN: 0-444-889936-1

This book is printed on acid-free paper.

Printed in The Netherlands

Preface

This book is an updated English-language version of the Czech textbook *Geophysical Methods in Hydrogeology and Engineering Geology*. The preparation of this version began in May 1989 as part of a cooperative research undertaking on the application of geophysics to environmental problems. The world has changed dramatically since the spring in Prague when we began this collaboration and our efforts are now partially supported by the U.S. National Science Foundation and the Czechoslovakian Academy of Sciences.

The chapters in the original Czech version were authored as follows: Chapter 1 — all authors; Chapter 2 — Mareš, Landa, Müller; Chapter 3 — Karous, Mareš, Mazáč, Landa; Chapter 4 — Karous, Mareš, Mazáč; Chapters 5 and 6 — Müller and Müllerová; and Chapter 7 — all authors. The English translation by H. Zdruková was revised and completed by the Chief Editor, W.E. Kelly.

We are indebted to the Department of Civil Engineering, the College of Engineering and Technology, and the Conservation and Survey Division of the University of Nebraska-Lincoln, and the Department of Applied Geophysics and the Faculty of Sciences at Charles University-Prague for assistance in preparation of the manuscript. Carolyn and Susanna Kelly assisted in typing the manuscript and Wilma Ennenga prepared the final camera-ready version of the manuscript.

William E. Kelly
Stanislav Mareš
Prague, Czechoslovakia
May 1992

Table of Contents

Chapter 1

Introduction

In today's highly developed industrial society, the *importance of hydrogeology* may be attributed to its close relation to national economic activities such as ensuring adequate supplies of drinking water and water for municipal, industrial, and agricultural purposes; providing appropriate conditions for development and exploitation of mineral resources; protecting the environment from agricultural and industrial production; and the increasing concern of governments for public health and safety.

Goals for hydrogeological investigations include:

1. Locating new ground-water resources
2. Developing an optimum scheme for utilization
3. Proposing measures for protecting quality and quantity, including changing surrounding hydrogeological conditions
4. Proposing the most effective measures for protection of ground water from pollution and depletion

This last task requires assessing the effects of all possible influences, both natural and artificial, and their changes in time and space. With some reservation, we regard as natural, changes in climatic, hydrogeological, hydrochemical, and analogous conditions. Effects such as changes in the chemistry of ground water in the proximity of industrial, agricultural and municipal waste tips, or changes in hydrogeological conditions due to industrial, agricultural, and urban development are regarded as artificial.

Protecting ground water from pollution requires first identifying the sites where sudden or gradual changes in the physicochemical properties of ground

water have occurred. Then it is necessary to propose and implement the measures needed for remediation of the polluted waters and elimination of the pollution sources. In cases where aquifer yield is threatened or hydrodynamic conditions have undergone marked changes, ways of increasing water reserves are proposed based on the results of hydrogeological investigations. The results of hydrogeological studies are also used for planning dewatering of mineral deposits, improving soil in agriculture, constructing building foundations and underground structures, storing hydrocarbons underground, and disposing of industrial waste.

The principal tasks to be accomplished in a hydrogeological investigation are the following: (1) establish the size and character of the hydrogeological structures, (2) identify interrelations between the various factors that influence the ground-water regimen in time and space, and (3) recommend regulating methods on the basis of the given criteria (geological, technical, economic, etc.).

The *goal of an engineering-geology investigation* is to provide the basic data to evaluate, as part of the engineering design, the interaction of the geological environment with the proposed structure. The investigations should ensure that the constructed facilities will be safe and economical with respect to both cost and time of construction, and that the structure will not unfavorably affect the geological environment. The degree of this interaction naturally depends on the type of structure and the geological conditions. The results of a geological investigation determine the method which is chosen for an engineering-geologic survey. The principal tasks of an engineering-geologic investigation, which are aimed at obtaining preferentially geotechnical information, are, briefly, the following: to provide the data needed to study the possibility of constructing engineering works with respect to the local geological conditions; to assess the interaction between the geological environment and the planned structures, and to propose an effective scheme for mitigating any harmful consequences of this interaction; and to assist in selecting construction procedures, construction types, and utilization of natural building materials.

Hydrogeology and engineering geology are applied sciences. In practice, they mainly use the knowledge and data provided by geological, physical, chemical, mathematical and biological studies. Also of importance are the results of other applied sciences such as geochemistry, geophysics, biophysics and biochemistry.

Using physical, astronomical, geological, and applied-mathematical data, geophysics studies the natural or artificially generated physical fields of the earth. *Applied geophysics* uses these studies to assist in determining geological conditions in the earth's crust, exceptionally also in the upper mantle. The earth's crust is inhomogeneous in general, and irregularities in geological structure are inevitably reflected in the pattern of the contingent physical field. The variations become more pronounced as the difference between the physical properties of the inhomogeneity-producing body and those of the environment become greater, and as the inhomogeneity comes closer to the earth's surface.

Applied geophysical methods are divided according to the character of the measured field (gravimetric, magnetometric, geothermal, geoelectrical, radiometric, nuclear geophysical, seismic and geoacoustic methods). Geophysical methods are used in several variants, usually as surface methods (measurements on the earth's surface), underground methods (measurements in boreholes, galleries, shafts, and other works), and remote sensing methods. Field methods, instrumentation, modes of elaboration and fundamental evaluation processes for individual methods are described in several textbooks on geophysics (for example, Telford et al., 1990; Mareš et al., 1984; Sheriff, 1989).

In using applied geophysics for investigations in hydrogeology and engineering geology, we will be concerned mainly with the uppermost parts of the earth's crust. Surveys to greater depths are usually required when exploring mineral deposits, conducting regional hydrogeological investigations, and when prospecting for mineral water resources. These conditions define, to a certain extent, the specificity of geophysical investigations for hydrogeological and engineering-geological purposes, which require an appropriate subset of

geophysical methods and field and evaluation procedures. Another factor that must be recognized and understood is the relationship between rock physical properties and the hydrogeological and engineering-geological parameters. However, the potential of applied geophysical methods in hydrogeological and engineering-geological surveys has to be reasonably considered. In some cases geophysical methods should be regarded primarily as indirect methods that cannot completely replace direct field measurements (borings, test pits, trenches). On the other hand, geophysical methods provide useful information about the structure or physical properties of rocks and soils between boreholes and, in favorable situations, may allow the number of direct measurements to be reduced. There are, however, problems where geophysical methods are irreplaceable (e.g., tracer tests in the study of transport properties and protection of ground waters). The primary benefit of geophysical methods is that they provide data of higher quality and reliability to be used, for example, in determining how ground water from a particular hydrogeological structure is to be used, on additional engineering-geological surveys or construction processes and, consequently, in reducing the cost of further investigations. The economic effect itself appears only in the final phase; e.g., in locating a water supply well at a site most appropriate to yield, or in selecting the most suitable damsite.

In order to ensure successful application of geophysical methods, it is important to respect three principles: investigations must be *integrated*, they must be carried out in *proper stages*, and they must be *economical*. The first principle demands that a set of geophysical methods be chosen, first, with respect to the physical properties of the environment and, second, with respect to the type of the hydrogeological structure and engineering-geological conditions, so as to obtain the maximum possible amount of useful information. The second principle requires that geophysical methods, where appropriate, be applied in all investigation stages, and that field investigations and data processing procedures be organized so that geophysical data and the results of special tests (hydrodynamic, physicomechanical, etc.) obtained at an earlier

stage might be used at later stages of investigation. Economics necessitates that the scope and type of a geophysical investigation be designed so as to obtain the maximum useful information at the minimum cost, and that duplication be avoided by exploiting the results of preceding investigations to the greatest extent. Close cooperation of a geophysicist with a hydrogeologist or engineering geologist is another prerequisite for successful investigations.

This book is intended chiefly for students of hydrogeology and engineering geology at universities and institutes of technology, and for practicing hydrogeologists and engineering geologists who may find some basic information on the use of applied geophysics in practice. The authors presume that the reader is acquainted with geophysical methods at least as they are given in selected chapters of Mareš et al. (1984), Sheriff (1989), or Telford et al. (1990). Therefore, only the principles of some specialized methods and procedures not included in those books are included herein. Because we expect that the book will also be useful to geophysicists engaged in hydrogeological and engineering-geological practice, a summary of the most important hydrogeological and engineering-geological terms is given in Chapter 2 to make the text more easily understandable.

The following list of the most frequently used abbreviations of the main geophysical methods and of important physical parameters should facilitate the orientation of readers in the text. Symbols for hydrogeological parameters are presented in Table 2.1.

LIST OF PRINCIPAL ABBREVIATIONS

AL	Acoustic log
LES	Lateral electrical sounding
PHL	Photometry
GA	Geoacoustic method
GGL-D	Gamma-gamma log density
GR	Gamma ray log

IM	Inclinometers
CL	Caliper log
CRP	Combined resistivity profiling
MSL	Magnetic susceptibility log
GC	Method of sliding contacts
NGL,NNL	Neutron-gamma and neutron-neutron log
MAM	Mise-a-la-masse method
ORT	Open radioactive tracers
PSP	Pumped storage plant
Ra	Resistivity logging; indices denote the system of electrodes applied (l - lateral probe; n - normal probe; ml, mn - microlateral and micronormal probes; LL - laterolog; MLL - microlaterolog)
RL	Fluid resistivity log
RWP	Radiowave profiling
SRP	Symmetric resistivity profiling
SP	Self-potential method (surface and logging variants)
TL	Temperature log
VLF	Very low frequency method
VES	Vertical electrical sounding
IP	Induced polarization method
WPT	Water pressure test

LIST OF SYMBOLS OF IMPORTANT PHYSICAL PARAMETERS

A	Amplitude (mV)
A^*	Relative complex parameter ($\Omega^{-1}m^{-1}$)
C	Concentration of dissolved solids in ground water (g l^{-1})
E	Energy (J)
E_d	Dynamic modulus of elasticity (MPa)
K_p	Coefficient of deformation calculated from geophysical data (%)
P_A, P_D, P_N	Porosity from acoustic, density and neutron logs (%)

P_{Sh}	Apparent shale porosity (%)
Q	Yield of well (m^3 s^{-1}), concentration of radioactive elements (Bq m^{-3})
V_f	Filtration potential (mV)
V_{sh}	Shale volume from logs (%), according to shale indicators
$\dot{X}$	Exposure rate (pA kg^{-1})
Z_a	Anomaly of vertical components of the earth's magnetic field (nT)
d	Borehole diameter (mm)
f	Frequency (Hz)
h	Depth below ground surface (m)
k_p	Wave number
m	Bed thickness (m)
r	Borehole radius (mm)
v	Velocity of water flow in the direction of borehole axis, sound velocity, elastic wave velocity, propagation velocity of electromagnetic waves (m s^{-1})
v_p, v_f, v_{ma}	Compressional wave velocity in the rock medium, water and matrix, respectively (m s^{-1})
v_s	Shear wave velocity in the rock medium (m s^{-1})
ΔU, ΔV	Potential difference (mV)
ΔT	Anomaly of total vector of the earth's magnetic field (nT)
α	Attenuation factor (m^{-1})
γ	Conductivity (S m^{-1})
ϵ_r, $\epsilon_{r,w}$	Relative permittivity of rocks and ground water, respectively
η	Polarizability (%), viscosity
ϑ	Temperature (°C)
κ	Magnetic volume susceptibility
λ	Thermal conductivity (W m^{-1} K^{-1}), wave length (m)
ρ	Resistivity (Ω m)

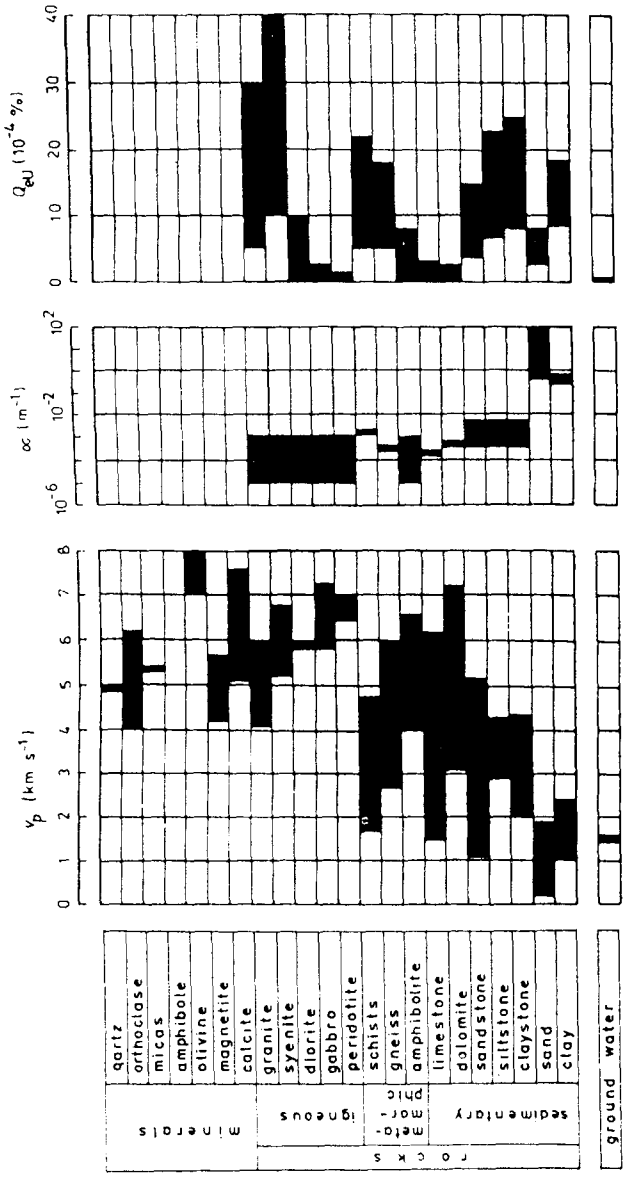

Figure 2.6 Velocity of compressional waves, v_p, coefficient of attenuation, α, and radioactivity expressed in the equivalent of U concentration Q_{eU} for selected minerals and rock types (compiled according to Clark et al., 1966; Matolín, 1970; Militzer et al., 1986, Volarovič et al., 1978).

Chapter 3

Geophysical Surveys for Hydrogeological Purposes

The methods of applied geophysics cannot be used to assess directly the presence of a ground-water body or an aquifer because they are invariably confined to a certain geological body. Nevertheless, we can determine, except in exceptional cases, the physical properties of the geologic medium, and thus of an aquifer or aquifer system, on the condition that it differs markedly in its physical properties from both the over- and underlying aquiclude. In such circumstances the methods of applied geophysics generally allow us to establish the thickness, depth and position of an aquifer (Section 3.1). In addition, they can be used to determine characteristics of ground water and ground-water flow such as total dissolved solids, density, temperature, filtration velocity, and velocity of flow; as well as aquifer lithology, porosity, permeability, transmissivity, storativity, and degree of weathering and jointing of an aquifer or water-bearing rock mass (Section 3.2).

3.1 Hydrogeological Structures and their Geophysical Models

The task of a geophysical survey is to assess the extent of individual elements of a hydrogeological structure and classify them on the basis of their physical properties. One of the basic elements of sedimentary hydrogeological structures is the *bed*. Geophysical methods are used to determine the dimensions of beds, their position in space, and occasionally, their deformational and physical structure and physical properties. In *sedimentary complexes*, geophysical methods may facilitate the process of lithological subdivision, determination of total thicknesses and thicknesses of individual beds, depth to basement, basement

surface relief and its tectonic structure, the extent of a sedimentary basin and similar features. In a *crystalline complex*, geophysics can assist in tracing fault zones and defining tectonics in general, determining rock contacts, thicknesses and degree of weathering, thicknesses of sedimentary cover, and zones of increased fracturing or the dominant strikes of fractures. In *karst areas* the assessment of the degree of karstification is of major importance.

3.1.1 Geological Beds and Geophysical Layers

A bed is a geological unit defined by its lithology. A *geophysical layer* is a tabular body differing from its surroundings in physical properties, such as resistivity and polarizability for a geoelectrical layer, or density and elastic wave propagation velocity for a seismic layer. A geological bed and geophysical layer need not be identical, and frequently are not. In some cases a geophysical method is able to separate a geological bed into several geophysical layers on the basis of physical properties, whereas in other cases an entire geological complex appears as a single geophysical layer. Accordingly, the surfaces separating individual geological beds need not correspond to boundaries between physically homogeneous layers.

The most frequently used criterion for classification of a *geoelectrical layer* is a difference in resistivity; less used are differences in polarizability and permittivity. A layer having the same resistivity parallel and transverse to its bedding throughout is considered a *homogeneous isotropic* geoelectrical layer with a resistivity ρ. The geoelectrical parameters of such a layer are resistivity ρ, thickness m, longitudinal conductance S, and transverse resistance T.

$$S = \frac{m}{\rho}, \quad T = m\rho \tag{3.1}$$

These parameters are determined by interpreting *vertical electrical sounding* (VES) curves. Where the layer thickness is sufficiently great relative to the thickness of the overlying complex, the parameters ρ, m, S and T can be

determined unambiguously. In the case of a schematic three-layer medium, however, the accuracy of the quantitative interpretation depends on the interrelationship between the resistivities of the overlying layer ρ_1, the layer examined ρ_2 and the underlying layer ρ_3; on the thickness of the layer relative to that of the overlying complex; and on the definitude of the sounding curve; i.e., on the accuracy of measurements and on the presence of complicating factors such as near-surface inhomogeneities and variations in topography. The most easily interpretable curves are of the H ($\rho_1 > \rho_2 < \rho_3$) and K ($\rho_1 < \rho_2 > \rho_3$) types. For a measurement error usually considered to be from 3 to 5%, layer thicknesses can be determined with a maximum error of 15%. The interpretation of the A-type (resistivities increase gradually with depth; i.e., $\rho_1 < \rho_2 < \rho_3$) and the Q-type (resistivities decrease gradually with depth; i.e., $\rho_1 > \rho_2 > \rho_3$) curves are least favorable; the error in thickness determination can be as much as 15 times greater than the measurement error, that is, up to 45 to 75%.

The thickness and resistivity of a bed observed in a boring can also be determined unequivocally by *lateral electrical sounding* (LES). By comparing geoelectrical parameters obtained from logging and VES results, both the inhomogeneity and the anisotropy of a bed can be established (Fig. 3.1).

For layers that are thin relative to the thickness of the overlying layer, the *principle of equivalence* will affect the interpretation. This means that sounding curves measured above layers of identical longitudinal conductance S, where the conductivity of the underlying complex is lower, or of identical transverse resistance T, where the conductivity of the underlying complex is higher, do not differ. According to the principle of equivalence, the thickness and resistivity cannot be determined from a sounding curve, but only their product where T equivalence exists (Fig. 3.2), or their quotient, where S equivalence holds. A unique interpretation for thickness or resistivity requires that one or the other be determined using an independent method. Methods used for this purpose are resistivity logging, refraction seismics or, for thickness determination, the geological profile inferred from a boring log.

Where the thickness of the layer is very small relative to that of the overlying complex, its indication on the sounding curve may, in an extreme case, be completely absent due to the *principle of suppression* (Koefoed, 1979).

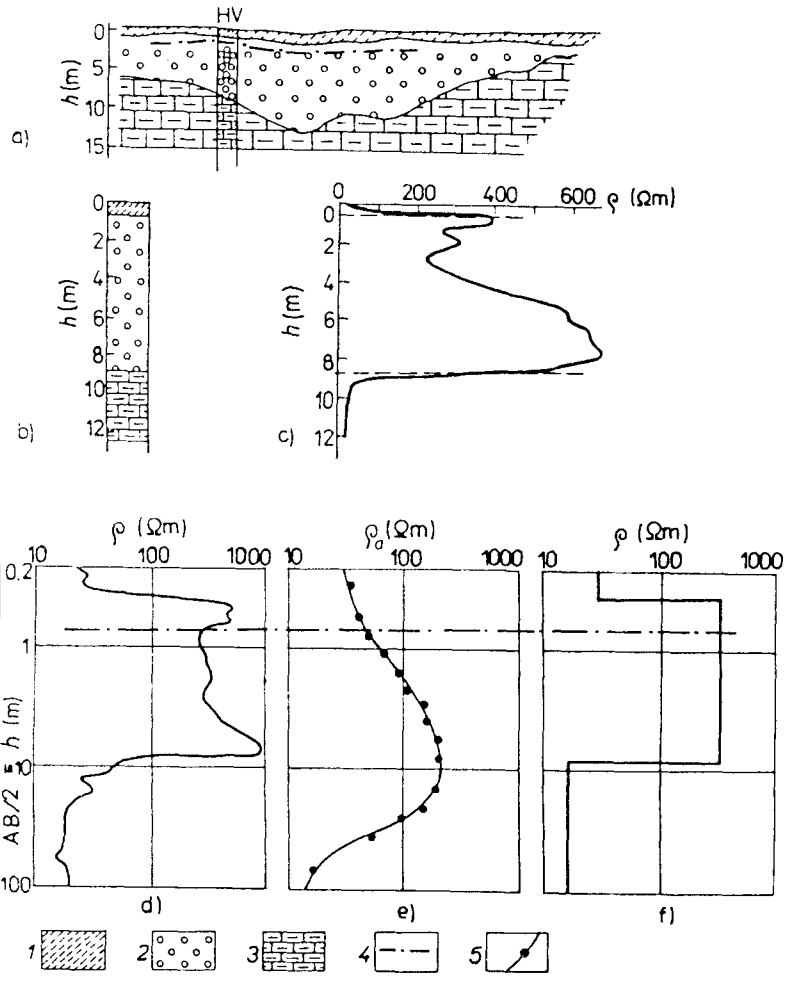

Figure 3.1 Relationship between the geological and geoelectrical model and the VES curve. (a) Vertical geological section. (b) Borehole profile. (c) Vertical resistivity profile according to LES. (d) Vertical resistivity profile at logarithmic scale. (e) Sounding curve. (f) Interpreted vertical resistivity profile. *1* — loam, *2* — sand and sandy gravel, *3* — marlstone, *4* — water table, *5* — measured values of apparent resistivity.

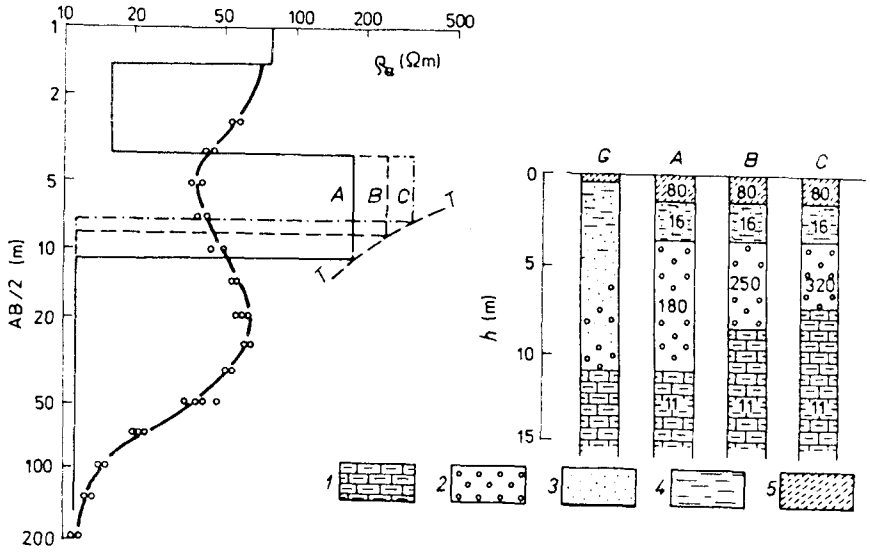

Figure 3.2 Interpretation of VES curve near borehole HV-112, at Písek near Chlumec nad Cidlinou, Czechoslovakia: *1* — Turonian marlstone, *2* — gravel, *3* — sand, *4* — clay, *5* — loam (with interpreted values of resistivity given in Ω m). *G* is the geological section according to boring results; *A*, *B*, and *C* are alternative sounding curve interpretations demonstrating the principle of *T* equivalence; *T* is the curve of transverse resistance.

The effect of the principle of equivalence may, in certain cases, be eliminated by combining stationary and inductive soundings for K and Q type curves, and be reduced for H and A type curves (Karous in Mazáč et al., 1986, Matveev, 1974).

In recent years, quantitative interpretation of VES curves has largely been done on computers (Fig. 3.3). A *correct interpretation*, however, requires that two conditions be satisfied (Mašková and Mazáč, 1985): first, the calculations must be precise; second, a reasonable geological concept or model must be incorporated in the interpretation process. Disregard of either can have a serious negative impact on the validity of the results of a geoelectrical survey for any locality.

Present-day interpretation procedures are based on the assumption of a one-dimensional medium. If this assumption is not satisfied, the results of the

interpretation will be incorrect and a two- or three-dimensional approach must be utilized (Dey and Morrison, 1979).

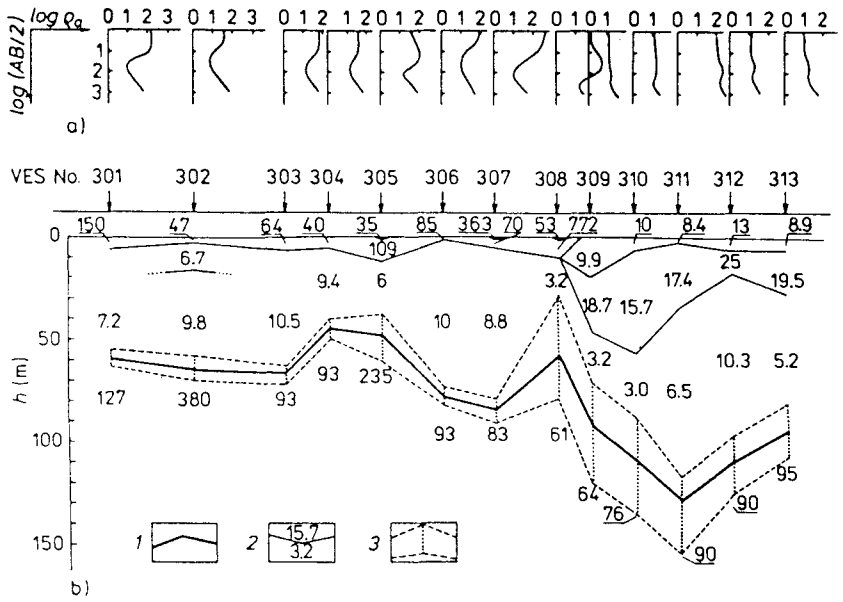

Figure 3.3 Interpretation of VES curves. (a) VES curves measured on profile P-3 in the Cheb basin (CSFR). (b) Quantitative one-dimensional interpretation of VES curves in the form of optimum and extreme parameters (according to Johansen in Koefoed, 1979). *1* — optimum course of bedrock relief with high resistivity (granite), *2* — boundary between geoelectrical layers with different resistivities in sedimentary cover where the formation with $\rho < 40\ \Omega$ m is predominantly shales and the formation with $\rho > 40\ \Omega$ m is predominantly psammites, *3* — extreme course of the relief with high resistivity.

If the resistivity in a geological bed changes gradually in the transverse direction or, as is more usual, increases with depth, we speak of a *gradational medium*. In such cases, interpretation of sounding curves is very difficult. A gradational medium is most commonly encountered in young, near-surface sedimentary rocks.

Most sedimentary beds display *anisotropy of resistivity*, due to the internal structure of the bed, which implies that parallel to the bedding or stratification the resistivity, termed the *longitudinal resistivity* (ρ_l) differs from the *transverse resistivity* (ρ_t) normal to the bedding. For an anisotropic layer, the *mean resistivity* (ρ_m) is defined as the geometrical mean of the longitudinal and transverse resistivities

$$\rho_m = \sqrt{\rho_t \rho_l} \qquad (\rho_l < \rho_m < \rho_t) \tag{3.2}$$

and the *coefficient of anisotropy*

$$\lambda = \sqrt{\frac{\rho_t}{\rho_l}} \quad (\lambda \geq 1) \tag{3.3}$$

An anisotropic layer is manifested on a sounding curve by its mean resistivity ρ_m and a thickness λ times its actual thickness. Therefore, the layer thickness cannot be determined from a VES unless the coefficient of anisotropy is known. This can be assessed by a combined analysis of resistivity logging results and sounding curves. Figure 4.12a shows an example of resistivities interpreted from LES and VES results over an anisotropic layer. The coefficient of anisotropy and the appropriate resistivity for interpretation of VES measurements in the proximity were obtained by their comparison.

In hydrogeological investigations differentiation of layers according to *polarizability* η can be important. A relatively high polarizability is found chiefly in water-saturated clayey sands to sandy clays. Their anomalous polarizability is due to the fact that individual sand grains are covered, at least in part, with a thin clay coating. Clean water-saturated quartz sand, pure clay and dry sand and clay mixtures in essence do not polarize ($\eta < 1\%$) (Fig. 3.17b). To determine thicknesses of polarizing sediments, sounding by the induced polarization method (VES-IP) is used. Because of the anomalous polarizability values above unconsolidated sediments, the VES-IP is appropriate for exploration of shallow Quaternary deposits.

A significant characteristic that allows individual layers to be differentiated is the *velocity of seismic wave* propagation. A *seismic layer* is a layer within

which seismic waves propagate at broadly identical velocities. Depending on boundary depth, the relationship between the velocities in under- and overlying layers, the length of the measured profile, and other parameters, a reflected or refracted wave is used in a seismic survey; and accordingly, reflection and refraction seismic surveys are distinguished. Broadly speaking, reflection seismics is applied in investigations at greater depths, whereas refraction seismic methods are used mainly in shallow geophysical surveys. Accurate determinations of depth from seismic measurements depends on a precise knowledge of the vertical velocity profile. A high precision in determination of the depth of reflecting or refracting boundaries ($\Delta h < 10\%$) can be achieved by using the records of acoustic and seismic logging; i.e., parametric measurements in boreholes.

Rock *density* is one of the physical properties which is studied most frequently. Changes in rock density are reflected in changes of the gravitational field. The gravitational effect Δg of a horizontal layer is proportional to its thickness m and the differential density $\Delta\sigma$

$$\Delta g = 2\pi\kappa\, \Delta\sigma\, m \qquad (3.4)$$

where κ is the gravitational constant. Since the effect of the layer does not depend on its depth below the ground surface, depth is very difficult to establish in interpreting gravity anomalies. The thickness m, however, can be derived from the gravitational effect and density. Therefore, the interpretation of gravity measurements is chiefly concerned with determining thicknesses of entire sedimentary complexes.

Well logging is most appropriate for differentiation of layers; logging provides a wide range of possibilities for differentiating layers based on various physical properties (Section 2.3).

Sedimentary layers rarely differ markedly in *magnetic characteristics*. Magnetic surveys, however, may be of great assistance in studies of the bedrock of sedimentary basins. In this case, it is a useful tool for lithological differentiation

of the bedrock and location of changes in bedrock depth, especially where the changes are abrupt due to faulting.

3.1.2 Thickness of a Sedimentary Complex, Depth to Bedrock and Key Horizons

A layer of great areal extent which is traceable over a large area and differs markedly from adjacent rocks is called a *key geophysical layer*. The boundary between layers or media, broadly horizontal and with markedly different properties, is called analogously a *key geophysical horizon*. The most important key horizon in sedimentary basins is generally the overburden/bedrock interface.

Assessment of changes in the thickness of basin sediments, mainly the determination of up and down throws in the bedrock and localization of bedrock highs and lows, contributes substantially to the general knowledge of the tectonic structure of a sedimentary basin. The determination of bedrock highs and lows is a major task for geophysical surveys and hydrogeological investigations of shallow unconsolidated sediments.

In studies of *very thick sedimentary complexes*, the total sediment thickness or the depth to the bedrock surface is determining for the recognition of the structure. This problem is studied using geophysical sounding methods, mainly geoelectrical, and seismic and, less frequently, gravimetry and deep-borehole logging.

As bedrock generally differs markedly in resistivity from sediments, *geoelectrical methods* can provide information on the thickness of sediments relatively unequivocally and at a low cost. In the case where the bedrock has higher resistivities than the sediments, the telluric and/or magnetotelluric method can be used. At the present time these methods are used only to a limited extent because of the strong effect of horizontal inhomogeneities and distortions due to industrial and stray currents.

For deeper hydrogeological investigations, the relatively new method of transient sounding yields results similar to those obtained with VES. Transient

soundings require only a limited measuring area as compared to VES. The only disadvantage is that they cannot be applied for hydrogeological investigations of depths less than about 50 m.

Gravimetry is used to advantage in regional surveys of large sedimentary basins. As the densities of sedimentary complexes are usually lower than those of bedrock, variations in sediment thickness are manifested in varying local anomalies Δg_L, with the sediment thickness being roughly proportional to the gravity anomaly. To assess sediment thickness more precisely, we need to know the differential density $\Delta\sigma$; that is, the difference between the mean sediment density and the mean bedrock density. Using thicknesses determined by borings we can find an empirical relation between the anomaly Δg_L and thickness m (Fig. 3.4). An accurate interpretation requires a sufficiently uniform bedrock density.

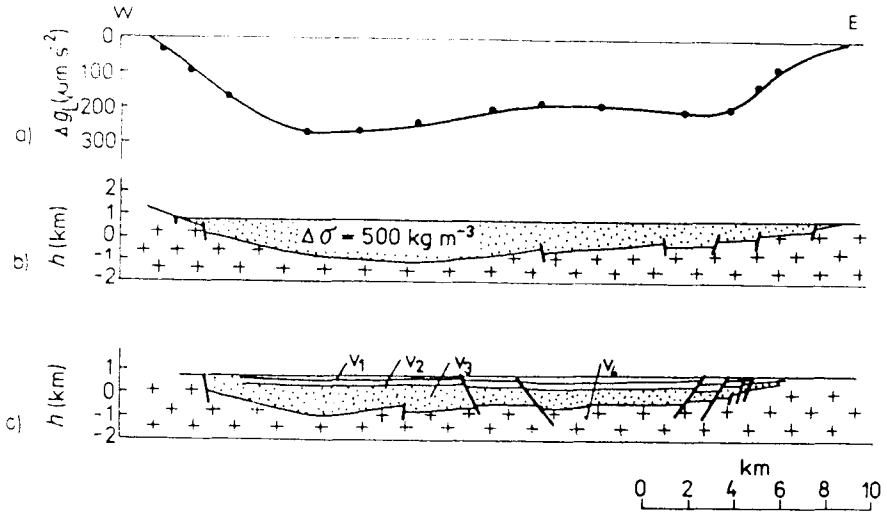

Figure 3.4 Profile of Bouguer anomaly across Indian Wells Valley, California and models interpreted from gravimetric and seismic measurements (Zbur, 1963): (a) Residual gravity anomaly. (b) Vertical section interpreted from gravity data ($\Delta\sigma$ = 500 kg m^{-3}). (c) Interpreted from refraction seismics v_1 = 1740 m s^{-1}; v_2 = 2210 m s^{-1}; v_3 = 2870 m s^{-1}; v_4 = 4600 to 5000 m s^{-1}.

The thickness of basin sediments can also be assessed by interpreting *seismic measurements* because there is usually a sharp contrast between the seismic velocities in sediments and bedrock. Seismic methods can, in many cases, also be used to delineate boundaries between sedimentary complexes (Fig. 3.4).

The accuracy of interpreted seismic boundaries depends greatly on the precision with which the distribution of velocities in the overlying complex has been determined. The complex is usually characterized by the medium velocity v_m, which is a weighted mean of velocities in individual homogeneous parts or layers. Another way is to determine the effective velocity of the overlying beds v_{ef}; it does not differ much from the medium velocity and is determinable either from the travel time-curves of reflected waves or from intersections of the travel time curves corresponding to direct and refracted waves. Discrepancies between thicknesses interpreted from seismic measurements and those established from borings indicates that an appropriate medium or effective velocity was not chosen, or that geological conditions do not permit the vertical profile to be simplified as a homogeneous whole or parts having constant vertical velocities.

Where the thicknesses of basin sediments do not exceed about 500 m, the method of vertical electrical sounding has proven suitable. The total thickness of sediments is established by successive interpretation of individual geoelectrical layers. For a preliminary interpretation of sediment thickness, statistical-empirical methods are often employed. They use the total longitudinal conductance of sediments S

$$S = \frac{m}{\rho_l} \tag{3.5}$$

where m is the total thickness of sediments, and ρ_l is the mean longitudinal sediment resistivity. This presumes the resistivity of the bedrock to be much greater than the resistivity of the sediments themselves. This approach is used chiefly because S can be unequivocally and simply determined from measured VES curves without any elaborate interpretation. To determine S, we construct

the tangent to the last points of the sounding curve at an angle of 45 degrees to the AB/2 axis. The longitudinal conductance S is the AB/2 value where the tangent intersects the value $\rho_a = 1\ \Omega$ m. The mean longitudinal resistivity of the sediments is inferred from the data obtained at a site where the sediment thickness (for example, from boring data) and the longitudinal conductance (from VES results) are known. The method fails where the longitudinal resistivity is so variable horizontally that its mean value cannot be determined. Even in such cases, a plot of longitudinal conductance gives an indication of bedrock topography and it broadly corresponds to the variation in thickness of the overlying sediments (Fig. 3.5).

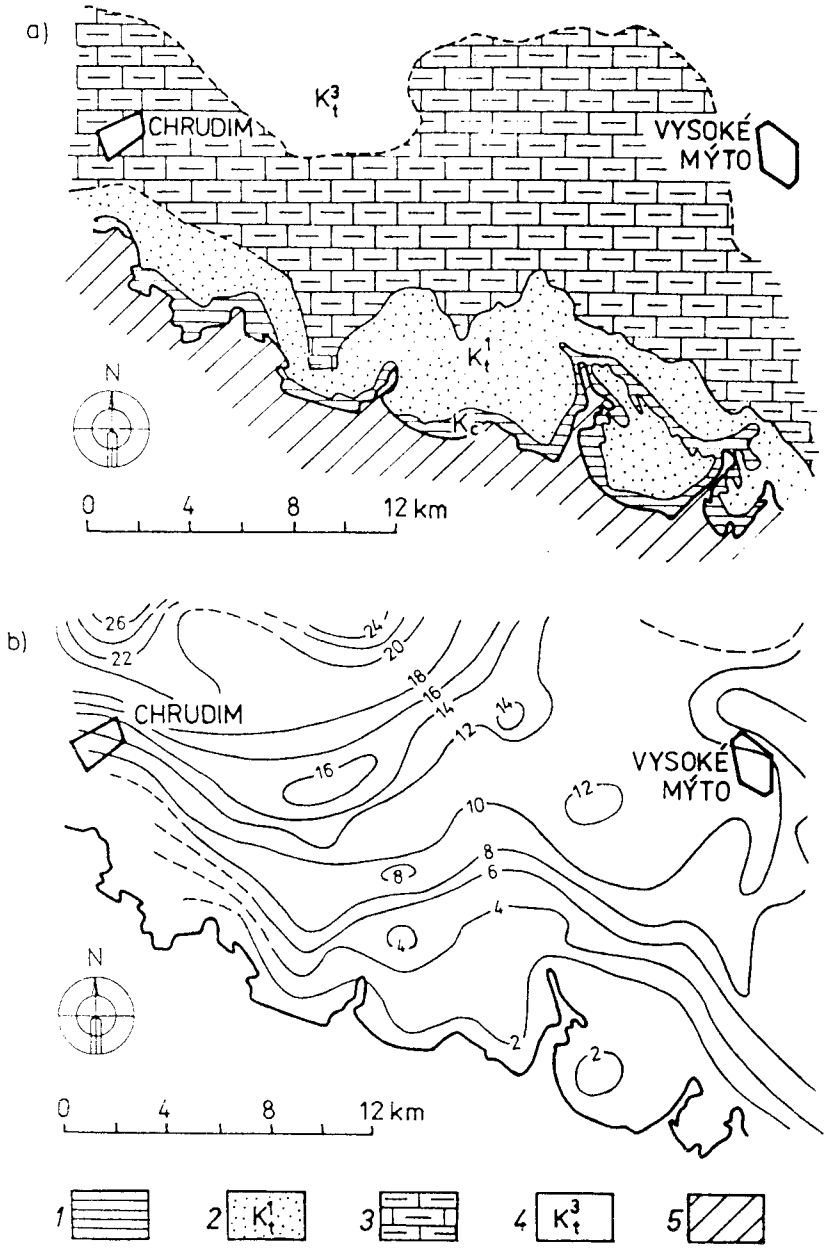

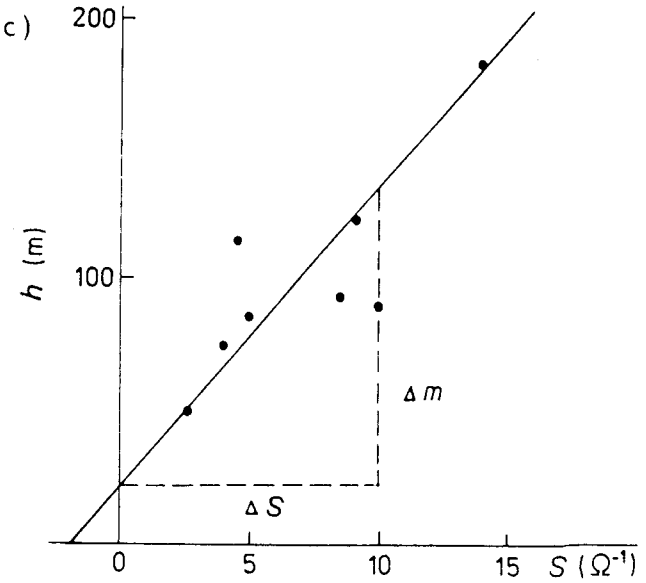

Figure 3.5 Results of a geoelectrical survey in a borderline part of the Bohemian Cretaceous Basin between Chrudim and Vysoké Mýto. **Facing page**: (a) Geological map. (b) Map of longitudinal conductance of sediments S according to VES. *1* — Cenomanian, *2* — lower Turonian, *3* — middle Turonian, *4* — upper Turonian, *5* — crystalline basement. **Above**: (c) Relation between longitudinal conductance, S, and thickness, m ($\rho_l = \Delta m/\Delta S = 5.8\ \Omega$ m).

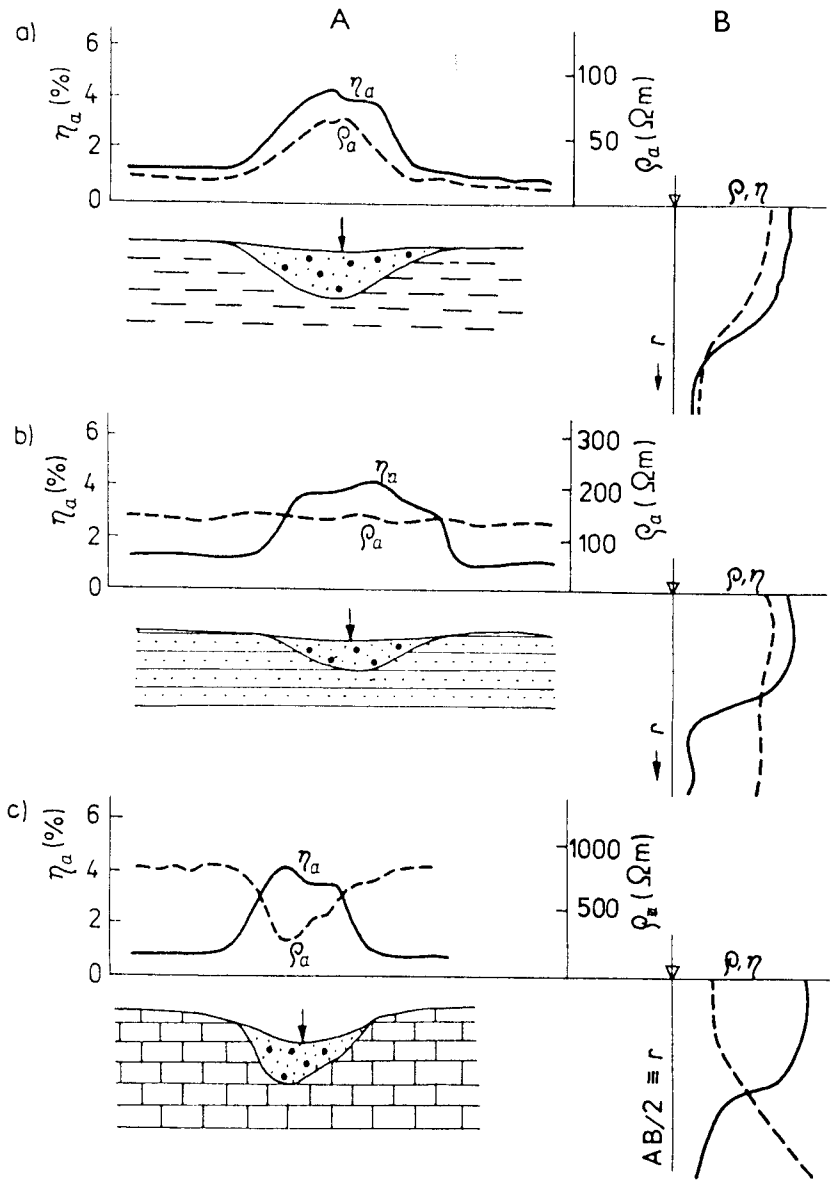

Figure 3.6 Characteristic profiling (A) and sounding (B) curves of apparent resistivity ρ_a and apparent polarizability η_a over unconsolidated sediments (according to Ogilvi, 1967): (a) bedrock of higher conductivity than the unconsolidated sediment, (b) bedrock of resistivity similar to that of sedimentary cover, (c) bedrock of lower conductivity.

Bedrock relief under thin unconsolidated sediments is usually determined with geoelectrical resistivity methods or the IP method, shallow refraction seismics, gravimetry, or magnetics where the bedrock has a magnetic character.

Once more, the method most frequently employed is vertical electrical sounding. The total thickness of unconsolidated sediments is defined by quantitative interpretation of VES sounding curves. Very often only qualitative results are assembled (for example, an isoohmic section, Fig. 3.11). In a complex of homogeneous sedimentary beds, the isoohmic section gives a picture of their vertical distribution. In the opposite case, the isoohmic section indicates facies changes. In optimum cases, where relatively homogeneous Quaternary sediments lie on a homogeneous bedrock, the method of double profiling can be utilized to obtain a continuous determination of sediment thickness. The thickness of the sedimentary cover can be determined from symmetrical *resistivity profiling* at two spacings (Karous, 1977).

As unconsolidated sediments differ from underlying solid rocks in anomalous polarizability, their thickness can be determined and areas of greater thickness located using induced polarization sounding (VES-IP) or profiling (IP) with relatively short electrode spacings. This method has proven successful in identifying Quaternary deposits even when they do not differ in resistivity from adjacent rocks (Fig. 3.6).

Where geoelectrical methods cannot be expected to be effective, shallow *refraction seismic* survey techniques may be employed. Shallow seismic equipment uses a hammer stroke as the source of the seismic pulse, hence the name *hammer seismics*. This method makes use of the contrast in velocities of seismic waves in unconsolidated and underlying solid rocks. In alluvial sediments seismic waves propagate at velocities ranging from 100 to 900 m s^{-1}, whereas underlying weathered rocks display velocities exceeding 1500 to 2000 m s^{-1}, with solid rocks having even higher velocities. In water, seismic waves propagate at a velocity of v = 1500 m s^{-1}, and thus seismics, in many cases, can determine the water table as a seismic interface (see also Section 3.2.5). The

depth of the seismic interface is determined from the travel-time curve. In measurements to shallow depths, two parts of the travel-time curves are used: H_{dw}, corresponding to the arrival of the direct wave, and H_{hw}, corresponding to the arrival of a head wave refracting at the shallow interface (Fig. 3.7). The first part carries information on velocities in the near-surface (shallow) bed and the other on the depth and shape of the refracting seismic interface, which is usually consistent with the boundary between Quaternary cover and bedrock or the water table.

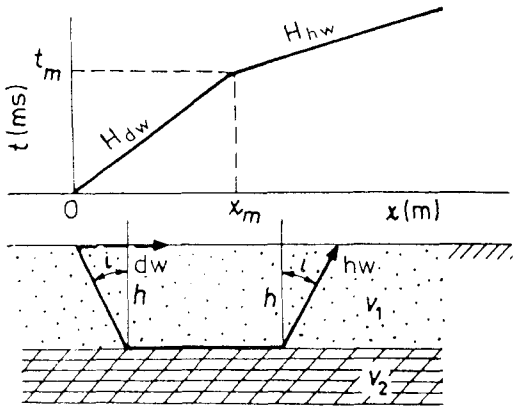

Figure 3.7 Origin of direct wave and head wave where H_{dw} is the travel-time curve of the direct wave (dw), H_{hw} is the travel-time curve of the head wave (hw) and x_m and t_m are coordinates of the intersections of direct and head wave travel-time curves. v_1 and v_2 are the velocities of seismic waves in sedimentary cover and bedrock, i is the critical angle at which refraction takes place, O is the point of explosion or impact, and h is the depth to the bedrock.

Tracing the arrival of the *direct wave* allows us to establish the velocity of direct wave propagation in the direction of measurement. Thus, for example, in investigating the course of a buried river channel, we can measure on a circle centered on the source. Then since in the direction of the latest wave arrival the waves propagate at the lowest rate, greater thicknesses of unconsolidated gravel are presumed to occur in this direction, defining the trend (Fig. 3.8).

To determine the depth to the seismic boundary, the entire shape of the

reversed travel-time curves of *head waves* for a certain sector should be used. There are a number of procedures used to establish this depth, the most frequently utilized being the method of mean velocities and the t_0 method. In both cases the medium above the seismic boundary is replaced by a medium with a mean velocity v_m, which is used for the calculation or reconstruction of its depth. Best results are obtained in a medium with a planar or nearly planar seismic boundary. The existence of elevations or depressions (i.e., a markedly curved boundary), the presence of a gradational medium with regard to the velocity of seismic wave propagation causing development of diffracted waves, and other phenomena render the resolution of seismic boundaries difficult, and special interpretation methods have to be applied (Mareš et al., 1984). The accuracy of determination of depths to seismic boundaries depends on the difference between the velocities v_1 and v_2 above and below the boundary, and on the preciseness of our knowledge of these velocities. In an ideal case the error in depth determination is less than 10%.

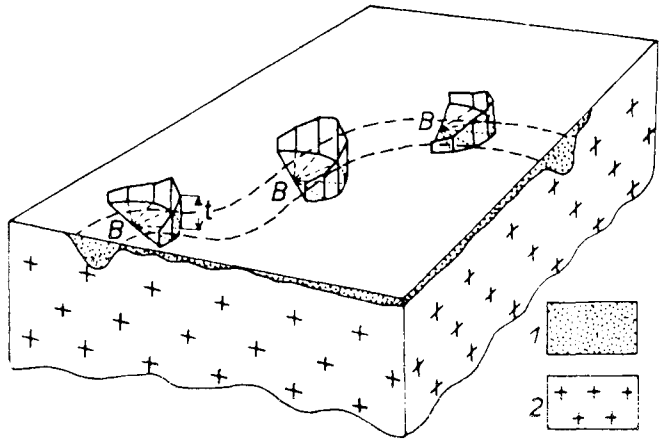

Figure 3.8 Principle of the application of shallow seismics, as demonstrated when tracing a buried river channel filled with stream alluvium (Davis and De Wiest, 1966). *B* — point of explosion, *t* — time of direct wave arrival, *1* — unconsolidated sediments filling the channel, *2* — solid underlying rocks.

Besides the velocity of compressional waves v_p, shear wave velocities v_s have recently begun to be determined in seismic surveys (Růžek, 1979; Proceedings, 1983). *Reflection methods* have also been used to investigate structures occurring at relatively shallow depths (Schepers in Sborník, 1976; Hunter et al. in Proceedings, 1989).

3.1.3 Displacement or Throw of Key Horizons

A displacement or throw of a key horizon in a tectonic zone may represent a reverse or normal fault. In both cases the depth of the key horizon is abruptly changed. From the geophysical point of view, it is usually unimportant whether a downfault or a normal fault with drag flexure occurred because geophysical methods can only measure the steepness of the angle at shallow depths. Displacement of a key horizon is indicated by a sudden change of its depth. If the change is small relative to its depth, it may be ignored in interpretation because the effect of the throw may be lost in the inaccuracy of interpretation. On the other hand, in many cases a quantitative interpretation of depth is not necessary for localization of a fault, and simpler more equivocal procedures may be used.

On a *gravimetric map*, a normal fault is indicated by the bending of or concentrating of isoanomalous lines. In a section perpendicular to the fault line, the anomaly Δg is indicated by an abrupt change; i.e., a pronounced horizontal gradient. The magnitude of the gradient depends on the depth and relative magnitude of the throw and on the differential density above and below the key horizon. Fig. 3.9 is an example of a residual anomaly Δg_L over a fault at different depths; the effect of displacement at a greater depth is shown by a smaller slope for the Δg_L curve. A lesser slope, however, is not necessarily the manifestation of a fault at a greater depth. It may also represent an oblique displacement at a shallower depth. For locating faults from gravimetric maps, Linsser's method (Mareš et al., 1984), or maps of horizontal gravity gradients are used.

In bedrock with high magnetic susceptibility, the *magnetometric method* may

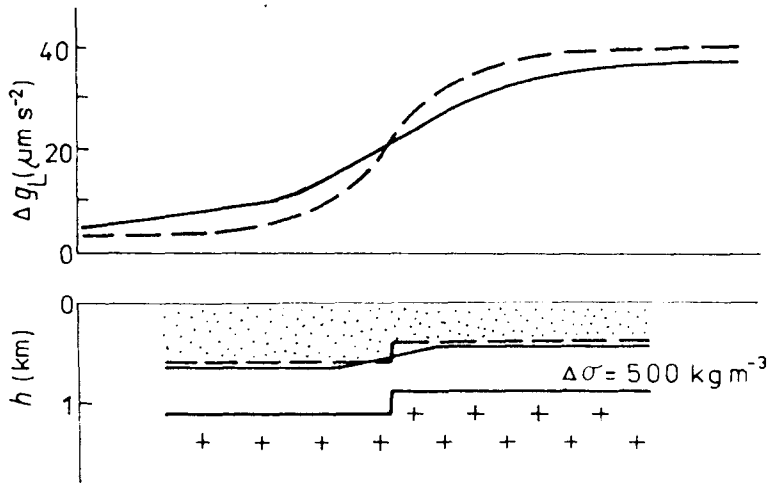

Figure 3.9 Indication of a downthrow on a gravity profile.

aid in locating faults. A marked horizontal gradient of ΔT or Z_a over a sedimentary basin may indicate a throw in the bedrock.

A break in a refracting boundary is manifested by a characteristic distortion of travel-time curves in *refraction seismics*. Two characteristic travel-time curves correspond to the zone of a refractory boundary following a break; one has the character of a wave diffracted on an edge and propagating beyond as a refracted (Love) wave, and the other corresponds to a wave that entered the refracting boundary behind the break through the bedrock. In most cases, however, only one wave can be recorded. Figure 3.10 shows the characteristic of a reverse travel-time curve above a break accompanied by a throw in the bedrock, or seismic key horizon. The throw may be interpreted from the interrelation between the travel-time curves corresponding to the segments before and after the throw. The depth of the refracting boundary and the amplitude of the throw is, however, in most cases determined as the difference in depths on either side of the fault. The travel-time curves of diffracted waves may be used to determine a more accurate location for the boundary edge.

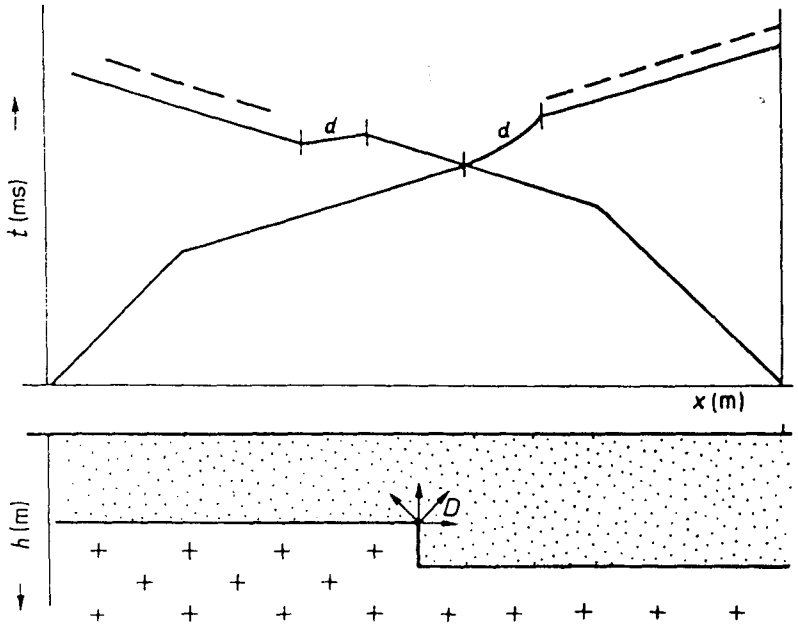

Figure 3.10 Character of reverse travel-time curves obtained by the refraction method at a throw in a seismic interface, where d is the sector of travel-time curve corresponding to the diffracted wave at the edge of the interface D.

Geoelectrical methods are the primary methods used for locating faults in hydrogeological investigations. If a fault occurs at a relatively shallow depth and the separation is reasonably large, it can be regarded as a contact between two rock types, and the resistivity methods and other variants of geoelectrical profiling prove most satisfactory (see Section 3.1.4). A fault with a relatively small vertical separation compared with its depth is identified by vertical electrical sounding (Fig. 3.11). The fault is revealed by a change in the apparent resistivity ρ_c for a given optimum spacing. The optimum spacing is determined from sounding curves as the spacing at which the difference in apparent resistivity ρ_a at both sides of the fault is significant. The values of apparent resistivity for a given spacing can then be determined by resistivity profiling with an optimum spacing at both sides of the fault. Profiling with the electrode array

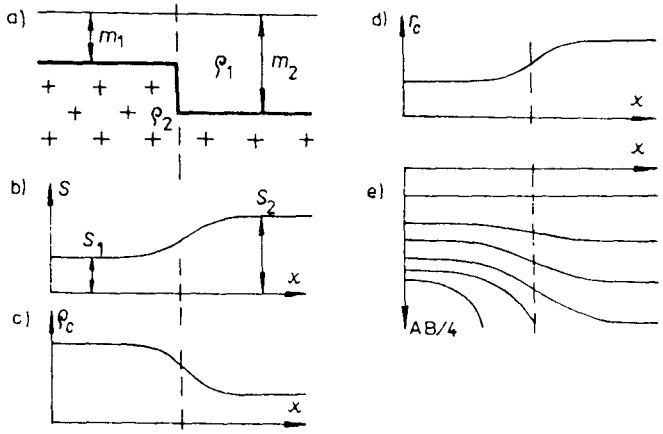

Figure 3.11 Parameters derived from the VES curve for the location of a throw in nonconductive bedrock (Karous, 1973). (a) Model of the throw. (b) Curve of total longitudinal conductance of sediments. (c) Values of apparent resistivity for a given spacing. (d) Spacing value for a given apparent resistivity. (e) Isoohmic pseudosection.

perpendicular to the profile is most suitable; a longitudinal array does not permit sufficient accuracy in determining the condition of the fault.

Another parameter which indicates the location of a fault by its change is the value r_c of the electrode spacing AB, at which the given apparent resistivity was measured. A downthrow in the bedrock or in a nonconductive key layer can also be seen in the isoohmic pseudosection. A dislocation accompanied by downthrow is evident from the change of sounding curves on both sides of the throw. Habberjam (1970) introduced a coefficient A for comparison of sounding curves which is, in fact, a simple measure of the difference between two neighboring sounding curves. Habberjam's coefficients attain anomalously high values in places of a change in a sequence of sounding curves; i.e., where resistivity conditions are changed. High A coefficients thus indicate tectonic disturbance.

In terrains of variable relief, where the vertical throw of a key horizon is smaller than the variations in relief, the methods described above cannot be employed because the parameters would represent more or less changes in ground surface elevation. A larger number of sounding curves has to be used

especially for an accurate location of a fault of a very small separation. The sounding curves make it possible to define conclusively only the total longitudinal conductance of the sediments S; according to Eq. (3.5), the mean longitudinal sediment resistivity ρ_l is the second parameter necessary for assessing the depth H of the key horizon (i.e., the total thickness m of the overlying sediments). The resistivity ρ_l can be obtained by statistical analysis of a representative set of sounding curves on either side of the fault (Karous, 1974).

3.1.4 Tectonics and Fault Zones

In igneous and metamorphic rocks, major ground-water accumulations and flows are found in tectonically altered areas and zones and in weathered portions of rock complexes. Water flowing through fractures in some rock types (limestones, dolomites, etc.) develops cavities which may be filled with clayey soils or water. Tectonically disturbed zones are often characterized by a pronounced change in rock physical properties allowing us to locate them directly using geophysical methods. Where the changes are too small to give rise to measurable geophysical anomalies, a fault zone may be located on the basis of indirect indications, taking into account other characteristic features of observed geophysical fields such as shifting or binding isolines, etc.

A *strongly fractured zone* can function as a drainage conduit or, if filled with clayey material, a dam which impedes ground-water flow. In either case it is expressed by a conspicuous reduction in resistivity. The most appropriate method for its location is therefore geoelectrical profiling in all its variants, especially resistivity profiling with the various electrode arrays (Fig. 3.12). The most suitable are asymmetric electrode arrays; i.e., combined profiling, method of combined middle gradient (Mareš et al., 1984), etc. Symmetric profiling is less appropriate for locating thin slab-like conducting bodies because the amplitude of the anomaly is easily hidden by the effects of surface inhomogeneities. Profiling with the electrode array perpendicular to the profile line also displays pronounced anomalies but field operations are fairly cumbersome. It is

utilized when an additional task is to be performed; for example, the assessment of a downthrow in nonconductive bedrock.

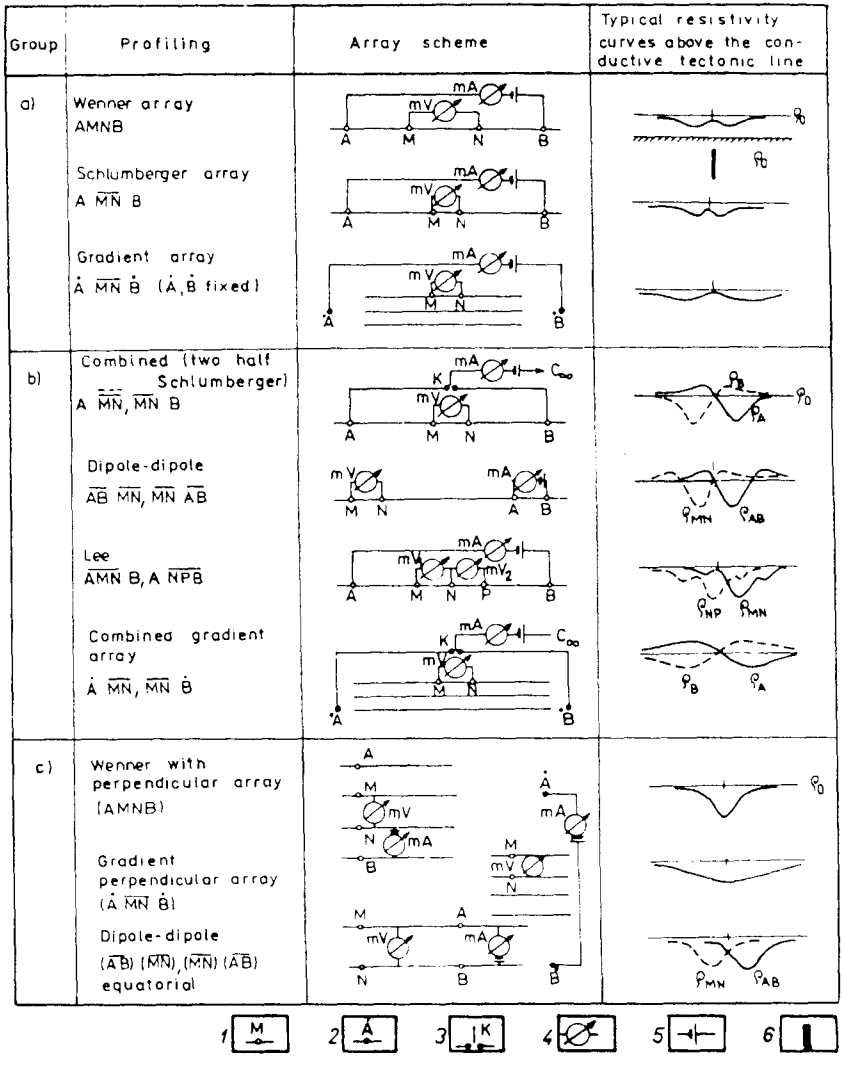

Figure 3.12 Overview of resistivity profiling methods and typical resistivity curves above a conductive tectonic line (Karous, 1978b). (a) Symmetric profiling. (b) Asymmetric profiling. (c) Profiling with perpendicular array. *1* — mobile (measuring) electrode, *2* — stable (current) electrode, *3* — change-over switch, *4* — milliammeter or millivolt meter, *5* — current source, *6* — conductive zone.

Of the remaining geoelectrical methods that may be economically utilized for detecting conductive zones, we recommend the electromagnetic methods using light-weight portable instruments. The *Slingram method*, and the *very low frequency method* in its inductive version (VLF), have proven most useful in hydrogeological surveys. Because transmitters for naval communication serve as a source for the primary field, the equipment for the VLF method has only a measuring component, simplifying field surveys.

Tectonic dislocations are also indicated by a decrease in density of the material filling fault zones which may therefore produce negative gravity anomalies. Deep fault structures accompanied by block subsidence are manifested by high gradients in the gravity field.

Dislocations can also be located by *thermal prospecting* and *measurement of* CO_2 concentrations in soil gas, since they often function as channels for rising ground water and gases. These methods detect temperature anomalies and high contents of CO_2 or other gases chiefly at the point where thermal or mineral waters rise along faults. In such cases, measurements in winter months at moderate depths are appropriate. *Remote sensing* of temperatures using a vehicle-mounted IR (infrared) indicator (Oelsner, 1977) is also a suitable procedure. Measurements should be performed during the late night hours, ideally shortly before dawn. Tectonic dislocations are manifested principally by a marked decrease in temperature in summer and, in contrast, by a temperature increase in winter (Fig. 3.13). The method is applicable even where all other direct methods for locating faults have failed. Deep structural lines may also be detected by *anomalous concentrations of metallic elements* in molecular form in the air or captured in artificial sorbents (Fig. 4.26b and Section 7.8).

Locations of ground-water ascent are often reflected in anomalies in *spontaneous polarization* (SP), due to the development of a filtration potential. The inflow of ground water into unconsolidated cover material is usually indicated by positive SP anomalies, whereas locations of leakage, for example, from a reservoir are indicated by negative SP anomalies (Fig. 3.14).

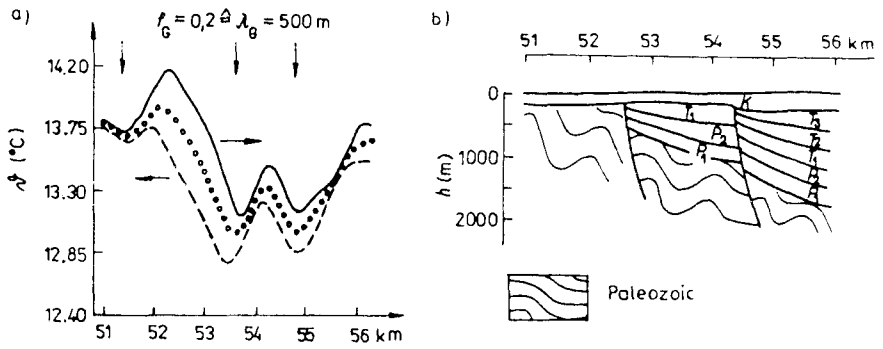

Figure 3.13 Temperature measurement, using IR method, in the area of the Central Germany fault line (according to Oelsner, 1977). (a) Temperature profile for the limiting wave length, λ_G = 500 m (horizontal arrows show the direction of vehicle movement; mean values are indicated by circles, vertical arrows show faults according to IR method). (b) Geological section based on borings and gradient gravity measurements. P_1 — Rotliegendes, P_2 — Zechstein, T_1 — Buntsandstein, T_2 — Muschelkalk, T_3 — Keuper, K — Quaternary.

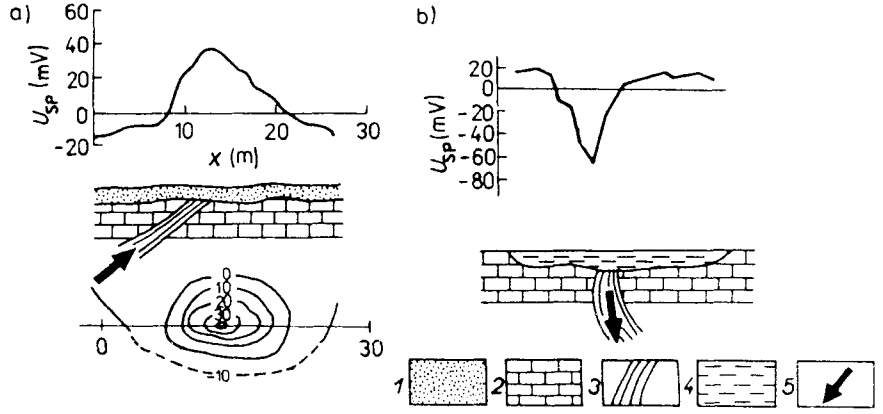

Figure 3.14 Examples of SP anomaly above a fault zone with ground-water flow. (a) Outflow of ground water (Stenzel and Szymanko, 1973). (b) Site of infiltration (Ogilvi, 1962). *1* — cover deposits, *2* — limestone, *3* — fault zone, *4* — water reservoir, *5* — direction of water flow along the fault zone.

A contact between two rock types, where there is no displacement, is determined using a geophysical method that distinguishes between the physical properties of the rocks involved. Resistivity profiling in a symmetric variant is usually employed. Frequently resistivity profiling with two electrode spacings

(i.e., with two depth ranges) is used, which permits the dip of the contact to be determined (Fig. 3.15).

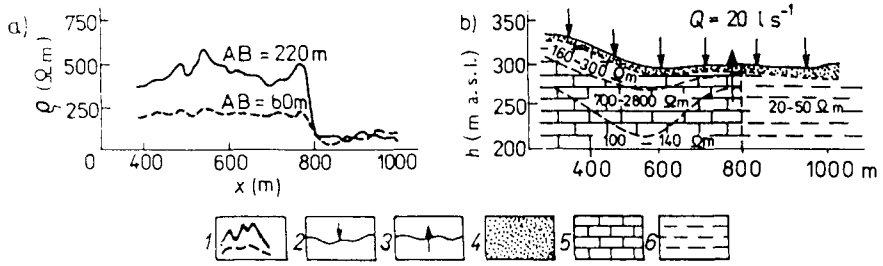

Figure 3.15 Curves of symmetric resistivity profiling over the contact between Mesozoic and Palaeogene rocks (Džuppa, 1973) near Ježova Ves nad Nitricou in the Strážovská hornatina Highland (Slovakia): (a) Resistivity curves. (b) Section interpreted from VES and SRP. *1* — SRP curves, *2* — location of VES, *3* — borehole, *4* — loam and gravel, *5* — Mesozoic rocks (limestone and dolomite), *6* — Palaeogene rocks.

A *magnetic survey* may be used where the rocks along a contact have different magnetic susceptibilities. In this way boundaries of recent volcanics, and buried volcanic layers can be located.

A broader fault zone may be indicated by a decrease in resistivity; in such a case, symmetric *resistivity profiling* (SRP) is used for its location. If a fault zone does not differ markedly in resistivity from the adjoining rock complex, we can make use of its *anomalous resistivity anisotropy* for its location, particularly if the adjacent rocks are electrically inhomogeneous or where varying thicknesses of conductive overburden have unfavorable effects. A fault zone shows a higher resistivity in the transverse direction (transverse resistivity) than in the longitudinal direction (longitudinal resistivity). According to the anisotropy paradox, however, surface resistivity methods will show a higher apparent resistivity in an array parallel to the elongation of the fault zone (Fig. 3.16). The anisotropy is measured by a symmetric resistivity procedure arranged in several (usually four) directions and with different spacings. The trend of the fault zone is given by the orientation of the array which gives the maximum

apparent resistivity. The degree of disruption is proportional to the ratio of the maximum/minimum apparent resistivity, which corresponds to the coefficient of anisotropy $\lambda = \rho_{a\,max}/\rho_{a\,min}$.

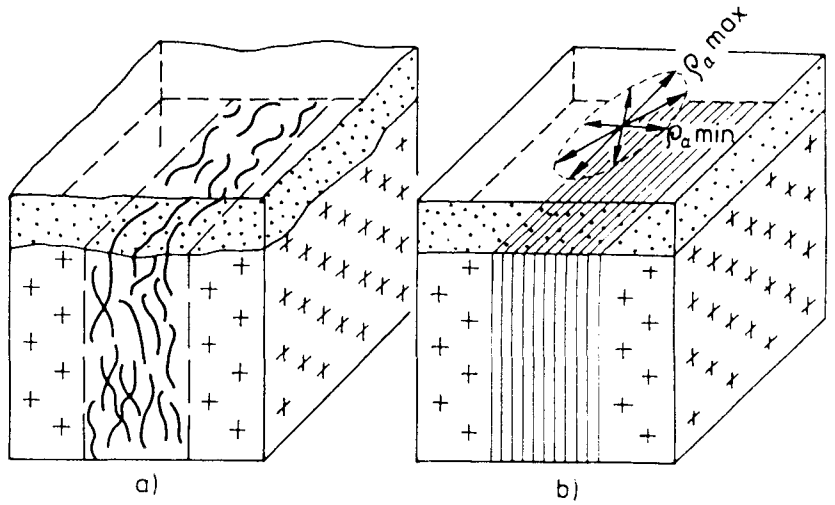

Figure 3.16 Radial resistivity measurement used for locating a fault zone on the basis of resistivity anisotropy. (a) Geological block diagram of a fault zone. (b) Geoelectrical model with anisotropic plate and the ellipse of resistivity anisotropy determined by radial resistivity measurement.

In searching for dislocations of a significant width, we can also use geophysical methods used for the determination of the thickness of a weathered overburden; that is, vertical electrical soundings and shallow refraction seismics, recognizing the greater thickness of weathered rocks in the fault zones.

3.2 Determination of Hydrogeological Parameters of Geological and Water Bodies by Geophysical Methods

Some hydrogeological parameters (for example, depth to ground water, direction and velocity of ground-water flow, degree of fracturing, shape of the cone of depression, etc.) can be directly evaluated from the results of geophysical

measurements, on the basis of universally valid theoretical relations or models. The remaining parameters, however, can only be assessed by correlation with geophysical parameters (Table 3.1); furthermore, the correlations are valid only within certain structures. For such determinations, both surface and logging methods as well as remote sensing methods are employed.

With respect to the applicability of the *hydrogeological interpretation of geophysical data* in practice, and to the effectiveness of an investigation, primary attention should be directed to:

- The quality of geophysical data (G_0) and their transformation to the apparent (G_a) and real (G_r) geophysical parameters of a hydrogeological body - the geophysical interpretation
- The accuracy of the hydrogeological (H_r) parameters determined from the geophysical parameters (G_0, G_a, or G_r) - the hydrogeological interpretation
- Formulation of equations for regression curves from the results of parametric measurements and the determination of the degree of correlation between the parameters being compared
- A reasonable number of parametric data to ensure the reliability of the calculated regression curve within the given range

Regression relations, and the minimum number of the measured parametric pairs for a given confidence range for the examined hydrogeological parameter, are determined by the methods of mathematical statistics (see, for example, Rektorys et al., 1981; Sharapanov et al., 1974).

3.2.1 Lithology and Shaliness

Determination of the *basic lithological type* from geophysical measurements is fairly complicated and only in the simplest cases can a single geophysical method suffice for this. Usually a set of surface and logging methods should be employed.

Table 3.1 Survey of geophysical methods and measured parameters with respect to their application in hydrogeology and engineering geology

Geophysical methods	Measured parameter symbol (unit)	Application in	
		Hydrogeology	Engineering geology
		Parameters that can be determined	
Gravimetric			
Gravimetry (profiles, regular or irregular nets)	Acceleration of gravity g ($m\ s^{-2}$)	Thickness of sediments, changes in bedrock surface, major dislocations, karstified layers in limestones	Delineation of quasi-homogeneous blocks, location of major tectonic ines, bulk density *in situ* (between points of investigation), underground cavities
Microgravimetry (ground, mining works)			
Measurement of vertical and horizontal gravity gradient	Gradient of gravity acceleration $\frac{\partial g}{\partial z}, \frac{\partial g}{\partial x}, \frac{\partial g}{\partial y}$ (s^{-2})		
Magnetometric			
Air-borne magnetic survey, ground magnetic and micromagnetic measurements	Components of magnetic field T, Z, H (nT) and their vertical gradient $\frac{\partial T}{\partial z}, \frac{\partial Z}{\partial z}$ ($nT\ m^{-1}$)	Character of bedrock of large basin structures, occurrence of basic bodies in crystalline basement, tectonic contact of volcanites with sediments	Delineation of quasi-homogeneous blocks, anisotropy of rock blocks, structural elements
Measurement with kappameters (mining works, exposures)	Magnetic susceptibility κ (SI units)		Changes of lithology in exposures, trenches, galleries, borehole profile
Magnetic susceptibility logging			
Radiometric and nuclear geophysics			
Airborne radiometry, gamma ray survey, gamma spectrometry (ground, boreholes, mines)	Exposure rate $\dot{X}$ ($pA\ kg^{-1}$) Content of elements K (%), eU (ppm), eTh (ppm)	Structural-geological elements, shaliness of sediments	Delimitation of quasi-homogeneous blocks, changes in lithology of rocks (in galleries and boreholes)

Table 3.1, continued

Geophysical methods	Measured parameter symbol (unit)	Application in: Hydrogeology	Application in: Engineering geology
		Parameters that can be determined	
Emanometry	Concentration of Ra emanation Q (Bq m^{-3})	Fault zones	
Measurement of cosmic radiation intensity	Exposure rate $\dot{X}$ (pA kg^{-1})	Discontinuities in a massiff	
Gamma-gamma method (mining works, boreholes)	Bulk density σ (kg m^{-3})	Bulk density *in situ* Total porosity	
Neutron-neutron method (pits, mining works, boreholes)	Moisture content W_o(%), neutron porosity P_N (%)	Moisture content *in situ* Total porosity	
Geothermal			
Airborne and ground survey using infrared method (contact-free)	Temperature ϑ (°C)	Faults	Discontinuities in rock massif
		Sites of surface water infiltration and of hidden ground-water discharge	
Measurement with thermometers (ground, mining works, boreholes		Geothermal gradients	
		Water dynamics in boreholes	
Geoelectrical			
Vertical electrical sounding	Apparent resistivity ρ_a (Ω m)	Depth to bedrock, thickness of aquifer, throws	Delimitation of quasi-homogeneous blocks, degree of tectonic deformation
Resistivity profiling (ground, mining works)		Thickness of zone of weathering, faults, fissures, cracks	
Resistivity logging		Changes of lithology in bore profile	
		Interstitial aquifers, open porosity, fracture aquifers	Degree of weathering and of tectonic deformation

Table 3.1, continued

Geophysical methods	Measured parameter symbol (unit)	Application in: Hydrogeology	Application in: Engineering geology
		Parameters that can be determined	
Self-potential SP method (ground)	Natural potential (filtration, electro-chemical, redox) ΔV (mV)	Sites of ground-water outflow, sites of infiltration, ground-water flow paths	
		Shape of cone of depression	Sites of corrosion of water and other pipelines
SP method (boreholes)		Lithological differentiation of borehole profile, interstitial aquifers, shaliness of clastics, dissolved solids content in ground water	Percolation properties of the medium, dissolved solids in ground water
Induced polarization (IP) method (ground, boreholes)	Induced potential ΔV_{IP} (t_i) (mV), primary potential ΔV_{Ra} (mV), apparent polarizability in time t_i $\eta_a(t_i) = \frac{\Delta V_{IP}(t_i)}{\Delta V_{Ra}}$	Thickness and area of sandy aquifer in clayey sediments	Assessment of engineering-geological and hydrogeological conditions in a rock massif
	Rate of discharge curve $\alpha_{IP} = \frac{V_{IP}(t_1)}{V_{IP}(t_2)}$	Appraisal of grain-size distribution of the aquifer (permeability)	
	Specific complex parameter $A^* = \frac{\eta_a(t_1) - \eta_a(t_2)}{\rho}$	Lithological differentiation of sandy-clayey sediments	
Mise-a-la-masse method	Potential difference ΔV (mV)	Direction and velocity of ground-water flow, filtration and migration parameters of rocks	
			Trends of discontinuites in rock massif
Very low frequency method	Magnetic components Re Hz (%) and Im Hz (%) of electromagnetic field of radiostations	Conductive tectonic lines and fracture zones	

Table 3.1, continued

Geophysical methods	Measured parameter symbol (unit)	Application in: Hydrogeology	Application in: Engineering geology
		Parameters that can be determined	
Electromagnetic methods	Ratio of vertical magnetic field components Hz_1/Hz_2 (%) and phase shift ϕ (deg)	Significant tectonic lines	Cables, subsurface metal pipelines, direction of horizontal boreholes
Dipole electromagnetic profiling (DEMP)	Conductivity γ (S m^{-1})		
Radiowave profiling	Wave number k_p (m^{-1})	Lithological division of near-surface beds, moisture content, salinity	
Electromagnetic measurements between boreholes and galleries	Transit time of radio signal t (s), coefficient of attenuation α (%)		Delimitation of quasi-homogeneous blocks and of discontinuites in the massif
Radar (ground)	Transit time t (s), velocity of radar impulse propagation v (m s^{-1})	Ground-water table	Cavities at shallow depths, lithology of near-surface beds, faults, joint and fold systems, changes in lithology and physical properties of rocks
(airborne)			
Seismic			
Seismic refraction survey (ground, mining works)	Transit time t (s), velocity of propagation of compressional v_p and shear waves v_s (m s^{-1}), attenuation factor α (m^{-1}), amplitude A (mV), frequency f (Hz)	Thickness of Quaternary deposits and weathered layers, depth to bedrock	
		Depth to ground-water table	Delimitation of quasi-homogeneous blocks, deformation of rocks, Young's modulus, Poisson's ratio
Seismic reflection survey (ground, mining works)		Depth to bedrock of major basinal structures	
Acoustic and seismic logging		Porosity, fracturing, elastic moduli	

Table 3.1, continued

Geophysical methods	Measured parameter symbol (unit)	Application in: Hydrogeology	Application in: Engineering geology
		Parameters that can be determined	
Cross-hole seismic measurement and measurement between mining works			Structural elements and weakened zones, deformation of rocks, zones of diverse stresses about mining works
Vibration methods (ground, mining works)			Deformations of ground surface, effects of explosives on structures, occurrence of underground cavities
Microseismological methods (ground, mining works)	Amplitude A (mV), activity N (s^{-1}), frequency f (Hz), velocity of sound propagation v (m s^{-1})		Stressed zones in a massif, effect and changes in stress-deformation process in a massif, assessment of seismicity of the area
Geoacoustic method (special boreholes)	Activity N (s^{-1}), relative amplitude A_p(μV s^{-1}), frequency f (Hz)		Same as above
Logging (besides those mentioned above)			
Caliper log	Borehole diameter (mm)	Delineation of an aquifer	Degree of massif deformation
Directional survey	Azimuth φ and inclination δ (deg) of borehole	Borehole drift	
Temperature log	Water temperature ϑ (°C)	Dynamics of water in borehole, yield of inflow	
Fluid resistivity log, also after water treatment with NaCl	Resistivity of water ρ_w, ρ_m (Ω m)	Vertical and horizontal flow rates, filtration velocity, hydraulic conductivity	
Photometry, also after water treatment with dye	Transparency of water, concentration of dye C (mg l^{-1})	Same as above	

Metode Geofizice	Simbolul parametrului masurat	Aplicatie in	
		Hidrogeologie	Geologie Inginereasca
	Parametrii ce pot fi determinati		
Gravimetrica			
Gravimetrie(profile, retele regulate si neregulare)	Acceleratia gravitationala g (ms^{-2})	Grosimea sedimentelor, schimbari ce apar pe suprafata rocii, dislocatii majore, strate carstificate in calcare	Dezalinierea blocurilor cvasiomogene, locatia celor mai importante inele tectonice, media densitatii *in situ* (intre diferitele puncte de investigatie), cavitati subterane
Microgravimetrie (lucrari la suprafata si miniere)			
Masuratori verticale si orizontale ale gradientului de gravitatie	Gradientul acceleratiei gravitationale $\partial g/\partial z$, $\partial g/\partial x$, $\partial g/\partial y$ (s^{-2})		
Magnetometrica			
Masurarea undelor magnetometrice din avion, masuratori magnetice si micromagnetice la nivelul solului	Componentele campului magnetic T, Z, H (nT) si gradientii lor verticali	Caracterul rocilor din structurile cu bazilne mari, ocurente ale corpurilor de baza in amplasamente cristaline, contactul tectonic dintre vulcanite si sedimente	Dezalinierea blocurilor cvasiomogene, anizotropia blocurilor de roci, elementele structurale
Masurarea cu ajutorul kappameters (lucrari la suprafata si expuneri)	Susceptibilitate magnetica k (unitati SI)		Schimbarea litologiei la suprafata, santuri, galerii, profile ale forajelor
Catalogarea susceptibilitatii magnetice			
Geofizica radiometrica si nucleara			
Radiometrie din avion, masurarea undei gamma, spectometru gamma (suprafata, foraje, mine)	Rata de expunere X ($pA\ kg^{-1}$). Continutul de elemente K (%), eU (ppm), eTh (ppm)	Elemente structural geologice, sistuozitatea sedimentelor	Delimitarea blocurilor cvasiomogene, shimbari in litologia rocilor (in galerii si in foraje)
Emanometrie	Concentratia emanatiilor tip Ra Q ($Bq\ m^{-3}$)	Zona de faliere	
Masurarea intensitatii radiatiei cosmice	Rata de expunere X ($pA\ kg^{-1}$)	Discontinuitatea intr-un masiv	
Metoda gamma-gamma (lucrari miniere, foraje)	Densitatea medie σ ($kg\ m^{-3}$)	Densitatea medie *in situ* Porozitatea totala	
Metoda neutron-neutron (gropi, lucrari miniere,foraje)	Continutul de umeazeala W_0 (%), porozitate neutronica P_N (%)	Continutul de umeazeala in situ Porozitatea totala	
Geotermala			
Masurarea din avion sii de la suprafata solului utilizand metoda infrarosu (fara contact)	Temperatura ϕ (^0C)	Falii	Discontinuitatea in roci masive
		Locuri ale infiltrarii apei de suprafata si a descarcarii apei de suprafata ascunse	
Masurarea cu ajutorul termometrelor (suprafata, lucrari miniere, foraj)		Gradienti geotermali Dinamica apei in foraje	
Geoelectrica			
Sonar electric vertical	Rezistivitate aparenta p_a (Ω m)	Adancimea rocilor, grosimea acviferului,	Delimitarea rocilor cvasiomogene,

		distanta	gradul de deformatie tectonica
Calcularea rezistivitatii (suprafata, lucrari miniere)		Grosimea zonelor de umezeala, falii, fisuri, crapaturi	
Notarea rezistivitatatii		Schimbari ale litologiei in profilul gaurii	
		Acvifere interstitiare, porozitati deschise, acvifere fracturate	Gradul de alterare si de deformatie tectonica
Potential propriu Metoda SP (la suprafata)	Potential natural (infiltrare, electrochimic, redox) DV (mV)	Izvoare, infiltrari si canale de scurgere	
		Forma conului de depresiune	Coroziunea cauzate de apa, alte cauze
Metoda SP (foraje)		Diferentele litologice ale profilelor forajelor, acvifere interstitiare, sistuozitatea clastelor, continutul solid dizolvat in apa din sol	Proprietatile mediului, elemente solide dizolvate in apa din sol
Metoda polarizarii induse (IP) (la suparafata, foraje)	Potential indus ΔV_{ip} (ti) (mV), potential primar ΔV_{Ra} (mV), polarizare aparenta in timp t_i $\eta_a(t_i)= \Delta V_{IP}(ti)/ \Delta V_{RA}$	Grosimea si suprafata acviferului nisipos, in sedimentele argiloase	Calcularea conditiilor geologico-ingineresti si hidrogeologice intr-un masiv
	Curba ratei de descarcare $\alpha_{IP}=V_{IP}(t_1)/V_{IP}(t_2)$	Calcularea permeabilitatii unui acvifer	
	Parametru specific complex $A^{\sim}=(\eta_a(t_1)- \eta_a(t_2))/p$	Diferentierea litologica intre sedimentele nisipoase si sedimentele argiloase	
Metoda Mise-a-la-masse	Diferenta de potential DV (mV)	Directia si viteza curgerii apei de suprafata, parametrii de filtrare si de migratie a rocii Tendinte de discontinuitate intr-un masiv	
Metoda de frecvente extrem de joase	Componente magnetice Re Hz (%) si Im Hz (%) ale campului electromagnetic al statiilor radio	Linii tectonice conductive si zone de fractura	

The basic lithological type can be established most reliably by *geophysical logging*, which enables the physical properties of rocks to be determined with a much greater exactness than by a surface geophysical survey. The logging methods are chosen depending on the rock type expected; the method selected for clastic sandy-clayey rocks will differ from that for a carbonate complex or in igneous or metamorphic rocks.

In clastic sandy-clayey rocks, evaluation of the basic lithological type is reduced to determination of shaliness V_{sh} (usually clay and silt content) and total porosity P. The shaliness V_{sh} is determined chiefly by using gamma-ray logging GR and the record of self-potentials SP and also often the true formation resistivity ρ_t. These methods are considered to be *shale indicators*. The shale content V_{sh} is calculated from relations that can be expressed in the form

$$V_{sh} \leq \frac{X-A}{B-A} \qquad (3.6)$$

where X is the mean value of the measured parameter (GR, SP, ρ_t) opposite a particular layer and A and B are limiting values of the same parameter, corresponding to clean sands (sandstones) and clays (claystones), respectively. The relation (3.6) gives rather high values of shaliness, in the optimum case approaching the true V_{sh} value.

In addition to the one-parameter shale indicators there are two-parameter shale indicators based on porosity data obtained by neutron logging (P_N) combined with formation density logging (P_D), or by acoustic logging (P_A) combined with formation density logging (P_D). The shale content determined in this way is the nearest to reality.

The determination of the basic lithological type in boreholes in carbonate, igneous or metamorphic rocks requires that as many independent parameters a_i be measured as there are rock types observed in the borehole. It is recommended that the physical parameters which clearly differentiate between the individual rock types be used for this (Figs. 2.4 to 2.6). The proportions of

the rock components X, Y, Z, etc., represented in a given depth interval are calculated using the relations

$$a_i = a_{ij}X + a_{ik}Y + a_{il}Z + \ldots\ldots + b_iP \qquad (3.7)$$

where a_{ij} to a_{il} and b_i are characteristic values of the measured physical parameter a_i for the different rock types and the ground water; they are tabulated or are obtainable by statistical analysis of logging data. P is the total volume of voids in the rock.

Determination of the lithological type from the results of a *surface geophysical survey* is not always as reliable as a determination made from logging results. Surface methods, however, have an undisputed advantage in that they allow the spatial variation of the geophysical parameters and thus also of the lithological type to be traced or mapped. Resolution of such problems is easier where near-vertical structures in metamorphic or igneous rock complexes are involved. Assessment of lithological type for sediments with nearly horizontal bedding is a very difficult task. The interpretation criteria have been most thoroughly developed for sandy-clayey reservoir rocks using the geoelectrical parameters ρ and A^* (Table 3.1); an estimation of shaliness (V_{sh}) (Fig. 3.17a) or of the clayey-sandy soil type (Fig. 3.17b) can be obtained.

3.2.2 Porosity and Fracturing of Rocks

The most favorable conditions for determination of porosity and fracturing using geophysical methods are provided by *logging*. Surface geophysical measurements can only be used under exceptionally favorable conditions.

In clastic *sandy-clayey sediments*, the following methods are used to determine porosity: neutron logging (NNL, NGL), the density variant of gamma-gamma logging (GGL-D), acoustic logging (AL, used only for deep structures), and under appropriate conditions, resistivity logging (laterolog Ra_{LL}, induction logging Ra_{IL}, and microresistivity logging) combined with SP or GR logs. The porosity of sandy-clayey sediments is calculated according to the relation

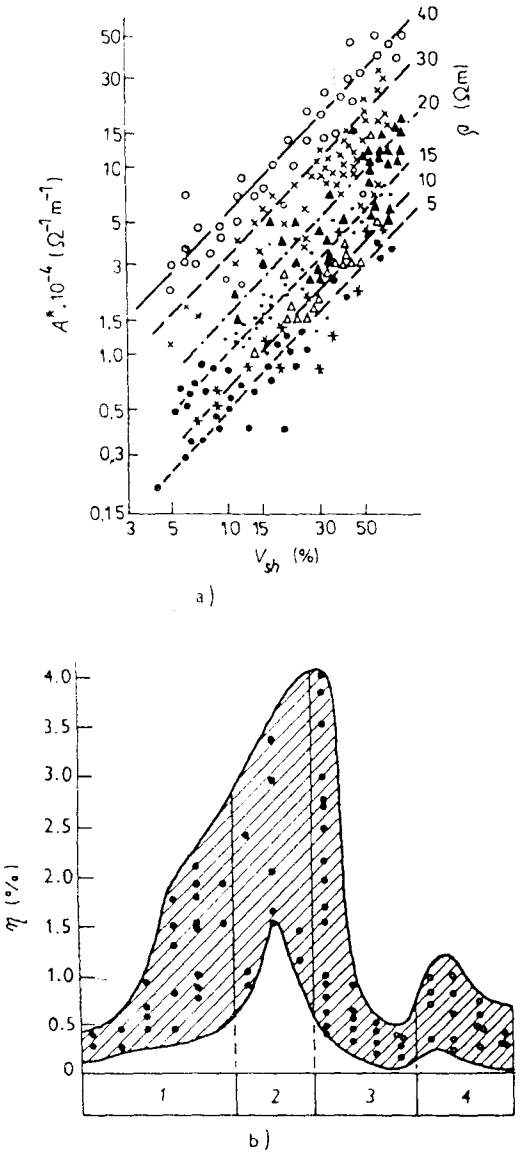

Figure 3.17 (a) Relationship $A^* = f(V_{sh})$ at various formation resistivities, ρ (Ω m) (according to Sharapanov et al., 1974). (b) Polarizability (η) as a function of the clayey-sandy soil type (according to Ogilvi and Kuzmina, 1972). *1* — sand, *2* — sandy loam, *3* — loam, *4* — clay.

$$P = P_i - V_{sh} P_{sh_i} \tag{3.8}$$

where P_i is the apparent rock porosity calculated from the results of the logging method applied and P_{sh_i} is the apparent porosity of shales measured by the same method assessed by statistical analysis of logs using cross plots.

The second term on the right side of Eq. (3.8) represents the correction for shale content V_{sh}, as the presence of an argillaceous component generally makes the calculation of porosity rather difficult. On introducing this correction into the calculation, the porosity derived from the relation (3.8) may most properly be denoted as open porosity P_0 (calculated from electrical logging) or as effective porosity P_{eff} (calculated from NNL, NGL, GGL-D or AL). The absolute error in porosity determination is usually less than $\pm 3\%$.

In *carbonate rocks* a combination of two logging methods is often applied (e.g., NNL and GGL-D, or NNL and AL), which makes it possible to assess the primary lithological type and total porosity simultaneously (Fig. 3.18). Total porosity involves the volume of pores (primary porosity P_1) as well as the volume of fractures and cracks (secondary porosity $P_2 = P_f$). Porosity determined by nuclear logging methods (NNL, GGL-D) most likely corresponds to total porosity. Acoustic and ultrasonic logging is more suitable for the determination of primary porosity; P_1 and P_2 can be established by their combination. Resistivity measurements are also used to determine fracturing (crack-to-space volume ratio) in these rocks (P_f). The equation for fracture porosity has the form

$$P_f = A \frac{\rho_w(\rho_b - \rho)}{\rho(\rho_b - \rho_w)} \tag{3.9}$$

where A is a constant depending on the complexity of the fracture system ($1.5 \leq A \leq 2$) and ρ, ρ_b, and ρ_w are respectively the resistivity measured by a certain system of electrodes, the resistivity of nonfractured rock, and the resistivity of ground water or drilling mud in rocks with a deep invaded zone.

Theoretically, all surface geophysical measurements methods whose parameters depend on P_0 (Table 2.3) may be used for determination of porosity P_0.

The resistivity methods are usually employed in a porous medium in practice (Worthington 1975, 1976). The relation between the aquifer resistivity ρ, open porosity P_0, resistivity of ground water ρ_w, and resistivity ρ_{ma} of the solid phase (including the shaley fraction) for a structural coefficient a and cementation exponent m (Worthington, 1976) is given by

$$\rho_0 = \left[\frac{1}{\rho_{ma}} + \frac{P_o^m}{a\rho_w}\right]^{-1} \qquad (3.10)$$

or by Eq. (2.20) or (2.21) in Table 2.3. The relative error ΔP_r in porosity determination is lowest as $\rho_{ma} \to \infty$ (Mazáč et al., 1978).

In a medium with fracture permeability, circular VES make it possible to establish both the *degree of fracturing*, P_f, as a function of apparent anisotropy (Fig. 3.18b) and the direction of fracturing, α_f. Using seismic methods the degree of fracturing is estimated as

$$P_f = \frac{v_f(v_b - v)}{v(v_b - v_f)} \qquad (3.11)$$

where v_b, v, and v_f are the velocities of the compressional waves in solid and fractured rock and fracture fillings (v_f = 1500 m s^{-1} where the fracture is filled with water). Fracture trends can be detected indirectly from circular measurements of spontaneous polarization (Fig. 3.36), provided that the fracture system relates to an environment in which filtration potentials are generated.

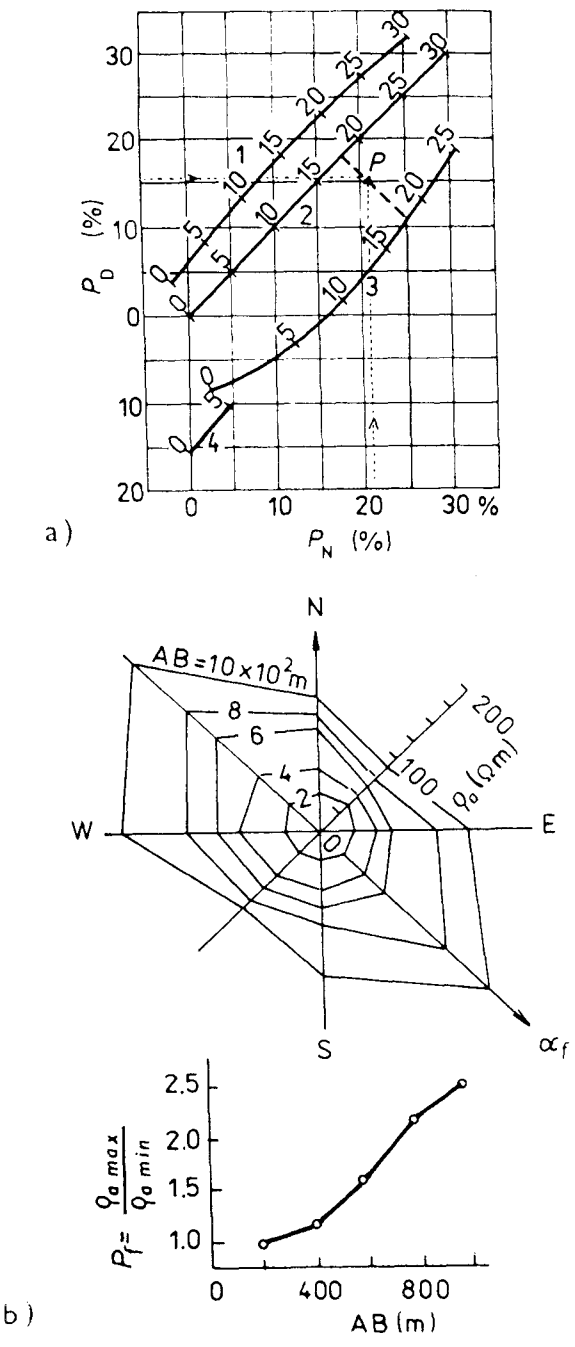

Figure 3.18 Facing page. Determination of porosity and fracturing by geophysical methods. (a) Cross plot of neutron porosity, P_N, and porosity derived from formation density log, P_D, used to assess the principal lithological type and total porosity, P (after Schlumberger, 1972a). (b) Determination of the direction of fracturing, α_f, and of changes in the degree of fracturing, P_f, with depth, as inferred from circular VES. *1* — sandstone, *2* — limestone, *3* — dolomite, *4* — anhydrite.

3.2.3 Moisture Content and Degree of Saturation

Moisture content W and water saturation S_w are determined chiefly for rocks and soils occurring above the water table; i.e., in the zone of aeration. In addition to the classical hydrogeological methods (Kuráž, 1978), moisture content and degree of saturation may also be determined by remote sensing methods (Chapter 7), surface methods and measurements in shallow boreholes, frequently in combination with penetrometer measurements.

Remote sensing methods are effective for assessing moisture contents over large areas to shallow depths (fractions of a meter to several meters). For this purpose, scanning in the range of the visible, infrared and microwave wavelengths can be employed. Interpretation of remote sensing results is hindered by changes in the resistivity ρ and permittivity ϵ of surface layers and variations in topography. To obtain absolute moisture values, remote sensing results must be calibrated against surface measurements.

Of the surface methods, we can use *resistivity and electromagnetic* methods. The application of resistivity methods is based on the principle that the resistivity increases with decreasing saturation S_w according to Eq. (2.20) or (2.21) in Table 2.3. These changes are greatest in compact rocks (at $W < 3\%$). Under such conditions we may also employ the resistivity variant of the electromagnetic very-low-frequency method (VLF) and electromagnetic dipole profiling (DEMP), using, for example, a Geonics EM-31 or EM-34 apparatus (variant of Slingram method).

Radiowave profiling (RWP, Chapter 7) is applicable for moisture determination only to shallow depths. The parameter being determined (wave number k_p) depends not only on moisture content but also on porosity, clay content and rock type. The RWP method is appropriate in soil improvement studies. The feasibility of using induced polarization has so far been little documented in practice (Sharaparov, 1974, Table 2.3).

The most reliable data on moisture content are provided by *hygrometers* based on measurements of the neutron flux density (neutron-neutron method) and of rock permittivity. Devices of the first type permit measurements at the ground surface (contact hygrometers) or in shallow holes made with a hand auger or in holes made by an electric cone penetrometer (Chapter 7). The neutron-neutron method provides a measure of the total hydrogen content in a rock. If all the hydrogen may be presumed to be bound in water molecules, the *neutron-neutron method* will give the volumetric moisture content W_0 directly. Apparatuses of the second type measure soil permittivity in shallow boreholes on the basis of changes in the inductance or capacitance of the sensing element. The relations given in Table 2.3 permit data on *relative permittivity* ϵ_r to be converted to values of volumetric or mass moisture content. The absolute accuracy of measurement with calibrated instruments is better than $\pm$ 2%.

3.2.4 Permeability, Hydraulic Conductivity, Transmissivity, and Protective Capacity

The permeability of a rock mass can be assessed using geophysical methods either qualitatively relative to other rocks, or quantitatively in terms of hydraulic conductivity k_f or transmissivity k_T.

Provided that at least one borehole is located within the hydrogeological structure of interest, *logging methods* provide the most reliable information on permeability. Criteria for the determination of permeable beds in a borehole depend on the type of permeability; i.e., whether it is intergranular or fracture permeability.

Aquifers bearing interstitial water (Fig. 3.19) are expressed in the following ways:

- on the SP record by a marked negative anomaly at $\rho_m > \rho_w$ and, in contrast, by a positive anomaly for $\rho_m < \rho_w$, for which electrochemical potentials are responsible
- on the microlog by the separation of the two resistivity curves measured $Ra_{mn} > Ra_{ml}$
- on lateral electrical sounding (LES) curves, provided that $\rho_m > \rho_w$, by

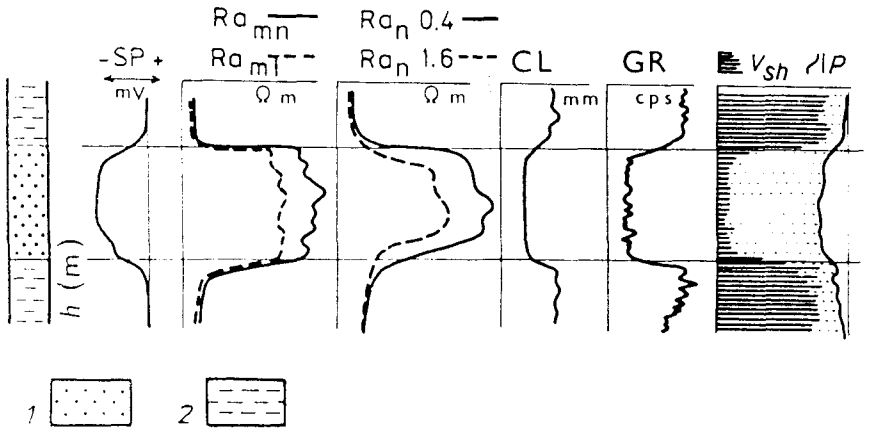

Figure 3.19 Characteristic features of an aquifer with interstitial permeability on the SP log, micrologs Ra_{mn} and Ra_{mt}, resistivity logs Ra_n measured by normal probes of different lengths, a caliper log CL, and a gamma log GR. The figure also shows the results of a computer processed diagram of formation volume analysis: *1* — sandstone, *2* — shale.

a markedly increased resistivity in the invaded zone; i.e., the apparent resistivities measured by short normal and lateral probes are distinctly higher than those obtained by long resistivity probes

- on a caliper log (CL) by a minimum well diameter, frequently smaller than the diameter of the drilling tool, due to the mud cake formed during mud invasion into a permeable bed
- on gamma-ray logs (GR) by a minimum value of exposure rate (a small content of a radioactive substance)
- on the graph of formation volume analysis (with automatically processed logs) by minimum clay content V_{sh} and maximum porosity values

Fractured aquifers in carbonate, igneous and metamorphic rocks are indicated in the following ways (Fig. 3.20):

- on SP records by narrow and comparatively sharp negative anomalies produced mainly by electrokinetic potentials
- on caliper logs (CL) by major or minor cavities

- on formation density logs (GGL-D) as layers with a lower bulk density, owing to the presence of fractures and cracks filled with water of $\sigma_w \ll \sigma_m$
- on NNL records as layers of a higher neutron porosity
- on formation resistivity logs as conspicuous conductive zones (ρ_a values attain tens or hundreds of Ω m) in contrast to solid rock blocks showing relatively high resistivities ranging from one to tens of kΩ m

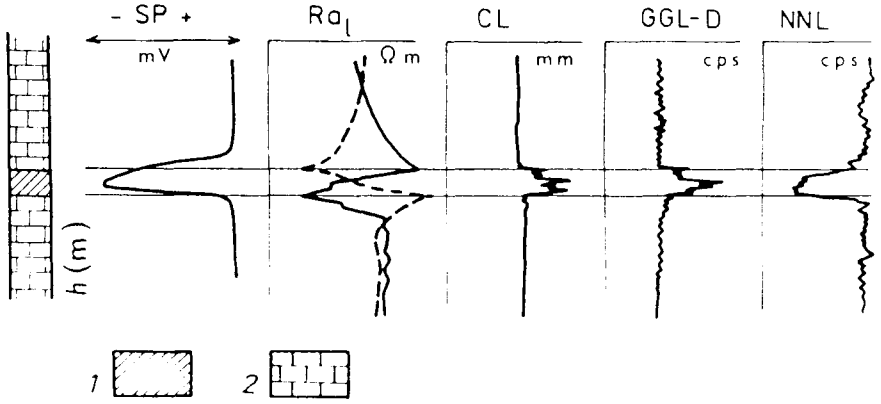

Figure 3.20 Characteristic features of a fracture zone on an SP log, resistivity logs (Ra_l), a caliper log (CL), a gamma-gamma log in density modification (GGL-D) and a neutron-neutron log (NNL). *1* — limestone, *2* — fractured aquifer.

For a quantitative determination of the *hydraulic parameters* of an interstitial or fractured aquifer where the flow can be assumed laminar, we use data on changes in the vertical volumetric flow rate Q' ($m^3\ s^{-1}$) over the depth of a borehole at a constant injection or withdrawal rate. Plots of flow rate versus depth obtained from the results of special logging methods (Section 4.5) make it possible to establish partial yields Q_i ($m^3\ s^{-1}$) or contributions from individual permeable beds and also establish their thicknesses m_i (m). The differences in water level s (m) relative to the static level h_0 are maintained intentionally small to minimize hydraulic losses. Under such conditions, the partial hydraulic

conductivity k_{fi} of confined and unconfined aquifers can be calculated using the simplified relation for radial flow to a well

$$k_{fi} = \frac{Q_i}{\Delta s_i m_i} A \qquad (3.12)$$

where Δs_i is the difference between the water level in the borehole and the piezometric level of separate aquifers, A is the steady-state well function which depends on well radius, the radius of influence R and the ratio $\Delta s_i/m_i$; for $\Delta s_i \ll m_i$, $A \rightarrow 1$ (Grinbaum, 1965).

The k_f values determined by geophysical logging are usually in good agreement with those determined from the conventional constant-discharge tests (Morin et al., 1988; Molz et al., 1989). An example of the determination of k_f is given in Fig. 3.21.

The partial transmissivity k_{Ti} in relation to the partial hydraulic conductivity k_{fi} and the thickness of a permeable bed m_i is defined by Eq. (2.15) in Table 2.2. In cases where the partial hydraulic conductivity can be derived from logging results, the partial transmissivity can also be calculated.

Under favorable conditions, both the hydraulic conductivity and the transmissivity are determinable using *surface geophysical methods*; i.e., resistivity and induced polarization. The most favorable conditions for utilizing resistivity methods in interstitial aquifers are for depths less than 50 m (Fig. 3.22c). The resistivity of such aquifers depends (at a constant resistivity of

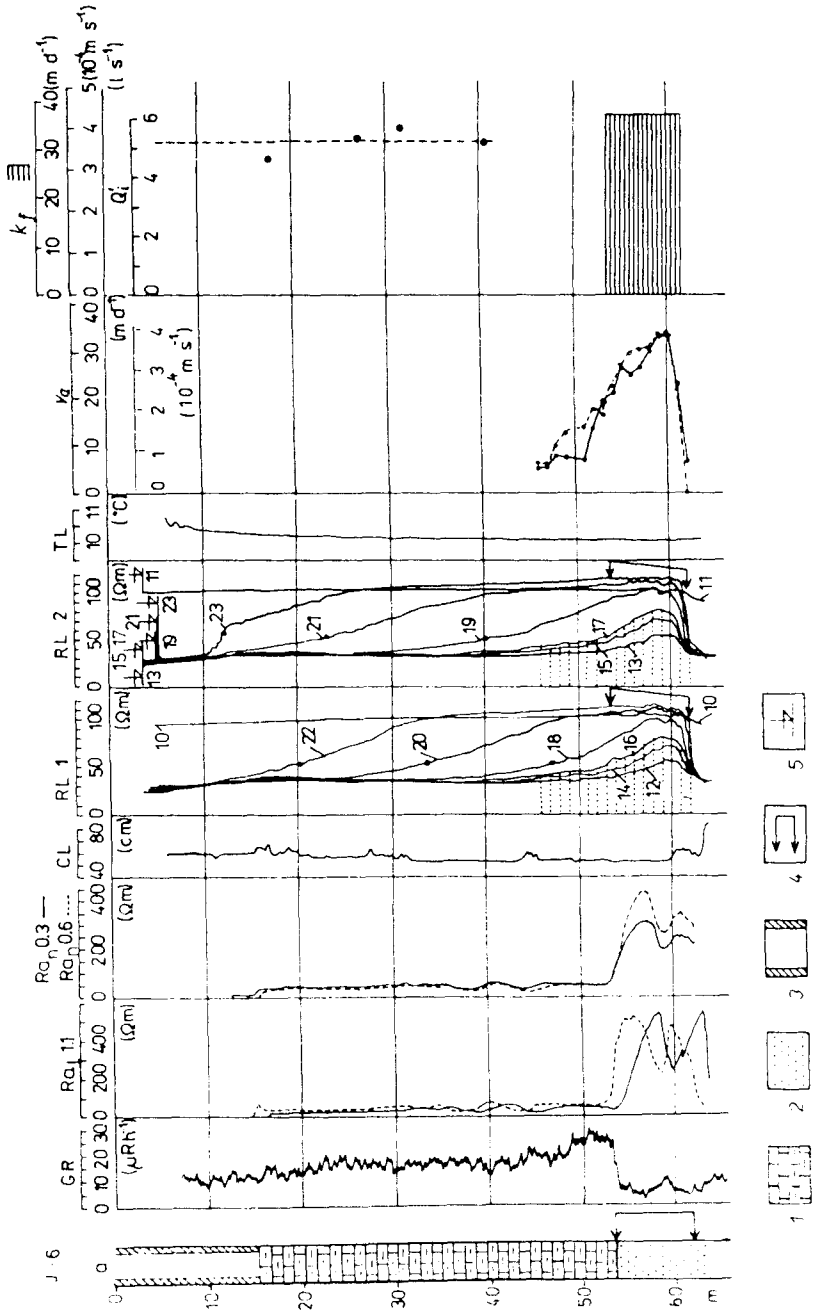

Figure 3.21 Facing page. Determination of hydraulic conductivity, k_f, and filtration velocity, v_a, in borehole J-6 (Jaroměř). GR — gamma-ray log; Ra_1 — resistivity logs measured with lateral probe (upper represented by dashed line, lower by solid line); Ra_n 0.3 and Ra_n 0.6 — resistivity logs measured with normal probes, spacing AM = 0.3 and 0.6 m; CL — caliper log; RL 1 and RL 2 — time series of fluid resistivity logs run down (1) and up (2); records 10 and 11 — under natural conditions; records 12 to 17 — after decreasing the fluid resistivity by the addition of sodium chloride, measured at stabilized water level in the borehole; records 18 to 23 — during pumping from a depth of 12 m, rate of pumping Q = 5 l s^{-1}; TL — temperature log; v_a — graphs of apparent filtration velocity calculated from RL 1 and RL 2 (records 12 to 17); Q_i' — graph of vertical volumetric flow rate calculated from RL 1 and RL 2 (records 18 to 23); k_f — diagram of the hydraulic conductivity. a — lithological section after logging. *1* — siltstones to sandy siltstones; *2* — sandstones; *3* — casing; *4* — inflow interval; *5* — water level in borehole.

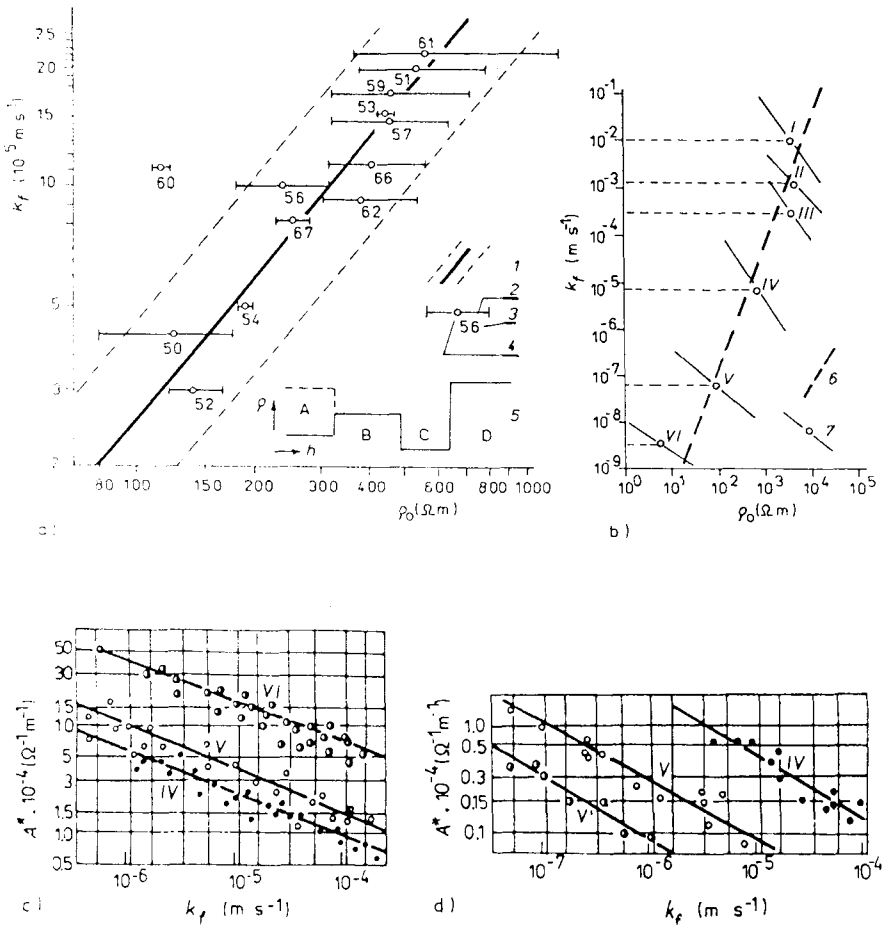

Figure 3.22 Relationships between geophysical and hydraulic parameters of an aquifer. (a) Correlation $k_f = f(\rho_0)$ for Quaternary terrace deposits along the Úhlava River (40 km south of Plzeň, Czechoslovakia), $k_f(10^{-5}$ m s$^{-1}) = 1.026 \times 10^{-2}\ \rho_0^{1.195}$; coefficient of correlation, $r_{k,\rho} = 0.871 \pm 0.070$; coefficient of determination, $D = |r^2_{k,\rho}|\ 100 = 76\%$ (according to Mazáč et al., 1985). (b) Similarly for a common hydrophysical model (according to Mazáč et al., 1985). (c) Relation $A^* = f(k_f)$ for rocks of water-bearing zone (after Sharapanov et al., 1974). (d) Similarly for the aeration zone (after Sharapanov et al., 1974). *1* — regression line ± standard error; 2 — range of extreme resistivities; *3* — number of borehole and VES; *4* — optimum resistivity; *5* — geoelectrical model (A — near-surface layer, dominantly with a lower, exceptionally higher resistivity ρ; B — water-bearing aquifer; C — weathered Palaeozoic complex; D — weakly weathered to unweathered Palaeozoic rocks). *6* — general trend depending on the rock type; *7* — mean values, trend in individual rock types designated. *I* — gravel, *II* — coarse-grained sand, *III* — medium-grained sand, *IV* — fine-grained sand, *V* — sandy-clayey sediments, *VI* — clay.

ground water ρ_w) mainly on clay content and porosity. The permeability of sandy aquifers is also closely related to porosity for clean sands and to clay content for clayey sands. Depending then on the environment, there exist both direct and inverse correlations between aquifer resistivities ρ_0 and hydraulic conductivities k_f, and the same between transverse resistance T and longitudinal conductance S and k_T (Fig. 3.22a, b). These relations depend both on the rock type and on the relation between the direction of ground-water flow, stratification and hydrogeological conditions in the aquifers (Mazáč et al., 1985).

These relations can be expressed in equation form

$$k_f = a\rho_0^{\,b} \quad \text{or} \quad k_f = a\rho_0^{\,\frac{1}{b}} \tag{3.13}$$

respectively, and

$$k_T = aT^b\, m^{(b-1)} \quad \text{or} \quad k_T = aS^b m^{(b-1)} \tag{3.14}$$

respectively, where a and b are regression coefficients obtained by statistical analysis of a set of parametric measurements (ρ_j, k_{fj}) or (T_j, k_{Tj}). The error in the determination of k_f or k_T depends on the statistical quality of the correlations 3.13 and 3.14 (Mazáč et al., 1979a). Induced polarization appears to be a promising method for determination of hydraulic conductivity. The steepness of the discharge curve can be characterized by the gradient α_{IP} (Table 3.1), which is closely related to the grain size of a sandy aquifer and thus to its hydraulic conductivity k_f. Equally good results are obtained by using the relative complex parameter A^* (Table 3.1), which normally correlates closely with the hydraulic conductivity (Fig. 3.22c, d). Under favorable conditions, k_f (or k_T) can be defined with a maximum error of 20 to 30%.

The *protective capacity* (k_n) of an aquitard may be estimated from the results of surface geoelectrical measurements or temperature logging under conditions of a steady thermal regime.

Under suitable conditions, the surface geoelectrical methods make it possible

to correlate the longitudinal conductance S of an aquitard overlying an aquifer with its protective capacity $k_n = f(S^{-1}) = f(t^{-1})$. The delay time t, may be of the following character (Henriet, 1976):

- Purely physical (t may be considered as the transit time for the percolation process)
- Sanitary (t may be correlated with the bacteria die-off curve)
- Remedial (t may be regarded as the time for a pollutant to penetrate from its source at the ground surface to the water table; i.e., the time available for remedial action)

A *map of longitudinal conductance* S_l (Fig. 3.23a) is a basic tool for assessing protective capacity k_n and can be transformed into a map of the hydrogeological parameters k_n or t, or it can be employed for their qualitative definition (Fig. 3.23b).

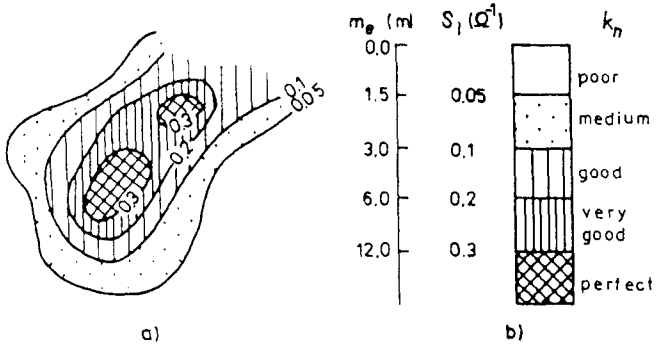

Figure 3.23 Map of longitudinal conductance of an aquitard (a) and its qualitative assessment (b). m_c — thickness of the aquitard (sandy-clayey bed), corresponding longitudinal conductance, S_l, and protective capacity of the aquifer, k_n (modified after Henriet, 1976).

For clastic sediments, there is a marked difference between the thermal conductivity λ of clays and sands (Fig. 2.5). For a constant heat flow the difference causes a change in the temperature gradient on the temperature log $\vartheta = f(h)$; impermeable silty and clayey layers (an aquiclude) show a noticeably

higher temperature gradient G than an aquifer composed of permeable sandstone and conglomerate layers (Fig. 3.24a).

In places the permeability of an aquiclude can be high enough that it should be regarded rather as an aquitard. Permeability increases can be due to an increased sand component or a higher fissure density. Local *changes of temperature gradient* may thus reflect changes in permeability $k_f^{\perp}$ perpendicular to the

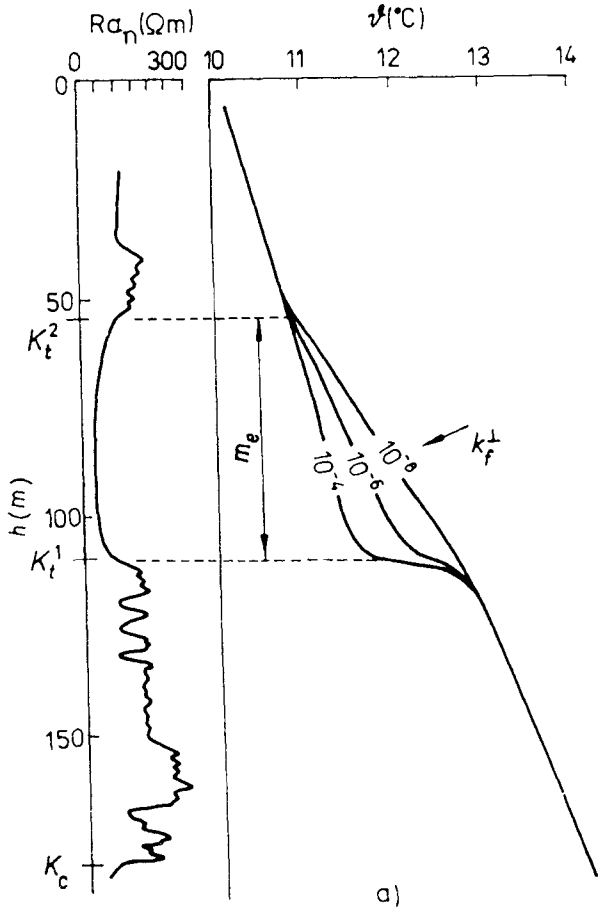

Figure 3.24a Determination of the protective capacity, $k_n = k_f^{\perp}\ m_e^{-1}$, by temperature logging. Temperature logs in a borehole at various coefficients of vertical permeability ($k_f^{\perp}$) of the aquitard — schematic plot of the situation in the Bohemian Cretaceous Basin.

stratification (Fig. 3.24b). Knowing the thickness of the aquitard, we can calculate the protective capacity k_n according to Eq. (2.16).

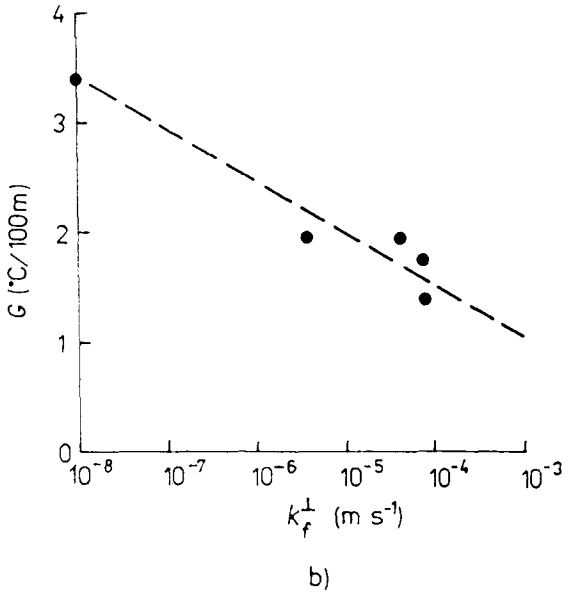

Figure 3.24b Relation of geothermal gradient to the coefficient of permeability $k_f^{\perp}$. K_c — base of the Cretaceous, K_t^1 — base of the lower Turonian in silty development, K_t^2 — base of the middle Turonian in sandstone development, Ra_n — resistivity log obtained by normal probe; m_c — thickness of aquitard.

3.2.5 Depth to Ground Water and the Shape of the Cone of Depression

The physical properties of an aquifer are constant in time, whereas the physical properties of rocks in the zone of aeration vary with time, depending on the instantaneous degree of saturation S_w (Fig. 2.1). Under favorable conditions, *depth to ground water* can be assessed indirectly by surface geophysical methods, and directly by logging (Fig. 3.25).

The accuracy of a depth determination using surface methods (seismics, VES and VES-IP) depends, in general, on the following factors:

- The thickness of the capillary fringe, m_k. Under conditions existing in

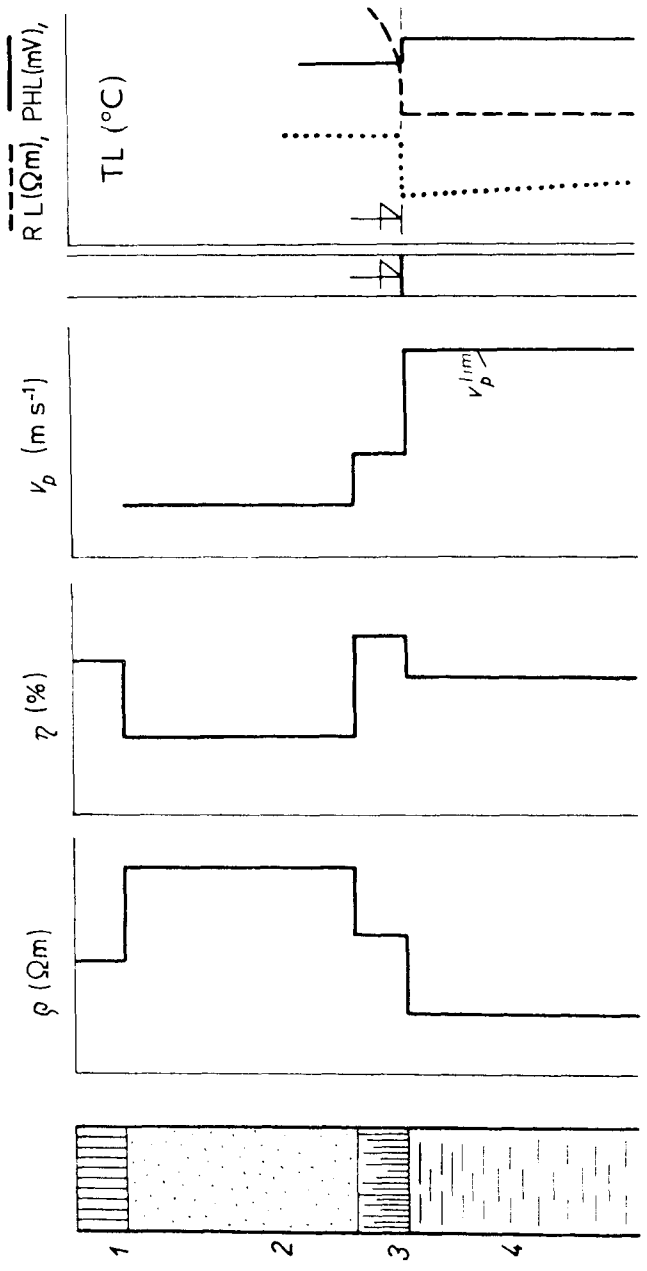

Figure 3.25 Scheme showing the influence of: *1* — the zone of suspended water, *2* — the intermediate zone, *3* — capillary fringe, and *4* — the water-bearing zone, on the resistivity values (ρ) according to VES, polarizability (η) according to VES-IP, velocity of compressional waves (v_p) according to seismic measurements, and the water level in the borehole on the fluid resistivity, RL, photometry, PHL, and temperature logs, TL.

clastic sediments, the thickness can reach 2 m and, extraordinarily, 3 to 4 m. A capillary fringe does not develop in a karst environment (Hynie, 1961).

- The fluctuation of the water table.
- The homogeneity and areal extent of the water-body with respect to depth (a homogeneous water body at a depth smaller than its areal extent provides optimum conditions).
- The regimen of the ground-water body and the thickness of the water-bearing aquifer.

A higher accuracy is attainable with confined ground water, where the level is also a marked petrographical boundary, than with an unconfined aquifer; the accuracy also increases with the thickness of the aquifer. The water table for unconfined water bodies represents a *definite seismic boundary*, which is usually not a lithological boundary. The velocities of compressional v_p and shear v_s waves in the zone of aeration ($S_w = 0$) and in the zone of saturation ($S_w = 1$) were studied by White et al. (1953), Levshin (1961), Berzon et al. (1958) and Biot (1956). The following results may be drawn from these studies (Fig. 3.26):

- Velocity v_p increases gradually with S_w, from 0 to 0.999, but at $S_w > 0.999$, v_p increases abruptly by 50 to 200%, depending on the depth of the water table H_z and porosity P.
- For this reason, seismic methods provide the most accurate estimates of the depth to the water table, particularly in unconsolidated sediments with interstitial permeability (Fig. 3.26a).

Figure 3.26 Facing page. Determination of the water table depth using seismic methods in a model medium (according to Lavshin, 1961). (a) Dependence of the threshold velocity (v_p^{lim}) for the zone of saturation $S_w = 1$, parameters $n = v_p/v_p^{lim}$, $1/m = v_s^{lim}/v_s$, and of the accuracy of depth determination of the water table (ΔH_z) on the depth of the water table (H_z (m)) with parameters of the rock medium $E_d = 10^5$ MPa, $\beta_{ma} = 1.05 \times 10^5$ MPa, $\mu = 0.15$, $\sigma = 2650$ kg m^{-3}, $P = 0.476$ and parameters of the ground water $\beta_w = 2.15 \times 10^3$ MPa, $\sigma_w = 1000$ kg m^{-3}; v_p, v_s, v_p^{lim} and v_s^{lim} are velocities of compressional and shear waves in the zone of aeration, ($S_w = 0$) and in the zone of saturation, respectively. (b) Theoretical model of the porous medium (cubic arrangement of ideal elastic spheres) with a porosity $P = 47.6\%$.

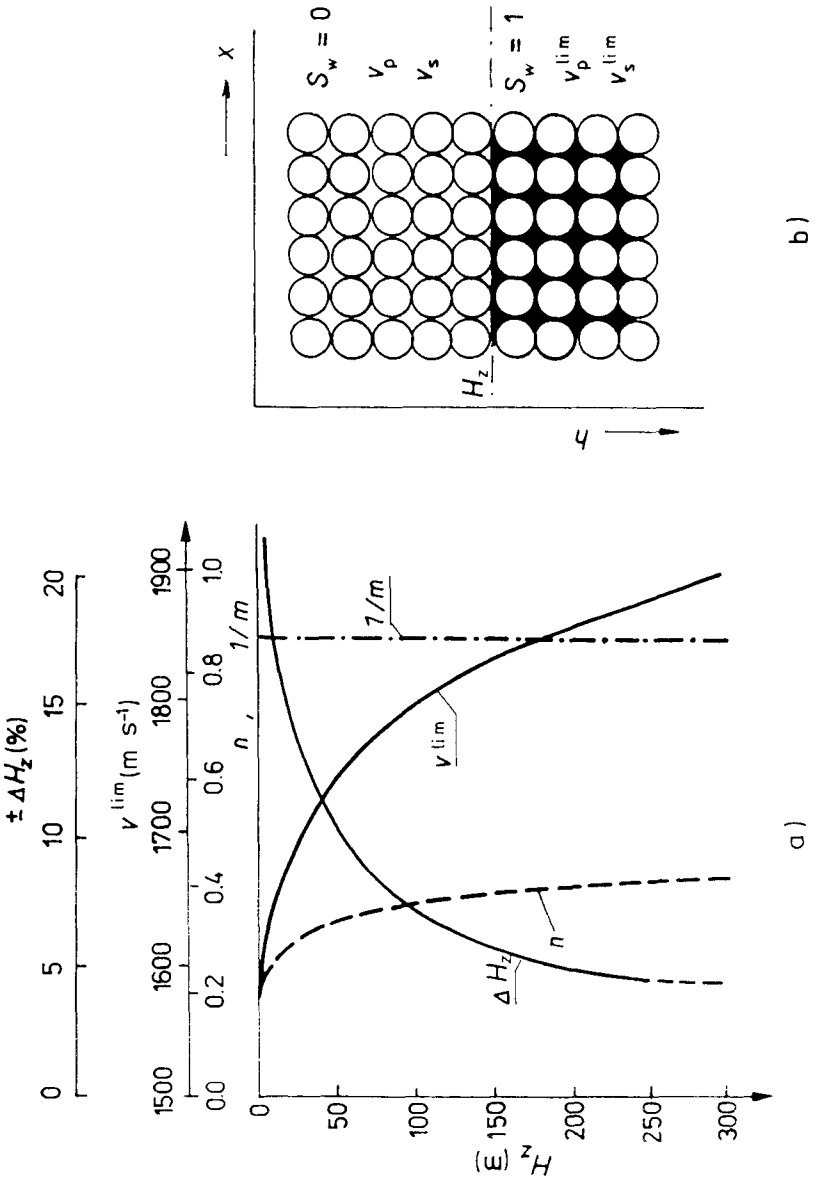

Determination of the water table in consolidated sediments and crystalline rocks is more difficult and less accurate. In any case, it is desirable that the thickness of the aquifer exceeds its depth below the surface. It is usually observed that

- The velocity v_s changes only slightly with changes in S_w and the $1/m$ ratio for limiting saturations (0 and 1) reaches 0.862.
- The velocity v_p in the zone of saturation invariably exceeds the velocity of sound in water (1470 m s^{-1}) and changes gradually with an increase in the depth of the water table H_z.
- Seismic properties of real media differ from those of the theoretical models of a sandy medium. Also, the presence of clay usually decreases v_p.

Application of vertical electric sounding in the resistivity variant is based on the difference in resistivities between the zone of aeration and the zone of saturation. Since even small changes in moisture content or degree of saturation S_w cause large changes in medium resistivity (Table 2.3; see also Keller and Frischknecht, 1966), the boundary established by this method will actually correspond to the upper boundary of the capillary fringe. The accuracy of determination of the depth to the water table by VES is thus, in general, smaller ($\Delta H = 20\%$) than the accuracy attained using refraction seismics (Janík et al. in Sbornik, 1976).

The use of *induced polarization* (IP) is based on the relation of the IP parameters to moisture content and the structure of aquifers. To attain a more reliable determination of the depth to the water table in sandy-clayey soils it is advisable to combine vertical electrical sounding in the resistivity and IP variants (Fig. 3.27).

In applying logging methods in boreholes tapping unconfined aquifers, the fluid resistivity RL, photometer PHL and temperature logs TL provide data on the depth to the water table with an accuracy of 0.1 m (Fig. 3.25).

Assessment of the *shape of a cone of depression* with observation wells is

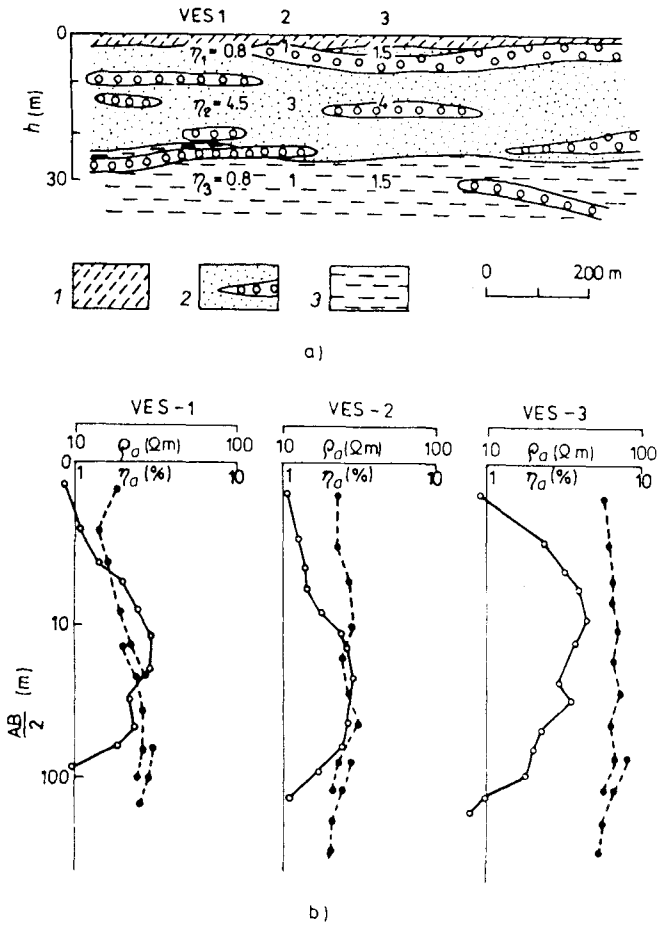

Figure 3.27 Assessment of water-bearing clayey sand deposits in the Sauk-su River Valley (according to Kuzmin and Ogilvi, 1965). (a) Geological section. (b) VES resistivity curves (dashed line), VES-IP curves (solid line). *1* — dry loam, thickness m = 1 to 2 m, η_1 = 0.8 to 1.5%; *2* — water-bearing, clayey sand deposits, m = 18 to 20 m, η_2 = 3 to 5%; *3* — bedrock, Mesozoic aleurites, $\eta_3 \approx 1\%$.

expensive and, as a consequence, not always very detailed. It is, therefore, advantageous to use geophysical methods; i.e., the methods just discussed or the method of spontaneous polarization.

When water (i.e., a weak electrolyte) flows through a porous medium, bonding of one type of ions (usually negative) in the diffuse layer produces a

surplus of negative charge where water enters a porous medium and, in contrast, a surplus of positive charge where it discharges (Fig. 3.28). This physico-chemical process produces filtration potentials V_f; that is, pronounced positive SP anomalies over the pumped well. The area under the SP curve on a measured profile is then directly proportional to the drawdown curve (Fig. 3.29).

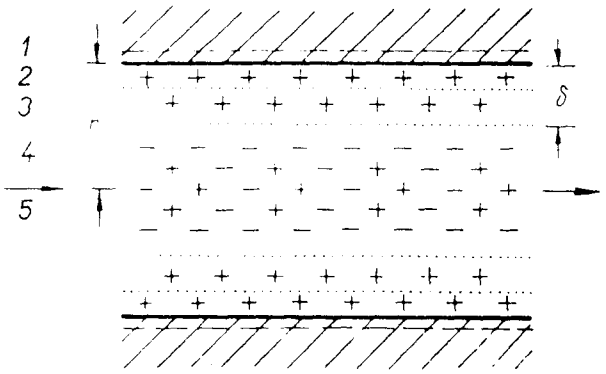

Figure 3.28 Development of filtration potentials in a porous medium. Scheme of electrical double layer on the wall of a pore channel with flowing water. *1* — wall of the pore channel with a negative surface charge, *2* — immobile ions of the Helmholtz layer, *3* — mobile ions of the diffuse layer, *4* — free pore solution, *5* — direction of free pore solution flow. r — radius of pore channel, δ — total thickness of the Helmholtz and diffuse layers.

3.2.6 Dissolved Solids Content in Ground Water

Resistivity ρ_w is closely related to the concentration of *total dissolved solids* in ground water C (g l^{-1}) (Table 2.1). Ground-water resistivity may be estimated primarily by geophysical logging and in suitable cases, also by surface resistivity methods. The more commonly used *logging* evaluation procedures are as follows:

- Calculation of ρ_w from the self potential anomaly SSP opposite a layer of well-sorted clean sand (without a clay component) according to

$$\rho_w = \rho_{mf} \exp\left[\frac{-SSP}{.434K_{dm}}\right] \qquad (3.15)$$

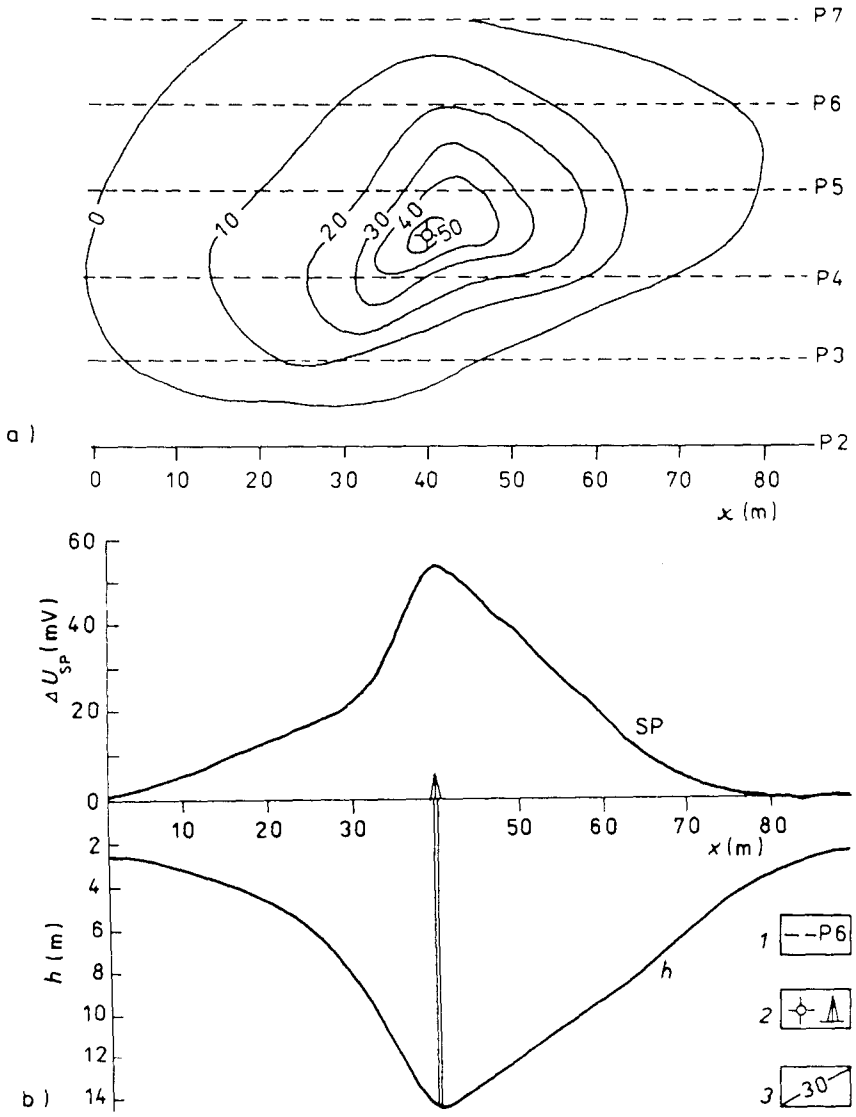

Figure 3.29 Determination of cone of depression's shape in glaciofluvial deposits, in the area of St. Petersburg, Russia, by the SP method and shallow refraction seismics. (a) Difference. ΔU (mV), in the SP field as measured before pumping and at the end of the pumping test. (b) Residual SP curve and depth h(m) of the water table established by refraction seismics along a line through the borehole location between profiles P4 and P5. *1* — location of profiles, *2* — borehole location, *3* — isoanomaly (mV).

where K_{dm} is the coefficient of electrochemical potential which depends on the temperature and chemistry of the ground water, and ρ_{mf} is the resistivity of the mud filtrate.

- If the chemistry of the ground water is known, the relation (3.15) for the known SSP (mV) and ρ_{mf} (Ω m) is solved numerically or by using a nomogram (Fig. 3.30). This procedure provides good results in sandy-clayey sediments with a high dissolved solid content in the ground water ($\rho_w < 1.0\ \Omega$ m, $C > 8$ g l^{-1}).
- From repeated SP records with two different resistivities of mud filtrate (ρ_{mf1}, ρ_{mf2}). The SP1 and SP2 anomalies opposite a sandy layer will,

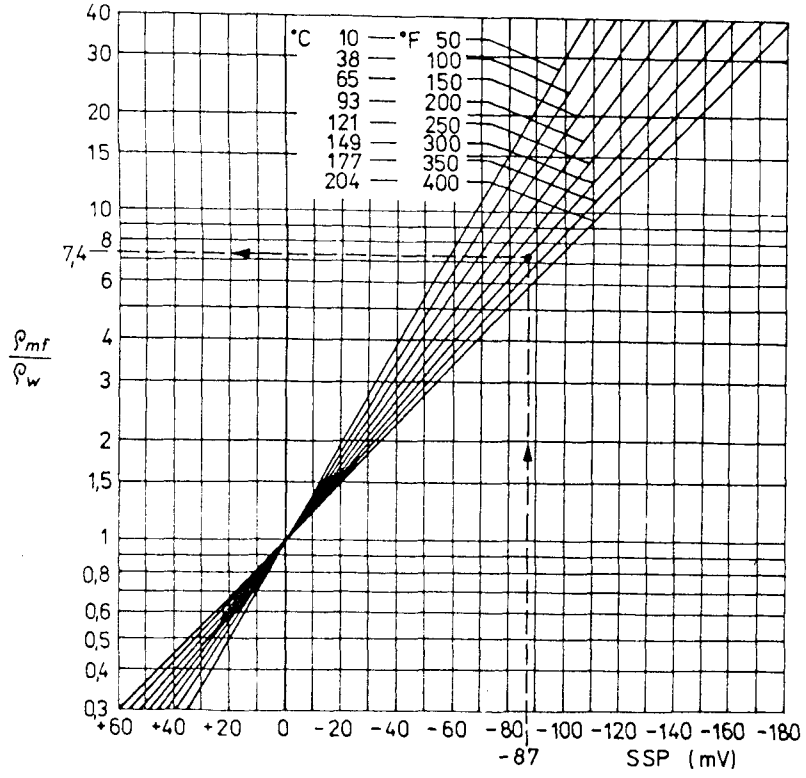

Figure 3.30 Nomogram for determination of the ρ_{mf}/ρ_w ratio, with a known static self potential anomaly SSP (mV) at temperature ϑ (°C) (according to Schlumberger, 1972 b).

combined with ρ_{mf1} and ρ_{mf2}, formally satisfy Eq. (3.15) and permit both ρ_w and K_{dm} to be calculated or graphically determined for $\rho_w = \lim \rho_{mf}$ as SP approaches 0 (Fig. 3.31a).

- Using automatic log processing and cross-plots SP - log (ρ_{xo}/ρ_t) or GR - log (ρ_{xo}/ρ_t), it is possible to establish the ρ_{xo}/ρ_t values corresponding to the minimum SP or GR values; i.e., to find clean sandy layers. For these it holds that

$$\frac{\rho_{xo}}{\rho_o} = \frac{\rho_{mf}}{\rho_w} = \text{constant} \rightarrow \rho_w = \frac{\rho_{mf}}{\text{constant}} \qquad (3.16)$$

This procedure (Fig. 3.31b) requires a combination of micro- and macro-resistivity measurements in a borehole; the micro- to determine the resistivity ρ_{xo} of the flushed zone (i.e., of the part of the aquifer at the borehole wall saturated by mud filtrate with resistivity ρ_{mf}), and the macro- to determine the resistivity ρ_o of the aquifer saturated with ground water with resistivity ρ_w.

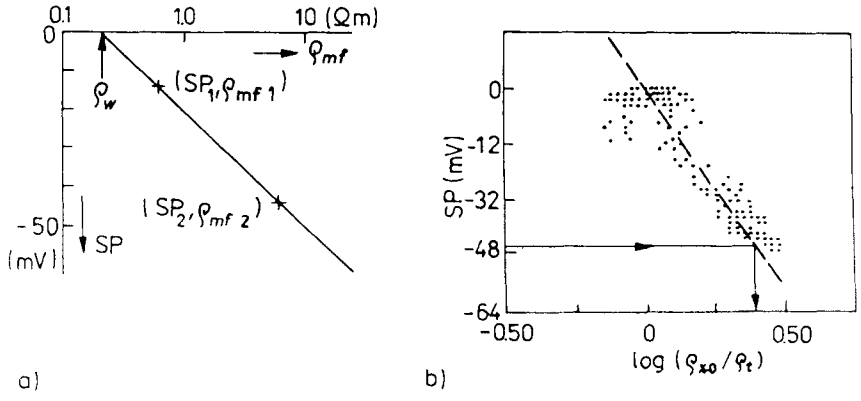

Figure 3.31 New methods of ground-water resistivity (ρ_w) determination from SP records. (a) Graphic method, when two pairs of values, (SP_1, $\rho_{mf\,1}$) and (SP_2, $\rho_{mf\,2}$), are known. (b) Determination of ρ_w using cross-plot of SP - log (ρ_{xo}/ρ_t); log (ρ_{xo}/ρ_t) = 0.4 $\Rightarrow$ ρ_{xo}/ρ_t = 2.5 for SSP = -46 mV and ρ_{mf} = 0.3 Ω m; ρ_w = 0.3/2.5 = 0.12 Ω m (schematicized according to Schlumberger, 1974).

- From resistivity measurements, using relation (2.20) or (2.21), which are to a certain degree equivalent. At first sight it is obvious that the most appropriate conditions for determination of ρ_w are where the ground water occurs in a clean clay-free, completely saturated aquifer ($S_w = 1$; $V_{sh} = 0$). In such cases, ρ_0 and ρ_w are directly proportional; i.e., $\rho_w = F^{-1}\rho_0$, the formation factor being a constant for the aquifer examined. Unless this condition is fulfilled, a correction for clay content must be introduced, using a shale indicator (Section 3.2.1).

Surface geophysical methods suitable for determination of total dissolved solids contents C (or ρ_w) are the resistivity and induced polarization methods. The determination of ρ_w on the basis of resistivity measurements is essentially identical with the procedure used with resistivity logging. In some cases, total dissolved solids C (g l^{-1}) have in practice been successfully established from VES records; in most cases, it has been accomplished in ground water saturating clean aquifers (Fig. 3.32). In such cases the error in determination is relatively small ($\Delta C < 50\%$) because the change $\Delta\rho$ produced by the maximum feasible difference in the aquifer porosity ($\Delta P_{max} = 30\%$) is less than the change caused by the maximum possible difference in the total dissolved solids content of the ground water (ΔC_{max} = 3 to 4 orders of magnitude). The induced polarization parameters A^* and η are less frequently used for the determination of C (Sharapanov et al., 1974).

3.2.7 Filtration Velocity, Ground-Water Velocity, and Direction of Ground-Water Flow

A test well provides the most suitable conditions for establishing the *filtration velocity* v_f by geophysical methods. Geophysical logging uses the *dilution technique*; the principle of this method was recognized some forty years ago (Grinbaum, 1965; Moser, Neumaier, 1957; Moser et al., 1957; Ogilvi and Fedorovich, 1964). In the interval to be tested, an tracer is introduced into the borehole and changes in concentration with time are observed. Sodium and

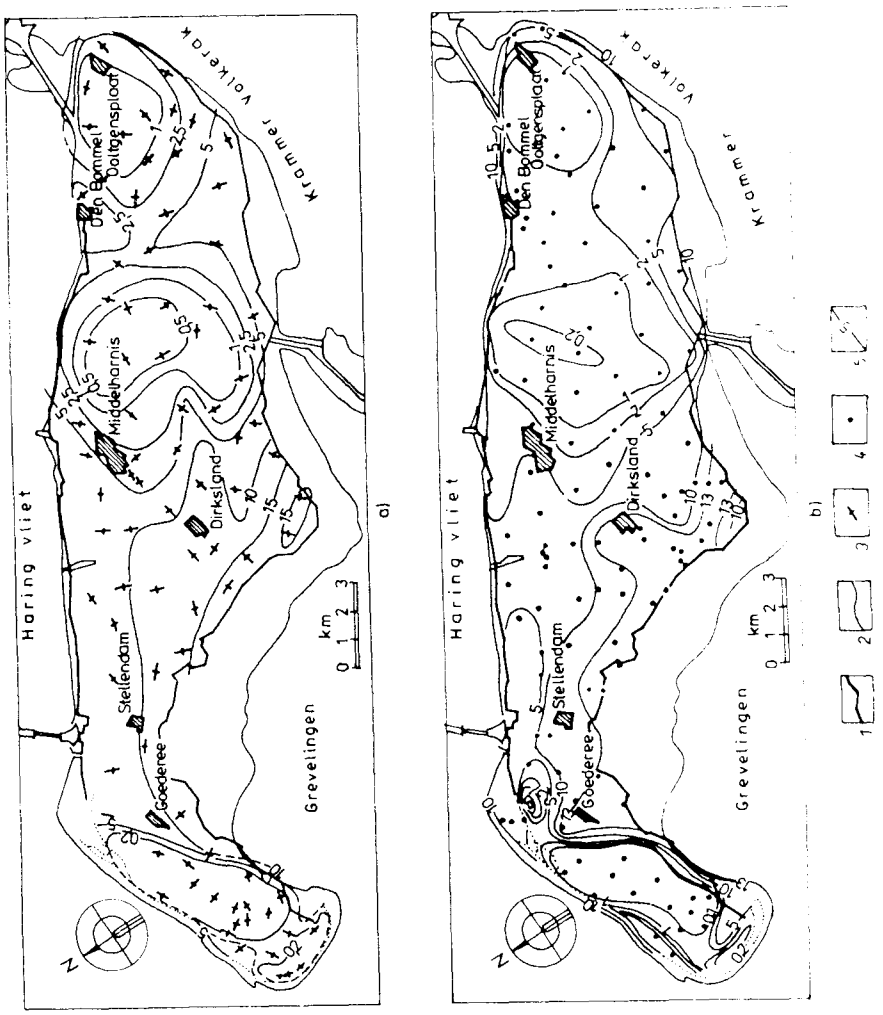

Figure 3.32 Comparison of data on total dissolved solids content C (g l^{-1}), in Pleistocene sands of Goeree Island, where the Rhine discharges to the North Sea, as obtained from 80 VES (a) and water samples from 140 observation boreholes (b) (after Walter, 1969). *1* — outline of the island, *2* — average ebb-tide line, *3* — locations of VES and direction of electrode array, *4* — locations of observation boreholes, *5* — isoline of total dissolved solids content C (g l^{-1}).

potassium chloride, organic dyes and open radioactive tracers are used as indicators (Drost et al., 1968, 1972; Drost, 1971; Halevy et al., 1967; Islam et al., 1969; Moser and Neumaier, 1958; Hulla et al., 1983). The filtration velocity is estimated from the change in concentration of the indicator. All relations may in essence be reduced to

$$v_a = 3.62 \frac{r}{t} \log \left[\frac{(C_t - C_o)}{(C_1 - C_o)} \right] \qquad (3.17)$$

where v_a is the apparent filtration velocity within the tested interval, usually about 1 m range (m s^{-1}); r is the borehole radius (m); and C_o, C_1, C_t are the concentrations of the tracer (indicator) in the ground water, immediately after introduction and at time t, expressed in normal units (g l^{-1}, mg l^{-1}, Bq m^{-3}).

To convert apparent filtration velocity v_a to true velocity v_f we need to know the correction factor α, the value of which depends on properties of the well casing and the hydraulic properties of the filter and the surrounding aquifer. Field techniques and the evaluation of measured values are described in detail in the literature (Grinbaum, 1965; Halevy et al., 1967; Mareš, 1976). An example of the determination of apparent filtration velocity in an uncased borehole is shown in Figure 3.21.

Ground-water velocity $v_{\Delta x}$ and the *direction* α_f *of flow* are usually determined by the *mise-a-la-masse method* (MAM). The hydrogeological variant of this method (Matveev, 1963; Gruntorád and Karous, 1972) is based on the introduction of an electrolyte into an aquifer through a borehole (Fig. 3.33 and 3.34) which creates a conductive body, the dimensions of which increase in the direction of the ground-water flow. The flow velocity is inferred from time changes of the velocity parameters v_g of the geoelectrical field (usually from the velocity displacement of equipotential lines) measured at the ground surface (Fig. 3.33b), and the flow direction from the elliptical shape of equipotential lines (see also Figs. 4.16, 4.17, 4.24).

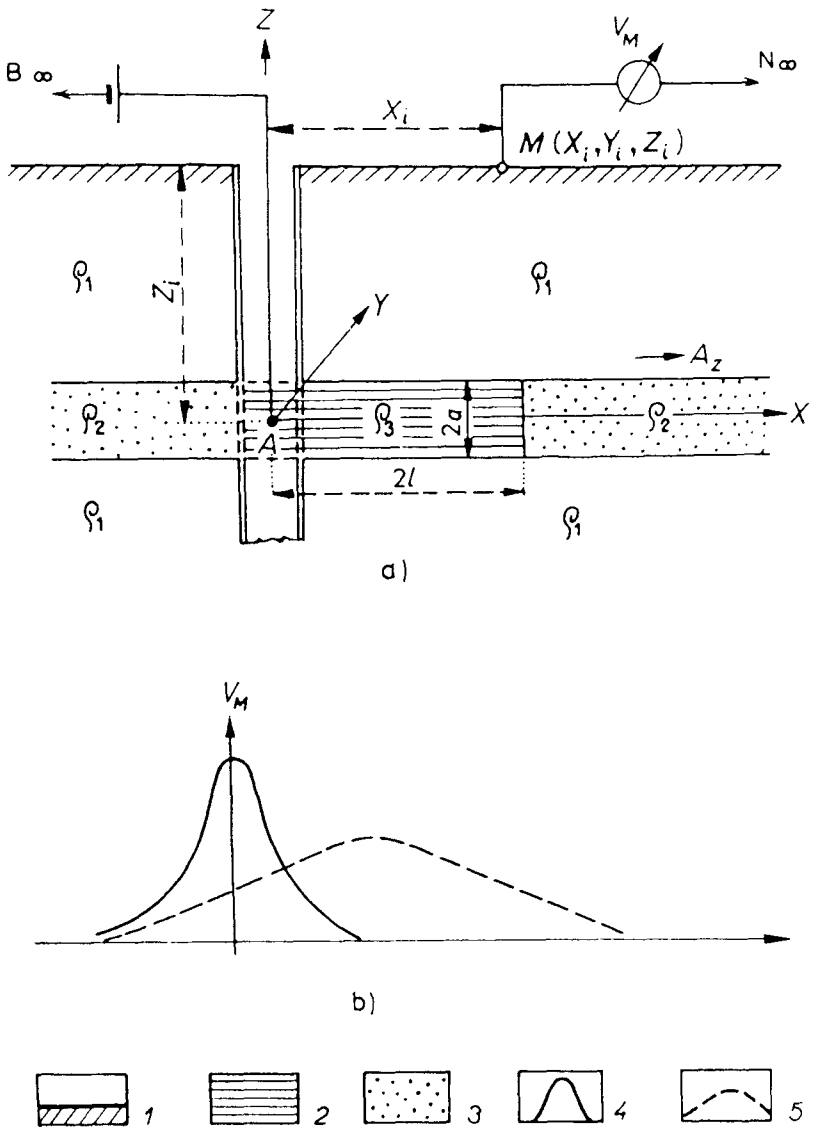

Figure 3.33 Principle of the hydrogeological variant of the mise-a-la-masse method (a) and the potential curves (b) (according to Gruntorád and Karous, 1972). *1* — ground surface, *2* — charged part of water-bearing aquifer supplied with NaCl, *3* — water-bearing aquifer, *4* — potential curve before NaCl introduction, *5* — potential curve after NaCl introduced.

The velocity parameter v_g can be converted to the velocity of ground-water flow $v_{\Delta x}$ using the relation $v_{\Delta x} = k\, v_g$, where the reduction coefficient k corrects for the difference between field conditions and the theoretical model (Mazáč et al., 1978).

The depth range and the accuracy of the method are characterized by the relative mean error $\Delta v_{\Delta x}$ (Fig. 3.34). To attain maximum accuracy at minimum expense, it is recommended that the MAM method be combined with VES or resistivity logging for the determination of ρ_1 and ρ_2, and with the dilution method to assess the filtration velocity.

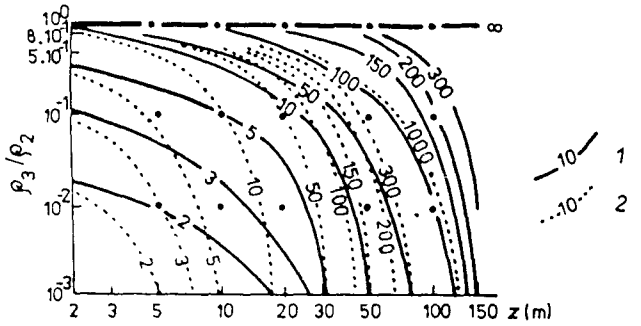

Figure 3.34 Relation $\Delta v_{\Delta x} = f(\rho_3/\rho_2, z)$ for a = 1 m, $\rho_1 I$ = 10 Ω m A (after Mazáč et al., 1978). *1* — isolines $\Delta v_{\Delta x}$ (%) $= f(\rho_3/\rho_2, z)$, with resolving power of measurements 10^{-1} mV; *2* — similarly with the resolving power of the measurement 10^{-2} mV.

The velocity and direction of ground-water flow in karst areas can be determined by a *special seismic method* (Arandelovich, 1969). A timed charge is introduced into the water-bearing karst structure through a natural sinkhole or a borehole. The explosion at a precisely determined moment causes seismic waves, which are detected by geophones and recorded by a signal recorder at the surface (Fig. 3.35), making it possible to estimate the coordinates of the hypocenter and epicenter of the explosion. By using charges with different time intervals of explosion, the further path may be traced over a rather long distance.

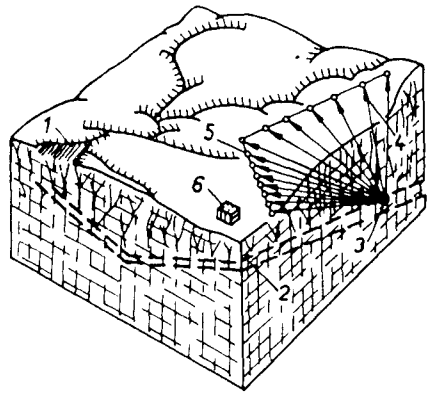

Figure 3.35 Scheme showing measurement of ground-water flow in karst areas, using seismic methods (according to Arandelovich, 1969). *1* — sinkhole, *2* — communication path of ground water (system of karst cavities), *3* — site of timed charge explosion, *4* — beam of seismic waves, *5* — geophones, *6* — seismic recorder.

Direction of ground-water flow at shallow depths may be determined by measuring the *filtration potential* under normal conditions; the fact that the potential increases in the direction of ground-water flow is also exploited. In practice, this phenomenon is of use only in a medium with a high hydraulic gradient saturated with a highly resistive ground water. The field survey is made on a square grid, or more simply, on a circle; the flow direction is perpendicular to the equipotential lines (Fig. 3.36).

Logging methods offer several procedures for establishing the direction of ground-water flow. Radiometric methods employ an open radioactive tracer, usually NaI^{131} or, better still, a colloid containing the radioisotope Au^{198}. A calculated amount of the radioisotope is introduced into the test interval through which flow across the borehole was observed (for example, by the dilution method). During a time interval, $t = 3.26\, d/v_f$, about 99% of the radioisotope is removed by seepage. The major part of it is absorbed unevenly on the borehole wall or casing filter, the greater part of it in the direction of the flow and the least in the opposite direction. Assessment of the direction of ground-water

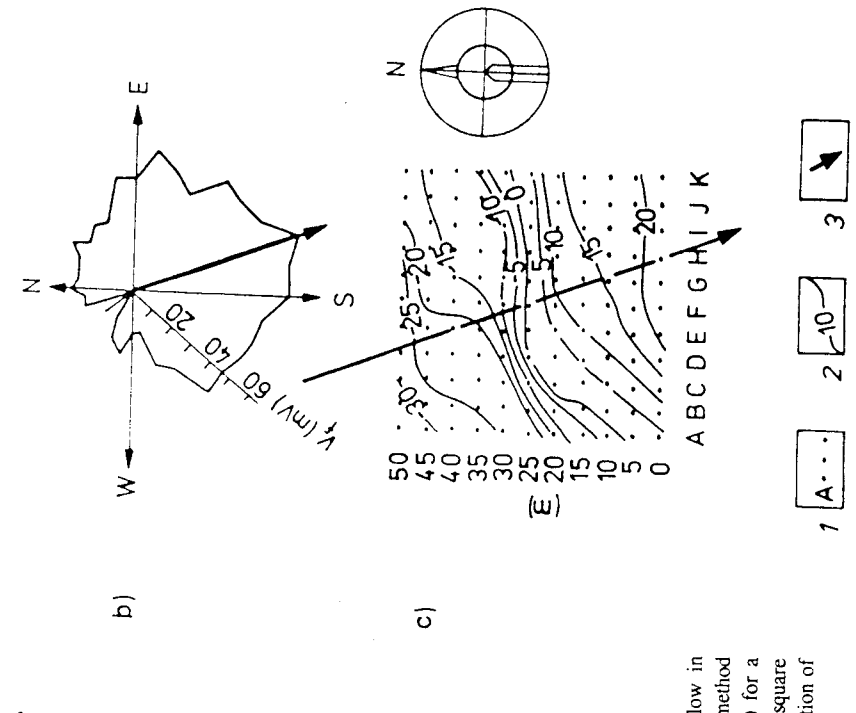

Figure 3.36 Determination of the direction of ground-water flow in Quaternary sediments of the Elbe (Czechoslovakia) by the SP method (according to Kolinger, in Sbornik, 1975). (a) Graph $V_f = f(A_z)$ for a circle of radius $R = 20$ m. (b) Polar diagram V_f. (c) Field v_f on a square grid. *1* — profiles and points measured, *2* — isolines V_f, *3* — direction of ground-water flow.

flow requires the exposure rate $\dot{X}$ to be analyzed directionally. For this purpose a radiographic probe (Niemczynowicz and Fraczek, 1967) or a logging radiometer is employed; the detector for the radiometer is contained in a lead shield with a revolving vertical slit controllable from the surface. The character of the record can be seen in Figure 3.37.

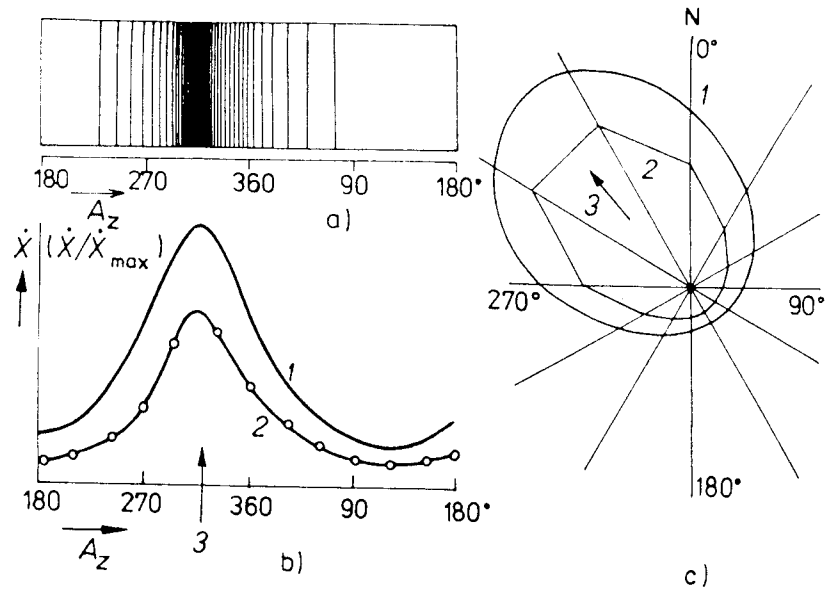

Figure 3.37 Direction of ground-water flow assessed by radiometric methods. (a) Schematic of radiographic probe record. (b) Graphs showing the relation between exposure rate and azimuth A_z. (c) Results plotted in the plane perpendicular to the borehole axis. *1* — according to radiographic probe, *2* — according to radiometer with a slit in revolving lead shielding, *3* — direction of flow.

Electromagnetic velocity meters for measuring flow velocities in estuaries, rivers, and pipelines (Cushing, 1973) can also be used in boreholes. If meters are equipped with two sensors, it is possible to determine the velocity and the direction of flow as the vector sum of two perpendicular components. To establish the orientation of a four-electrode system in the magnetic field of the coil relative to geographic North, a gyroscopic direction meter can be used.

Garkalenko et al. (1971) described an apparatus with a vessel containing dye, located in the center of a horizontal slit. Under the slit there is a magnetic needle in a hermetically sealed box lighted by two filament lamps. The objective of a camera operated from the surface is to photograph the dye trace, which extends from the vessel in the direction of ground-water flow, together with the position of the magnetic needle (Fig. 3.38).

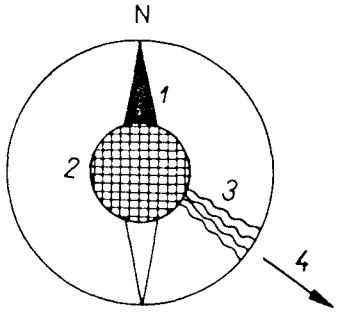

Figure 3.38 Character of the photograph of a dye trace and magnetic needle (according to Garkalenko, 1971). *1* — magnetic needle, *2* — tank with dye and gauze strainer, *3* — trace of dye in the plane perpendicular to the borehole axis, *4* — direction of flow.

3.2.8 Migration Parameters

Migration of a pollutant or tracer in ground water is governed by the characteristics of the rock medium and the ground-water flow. One-dimensional transport in a uniform flow field is defined by the one-dimensional convective-dispersion equation (Ogata, 1970):

$$D_L \frac{\partial^2 C_a}{\partial x^2} - v_x \frac{\partial C_a}{\partial x} = \frac{\partial C_a}{\partial t} \qquad (3.18)$$

where D_L is the coefficient of longitudinal dispersion, v_x the average pore-water velocity in the x-direction and C_a is the concentration of the solute a.

The essence of tests used in determination of the *migration parameters* (D_L, v_x or C_a) consists in supplying a tracer to the ground water through a borehole

and tracing C_a and changes in C_a with time t and distance (x, y); i.e., C_a viz. $\Delta C_a = f(t, x, y)$. The migration or transport parameters are determined from these data (Bachmat et al., 1988; Davis et al., 1980; Drost, 1989; Fried, 1975).

The geophysical methods that have the best likelihood of providing the required data are those which allow direct observation of tracer concentrations in the field (resistivity measurements for electrolytic indicators, photometry for organic dyes, radiometry for radioisotopes, thermometry for temperature changes) and the mise-a-la-masse method for determination of the flow velocity $v_{\Delta x}$, the direction of flow and the geometric form of the plume representing the tracer. The MAM method can also be used for checking the orientation of the injection and observation boreholes in order to ensure that they are properly located to record the changes in tracer concentration.

There are known cases where sudden leakages of pollutants approximate the conditions of a tracer test and thus their evaluation allows the migration parameters to be calculated. As such leaks or systematic pollution usually affect relatively large areas, it is possible to employ the customary surface geophysical methods to assess the changes in chemistry of the ground water (VES method, electrical profiling, etc.), the increased temperature of ground water (thermometry) or increases in the concentration of radioactive substances (radiometry), etc. In many instances the geophysical methods (for example, some tracer tests) become irreplaceable for determining migration parameters, because they provide a type of information about the process that cannot be obtained by any other method. The application of surface geophysical methods to determine plume geometry and concentrations is restricted to porous media and to aquifers occurring within a few meters of the ground surface.

Chapter 4

Methods, Techniques and Organization of Geophysical Surveys in Hydrogeological Studies

The selection of a geophysical method, its application in the field, and the evaluation and presentation of the results depend mainly on the purpose of the hydrogeological survey and the character of the hydrogeological structure being investigated. The distinctions which arise from these assumptions will be defined and differentiated in this chapter.

4.1 Regional and Detailed Hydrogeological Surveys

All geophysical methods, albeit to a different degree, are applicable in hydrogeological surveys. Statistical analyses of geophysical activities show that the geoelectrical methods are the most widely used followed by logging; seismic, geothermal (or geothermic) methods, gravimetry, magnetometry and radiometry are less frequently used. Recently, special aerial methods (e.g., remote sensing) have been introduced and their use is increasing.

Various combinations of geophysical methods are employed in surveys depending on the geological environment. In principle, the following environments can be distinguished:

1. Shallow hydrogeological structures
2. Deltas of large rivers and littoral areas, coastal zones, and islands
3. Sedimentary basins and consolidated sediments
4. Areas of neovolcanics
5. Crystalline areas
6. Karst areas

4.1.1 Shallow Hydrogeological Structures

Shallow hydrogeological structures typically involve young sedimentary complexes formed mostly of unconsolidated sediments. Despite their minor areal extent, they are of major importance because of their hydrogeological properties, including high permeability, high well yields, and recharge properties which are favorable for ground-water development. Ground water at shallow depths and ease of drilling contribute to easy development at reasonable cost. Lithologically, they consist of clays, silts, sands, and gravels of various grain sizes and degrees of sorting.

The physical properties of these sediments are favorable for geophysical exploration. Washed coarse-grained sediments have high resistivities and thus, if they differ in resistivity from surrounding layers mainly from the bedrock, their spatial extent can easily be delimited by electrical resistivity methods in both the profiling and sounding variants.

Clays, and fine-grained sandstones with substantial clay contents have lower resistivities so that the discrimination between clay and sand, or sand and gravel by geoelectrical methods is usually nearly unequivocal. Differentiation of rocks showing small contrasts in resistivity is facilitated by differences in polarizability which is assessed by induced polarization measurements.

In unconsolidated sediments, seismic waves propagate at much lower velocities than in solid underlying rocks, and therefore the thickness of alluvial or other Quaternary sediments can be determined as a depth to a refracting seismic boundary. The method known as shallow refraction seismics and the use of light-weight portable seismic equipment have often proved successful.

Microgravimetry, which uses the differences in density between unconsolidated sediments and underlying bedrock or between disturbed and undisturbed bedrock, is sometimes employed. Where the bedrock is homogeneous and made up of magnetic rocks, magnetic surveys are suitable.

Most data on *depth to bedrock* and *aquifer thickness* is provided by *vertical electrical soundings*. An example of the interpretation of VES curves over

Holocene deposits is illustrated in Fig. 4.1. Quantitative determination of the depths of boundaries between individual rock types requires a complete interpretation of all curves and a good knowledge of the geological setting. Layer

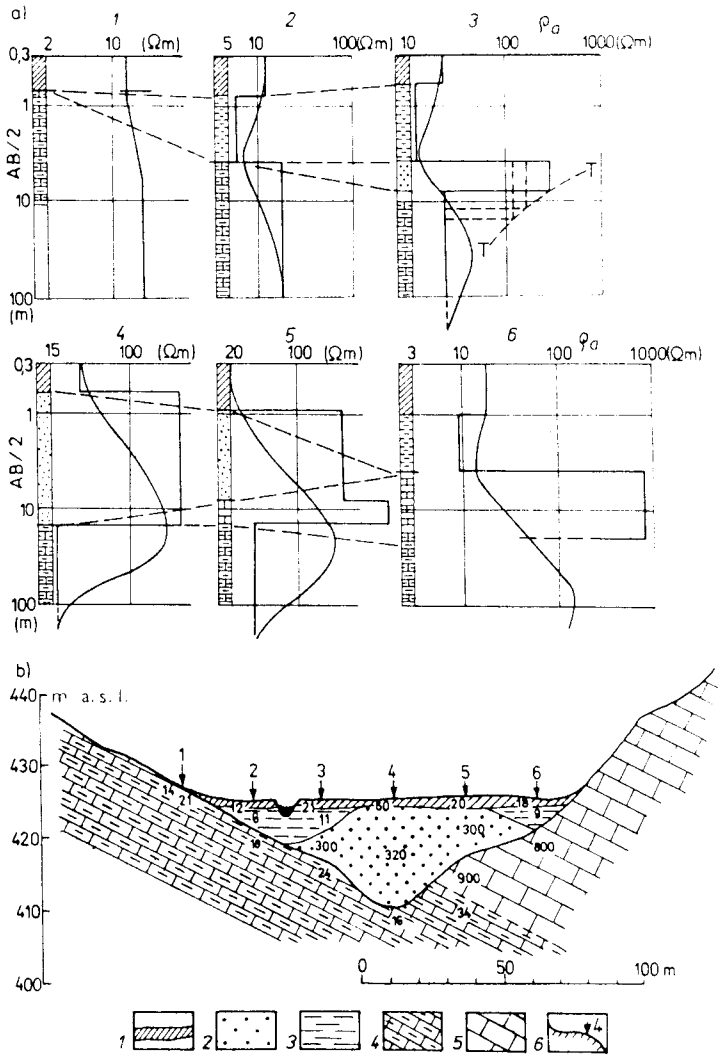

Figure 4.1 Soundings over Holocene alluvial deposits: (a) VES curves (b) cross section through the alluvial sediments. *1* — loam; *2* — sand, and gravel and sand; *3* — clay; *4* — calcareous siltstone; *5* — limestone; *6* — location of VES.

resistivities are determined from soundings in locations of maximum layer thicknesses.

The VES method makes economical and rapid mapping of wadi sediments possible which is a common assignment for hydrogeological surveys in arid regions. Figure 4.2 shows an example of a VES at a location near Markhah in Yemen, at the edge of the Rub-Al-Chali desert. In order to obtain a reasonable interpretation of the VES curves, and to constrain the influence of equivalence on the thickness interpretation, a constant resistivity of 12 Ω m was assigned to the basal conductive layer (conglomerates saturated with highly mineralized water). This value was determined by interpretation of VES curves near boreholes and lateral electrical sounding (LES) curves.

In sands and gravels of a constant resistivity with an appropriate resistivity contrast to the surrounding layers, the areal extent of the unconsolidated sediments can be mapped by *resistivity profiling* at an optimum electrode spacing (Fig. 4.3). Where the bedrock resistivity is fairly uniform, the method of *double profiling* using two current electrode spacings (Karous, 1977) can be used to economically determine sediment thicknesses.

In investigations of unconsolidated sediments at shallow depths, resistivity methods can be combined with shallow *hammer refraction seismics*. In this way the depth of the boundary between the unconsolidated sediments and underlying solid rock can be established simultaneously with an estimate of the degree of weathering of the bedrock.

Figure 4.4 is an example of interpreted seismic measurements. The survey made it possible to establish not only the boundary between the overburden

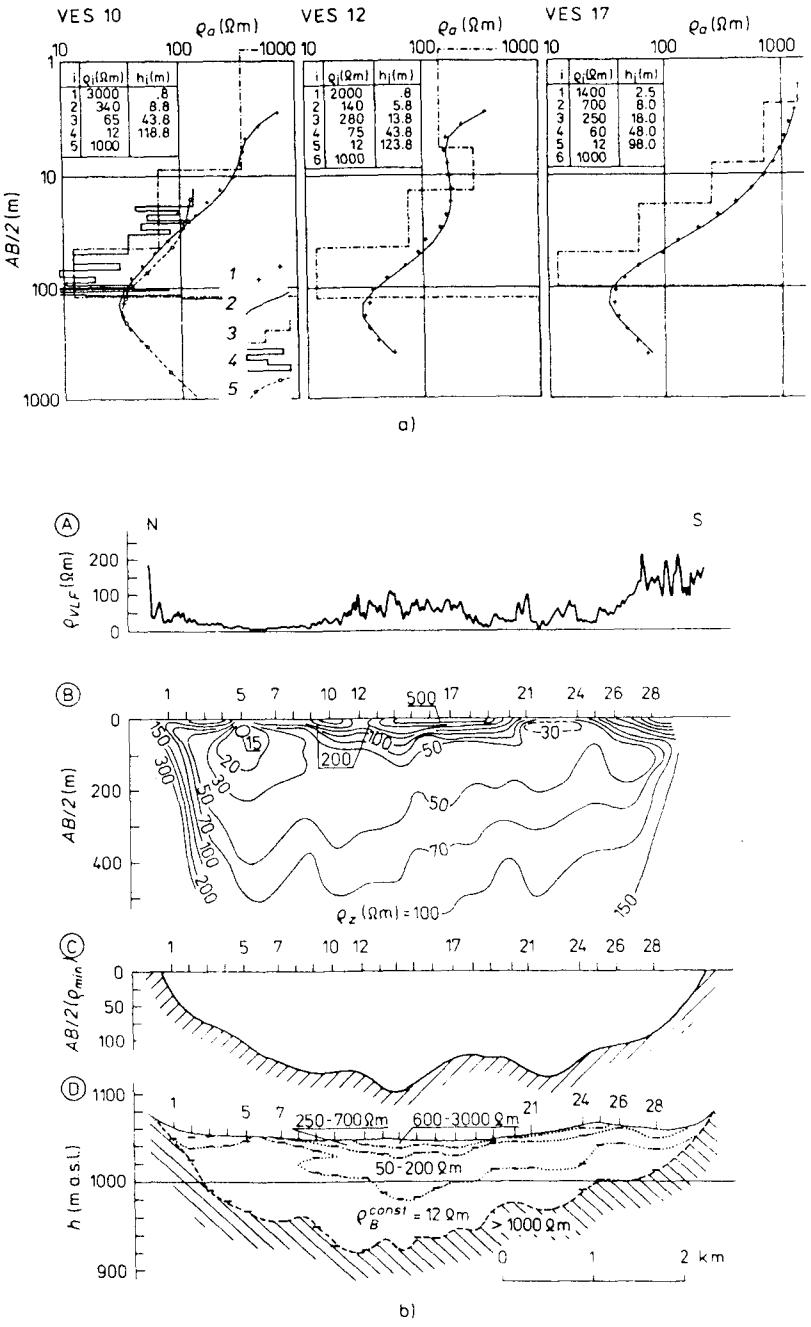

Figure 4.2 Facing page. Application of the vertical electrical sounding method to the hydrogeological exploration of sediments in the Khawrah wadi, PDR of Yemen (Karous and Kněz, 1984). (a) Measured VES curves and the results of computer interpretations: *1* — VES curves measured, *2* — constrained theoretical VES curve, *3* — interpreted vertical resistivity profiles, *4* — vertical resistivity profiles according to lateral electrical sounding, *5* — theoretical VES curves corresponding to resistivity logging. (b) Interpretation of geophysical profile VII across the Khawrah wadi: A — VLF resistivity profile curve, B — vertical isoohmic pseudo-section according to VES, C — AB/2 distances corresponding to the minimum apparent resistivity, D — resistivity section interpreted according to VES.

deposits and underlying crystalline rocks, but the distribution of seismic velocities in the bedrock which also indicated the degree of weathering. The lower velocity at point 201 corresponds to a tectonic dislocation, which was also identified by geoelectrical methods.

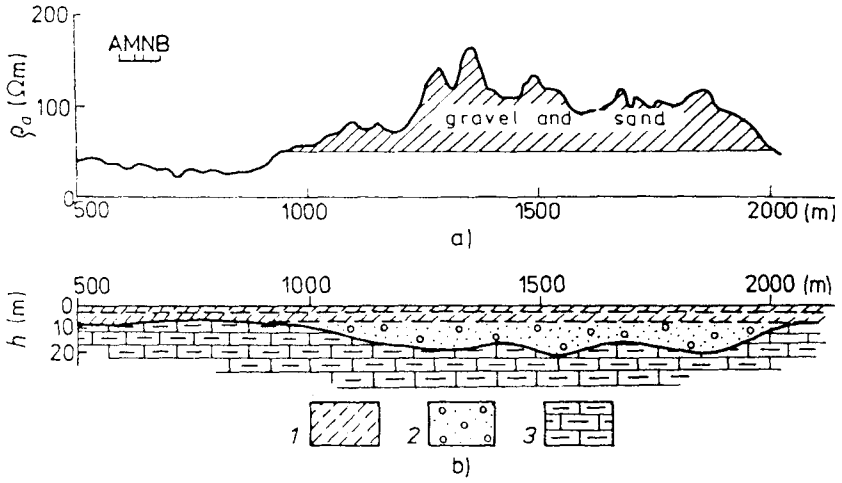

Figure 4.3 Symmetric resistivity profiling and vertical electrical sounding over the buried channel of the Labe River at Písek near Chlumec nad Cidlinou (Bohemia). (a) Resistivity profile 1. (b) Vertical section interpreted according to VES. *1* — loam; *2* — sand, and gravel and sand in the ancient bed of the Labe; *3* — underlying Turonian marlstone.

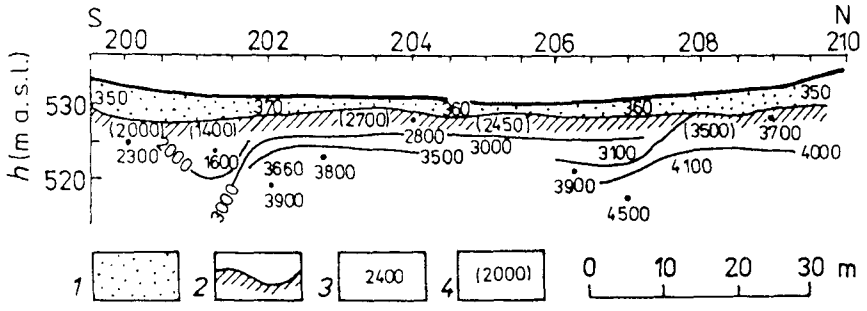

Figure 4.4 Seismic survey of unconsolidated sedimentary cover in the Těchobuz area of Mezilesí (Skopec, 1978). *1* — sedimentary cover, *2* — bedrock surface, *3* — velocity of seismic waves in the velocity section, *4* — velocity at the bedrock surface.

Seismic measurements can also assist in a more precise interpretation of VES curves. An example of a combined evaluation of seismic and geoelectrical survey results is given in Fig. 4.5.

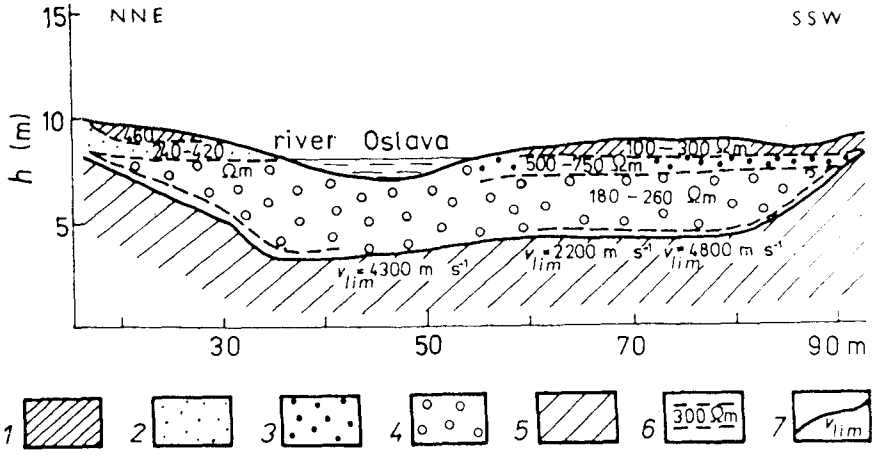

Figure 4.5 Application of vertical electrical sounding and shallow refraction seismics to the investigation of sedimentary deposits in the Oslava River Valley at Čučice near Oslavany, Czechoslovakia (Hašek et al., 1978). *1* — sandy loam, *2* — sand, *3* — stony debris, *4* — gravel and sand (water-bearing), *5* — bedrock, *6* — geoelectrical layer with interpreted resistivity, *7* — seismic boundary with velocity v_{lim}.

The use of *induced polarization* methods in investigations of shallow unconsolidated sediments has been limited so far by an inadequate interpretation theory and the small number of available theoretical curves (Komarov, 1972; Elliot, 1974, Mazáč et al., 1979b). Therefore IP methods can only be used to provide qualitative information on the distribution and depth of water-bearing layers (Fig. 3.27).

In a detailed ground-water survey it is important to determine the dynamics of the ground-water regime including directions of flow and ground-water levels. An application of shallow refraction seismics for determining the *depth to the water table* is shown in Fig. 4.6.

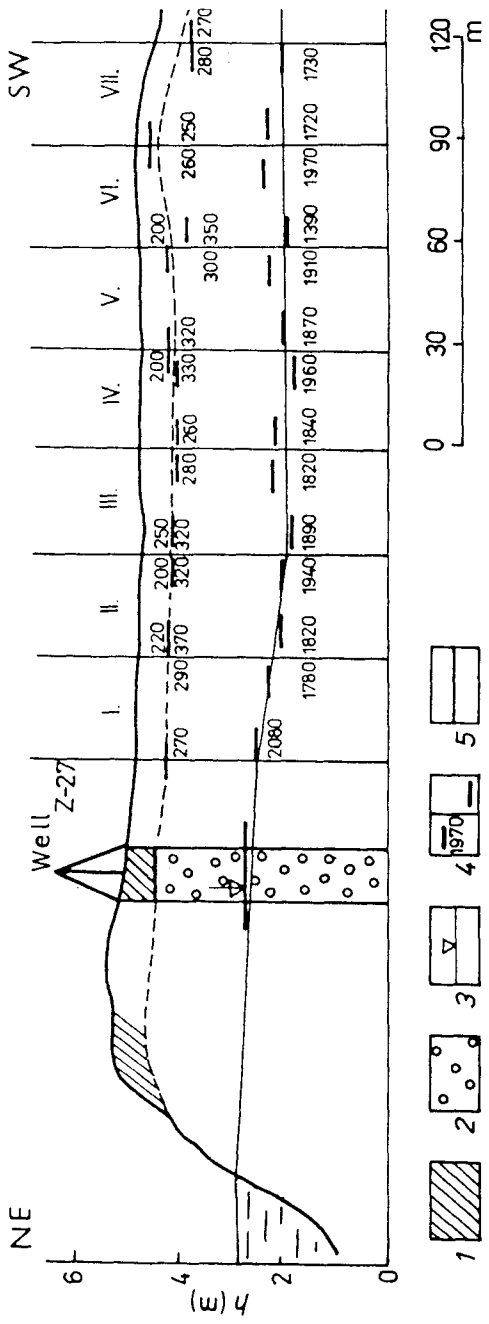

Figure 4.6 Assessment of water table using shallow refraction seismics at a location near Čunovo, south of Bratislava, Czechoslovakia (Janík and Olexa, 1975). *1* — sedimentary cover; *2* — sand and gravel; *3* — water table according to the well Z-27; *4* — interpreted seismic boundaries with velocities v_{lim} (m s^{-1}) in the deeper layer; *5* — water level according to the geophysical survey.

4.1.2 Major River Deltas, Littoral and Coastal Zones and Islands

Hydrogeological structures near salt-water bodies are basically dependent on the geology of the area and thus are similar to those discussed in other sections. However, they are dealt with separately because of one important difference - the saturation of such aquifers with seawater.

Owing to its high salt content, seawater has a lower resistivity (c. 1 Ω m) than fresh water; the resistivity of fresh water ranges between 20 and 100 Ω m (Table 2.1). The resistivities of aquifers saturated with seawater and fresh water therefore differ widely and resistivity methods, mainly the VES method, are used to locate their contact. However, the differentiation of impermeable clayey sediments from sandy layers saturated with seawater is difficult due to the equivocal interpretation of the resistivity methods.

An example of the use of geoelectrical methods in the investigation of a coral atoll is given in Fig. 4.7. A vertical resistivity section based on VES interpretations leads to establishment of the corresponding hydrogeological section.

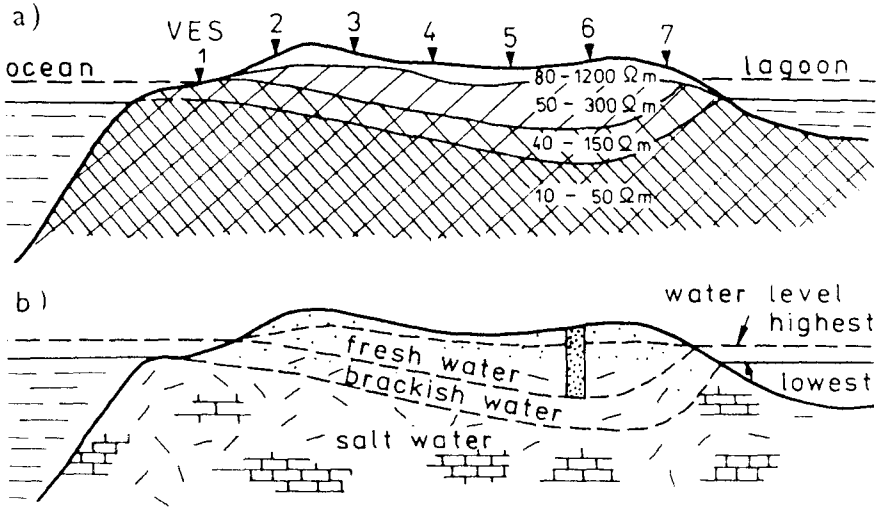

Figure 4.7 Idealized application of VES for differentiation of aquifers saturated with fresh, brackish and seawater on a coral reef. (a) Interpreted vertical resistivity profile according to VES. (b) Hydrogeological cross section.

Determination of the trend of layers saturated with fresh, brackish and salt water allows selection of optimum locations for fresh water wells.

In coastal areas, geophysical surveys are conducted to differentiate water-bearing strata according to permeability and sedimentary conditions and to assess the relief of impermeable bedrock. A frequent task is to find locations of outflows of fresh ground water into the sea. For these purposes, remote sensing, resistivity methods in both modifications (i.e., profiling and sounding) seismic and gravity surveys are used. Magnetometry has also been used successfully in investigations of volcanic island regions.

4.1.3 Sedimentary Basins and Consolidated Sediments

Important aquifers, represented by sandstone over- and underlain by impermeable clayey and marly sediments, frequently occur in extensive sedimentary basins. Geophysical surveys in these environments may be divided into two groups. The first group includes studies of the structural-geological and tectonic setting:

- Determination of the depth to the bedrock and bedrock relief, hydrogeological conditions of the bedrock
- Determination of the size of the basin area and the character of its limits
- Determination of the dip of beds, anticlinal and synclinal structures, thickness of beds, bed complexes and formations
- Location of faults, flexures, and other structures

The second group involves:

- Determination of lithology and facies changes
- Detailed division of aquifers corresponding to hydrogeological parameters
- Determination of direction of regional ground-water flows

For determination of the *depth to the basement* in a sedimentary basin, the following geophysical methods are utilized: resistivity methods, gravity surveys, seismic, magnetic, logging and air-borne methods; and to a lesser degree the telluric current and magnetotelluric sounding methods.

As sedimentary structures often have lower densities than underlying rocks, varying sediment thicknesses are reflected in varying values of *residual anomalies* Δg_L (Mareš et al., 1984), the thickness of sediments being approximately proportional to the absolute value of the residual anomaly. However, the prerequisite for a reliable determination of changes in basin sediment thicknesses is a uniform bedrock density. The converse is where changes in gravity anomalies reflect changes in bedrock density. An example of the interpretation of sediment thickness from gravity measurement is shown in Fig. 4.8. The accuracy of the interpreted depths depends on the precise determination of the differential density $\Delta\sigma$ and its steadiness in the horizontal direction.

The effectiveness of geophysical (chiefly gravity) surveys, even in sedimentary areas where the geology has been thoroughly studied, can be demonstrated

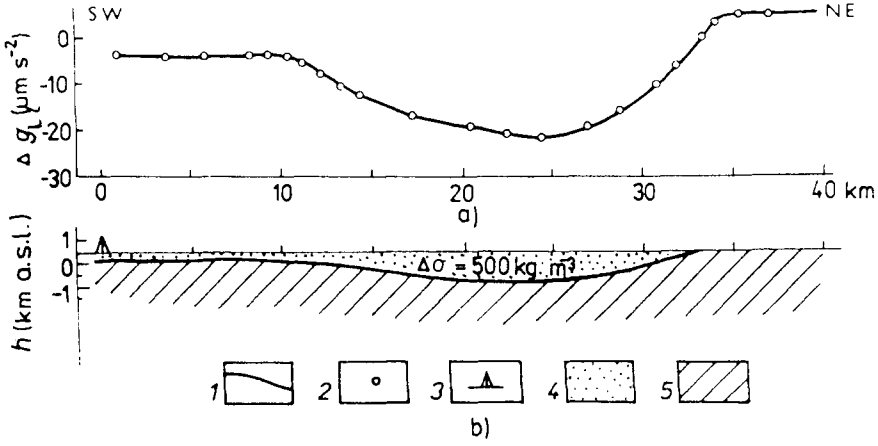

Figure 4.8 Interpretation of sediment thicknesses from gravimetric data obtained in the Kordofan province of Sudan (Ďuratný et al., in Sborník, 1972). (a) Profile of residual anomaly (Δg_L). (b) Interpreted cross section of the sedimentary basin (sand, sandstone, clay, shale siltstone). *1* — residual anomaly (Δg_L) corresponding to the interpreted cross section, *2* — measured values (Δg_L), *3* — key borehole, *4* — basin sediments (σ_1 = 2080 kg m^{-3}), *5* — Precambrian rocks of the basement (σ_2 = 2590 kg m^{-3}).

with an example from the Cheb basin (Dobeš et al., 1987). The survey, which was carried out in three phases, revealed a number of unknown structures in the basin basement, e.g., the Žírovice depression (Fig. 4.9), and provided an overall picture of the basin. On this basis the interrelations of individual structures in the regional tectonic system were recognized and assessed.

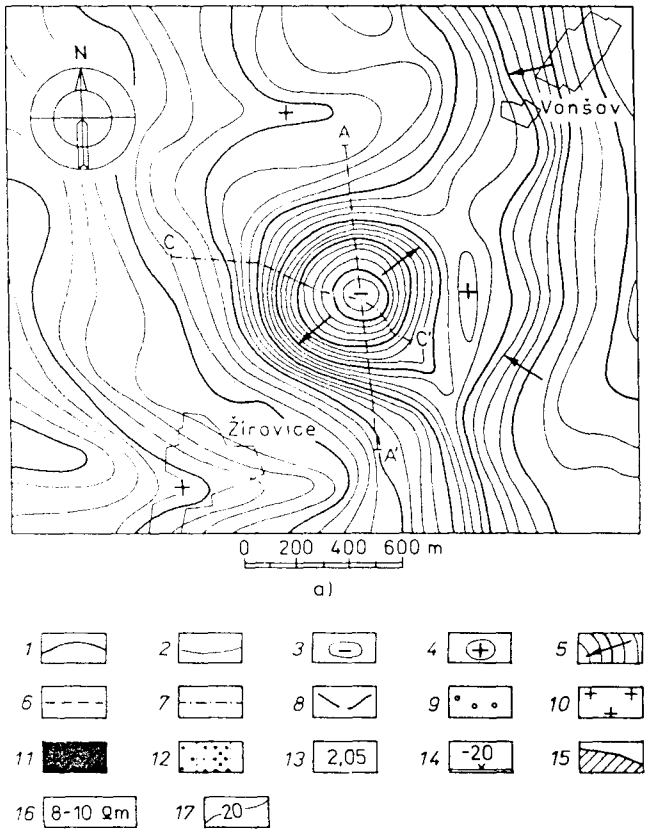

Figure 4.9 An example showing the contribution of geophysical measurements in a study of the Cheb basin, Czechoslovakia (according to Dobeš et al., 1987). **Above:** (a) Evidence of a local gravity minimum near Žírovice, 3 km north of Františkovy Lázně (Bohemia), on a schematized map of gravity isolines. **Facing page:** (b) Gravity profile A - A′ and its quantitative interpretation. (c) Geoelectrical section (results of quantitative VES interpretation) and a corresponding isoohmic section. *1* — gravity isoanomaly with an increment of 10 μm s^{-2}, *2* — gravity isoanomaly with an increment of 2.5 μm s^{-2}, *3* — local gravity minimum, *4* — local gravity maximum,

Seismic methods were effective in determining sediment thicknesses. The regional seismic survey of the Bohemian Cretaceous Basin showed that the thickness of Cretaceous sediments can be determined where the basement is formed by the crystalline complex. Where the Cretaceous is underlain by Permian rocks, the two systems cannot be distinguished on the basis of their seismic

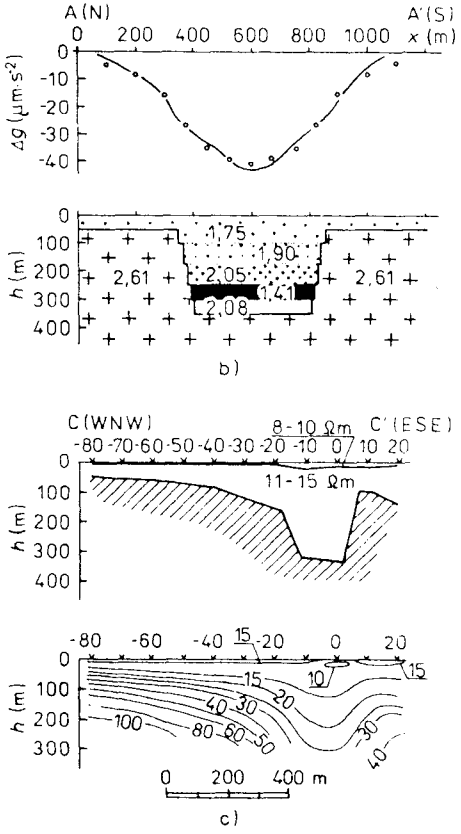

5 — increasing gravity in the direction of arrow, *6* — gravity profile A - A′ (see part b), *7* — VES profile (see part c), *8* — residual gravity curve, *9* — gravity effect of the model, *10* — Smrčiny granite, *11* — coal seam, *12* — Tertiary sediments, *13* — bulk density in g cm^{-3}, *14* — location of VES, *15* — geoelectrical boundary between the overlying sedimentary complex and the deepest layer of a higher resistivity, *16* — interpreted resistivities, *17* — isolines of apparent resistivity in isoohmic section.

velocities and the interpreted thicknesses represents their total thickness. Figure 4.10 presents a simplified geophysical cross section of the Bohemian Cretaceous Basin interpreted from the results of seismic surveys, VES's and borings. The boundary established from the seismic and VES measurements agrees in the northeastern part of the section where Cretaceous sediments lie on the crystalline complex. The resistivity and seismic measurements thus provide complementary information for constructing the cross section.

In addition to gravity and seismic surveys, resistivity methods, vertical electrical sounding in particular, are suitable for the study of basin sediments. Absolute and accurate results can, however, only be obtained by correlation with logging results from a sufficiently dense network of boreholes. A comprehensive analysis of resistivity logging and interpreted VES curves adjacent to boreholes (Figs. 4.11 and 4.12) makes it possible to establish the resistivity characteristics of individual geoelectrical layers and to determine their geological equivalents. For the Bohemian Cretaceous Basin, the basal sandstones, mainly those of Cenomanian age, form a key horizon over the entire basin. In the southeastern part of the Basin, the key nonconductive horizon is represented by lower Turonian sediments in coarse-grained sandy facies. The map showing the depth to the basin basement was compiled from quantative interpretation of VES curves (Fig. 4.13).

Changes in lithofacies often make correlation of geoelectrical layers with geological beds difficult. In such cases the resistivity measurements, especially maps of apparent resistivity for different electrode spacings (Fig. 4.14) can only provide a rough concept of the *spatial distribution of the facies*. In the Bohemian Cretaceous Basin the areas of higher resistivities ($\rho_a > 100\ \Omega$ m) are associated with the occurrence of coarse-grained sediments, which often represent important aquifers. The high gradient on the resistivity map provides evidence of a tectonic boundary (in Fig. 4.14 the Litoměřice fault at the NW margin); the low gradients indicate a gradual transition of the coarse-grained sandstone facies into a finer-grained facies towards the east.

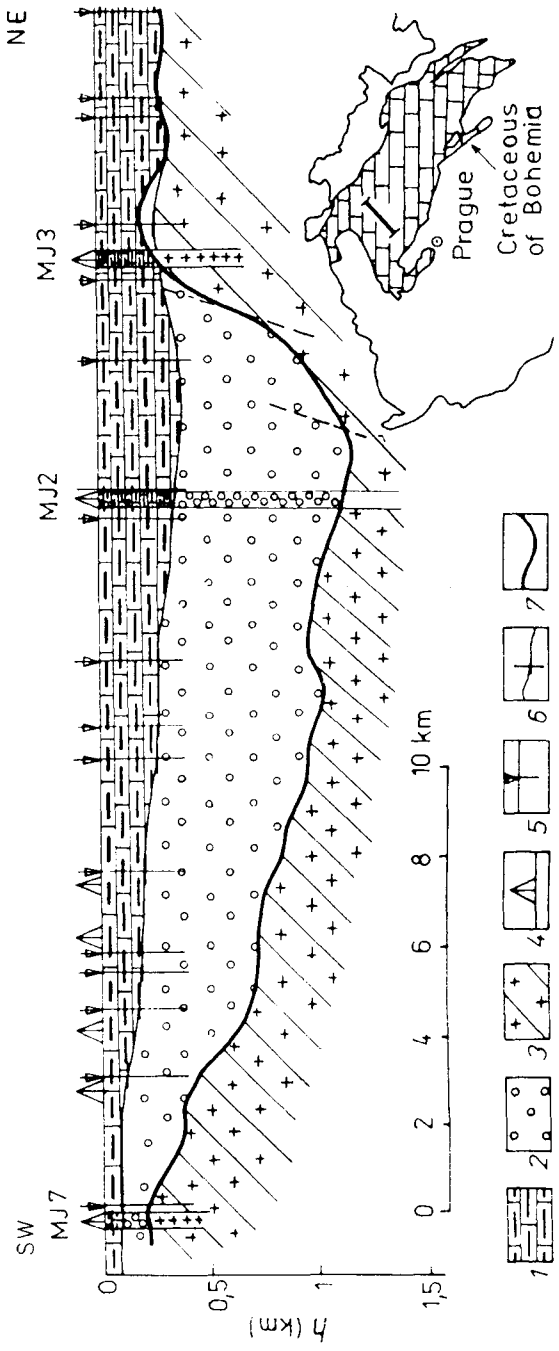

Figure 4.10 Simplified cross section of the Bohemian Cretaceous Basin compiled from reflection seismics (Hrách, 1973), vertical electrical soundings, and boreholes (Karous, 1972). *1* — Cretaceous sediments, *2* — Permian basement, *3* — crystalline basement, *4* — boreholes, *5* — location of VES, *6* — boundary interpreted according to VES, *7* — depth to the crystalline basement based on seismic results.

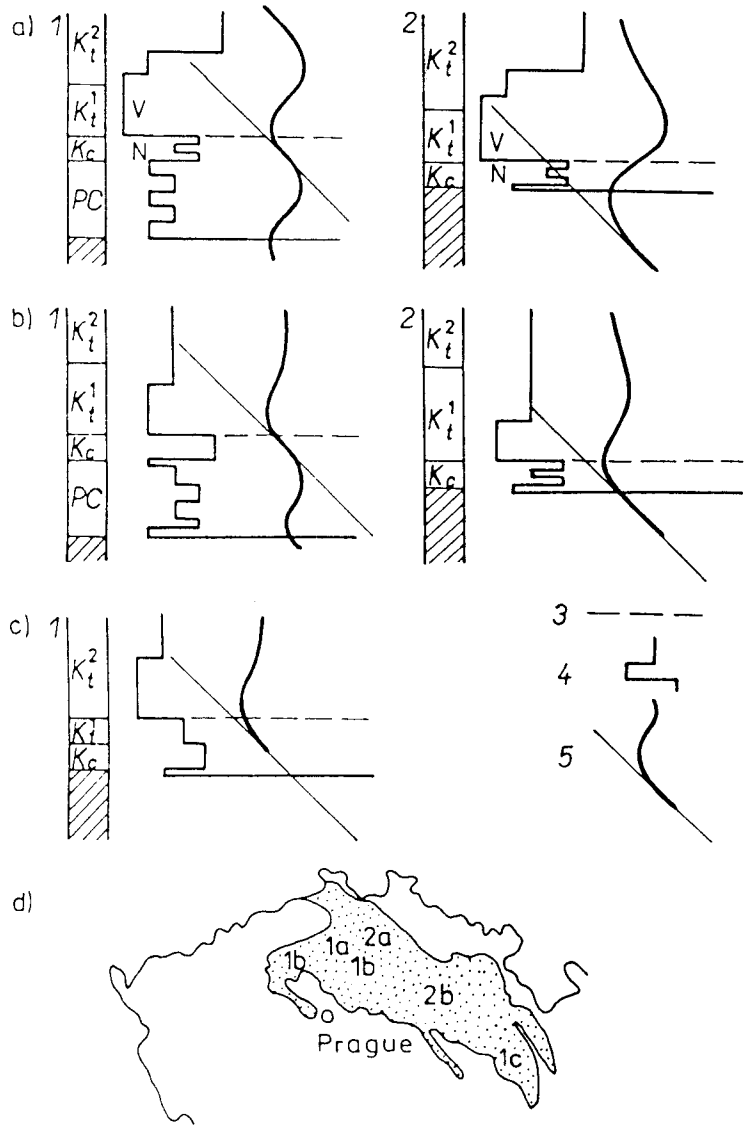

Figure 4.11 Characteristic vertical resistivity profiles across the Bohemian Cretaceous Basin (Karous, 1972). (a) Area of nonconductive middle Turonian sediments. (b) Area of conductive middle Turonian sediments. (c) Area of lower Turonian sandstone facies. (d) The Cretaceous area corresponding to VES types (a) to (c). *1* — Permian basement, *2* — older basement, *3* — key boundary, *4* — logging profiles, *5* — sounding curve with asymptote *S* (Logarithmic scale for resistivity and depths); *PC* — Permo-Carboniferous, K_c — Cenomanian, K_t^1 — lower Turonian, K_t^2 — middle Turonian.

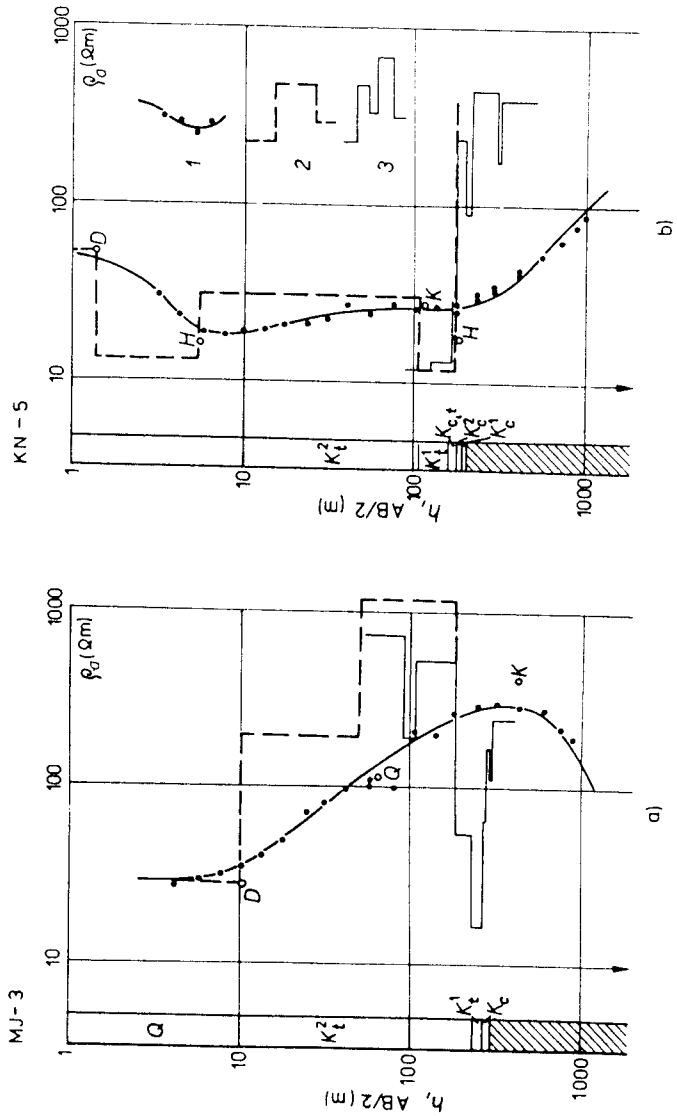

Figure 4.12 Interpretation of VES curves near boreholes investigated with lateral electrical soundings (Bohemian Cretaceous Basin). (a) Borehole MJ-3. (b) Borehole KN 5. *1* — measured VES points and interpreted sounding curve; *2* — interpreted vertical resistivity profile according to VES; *3* — interpreted resistivity profile according to LES; K_c^1 — freshwater Cenomanian, K_t^2 — marine Cenomanian, K_c^1 — intermediate zone, K_t^1 — lower Turonian, K_t^2 — middle Turonian, *Q* — Quaternary.

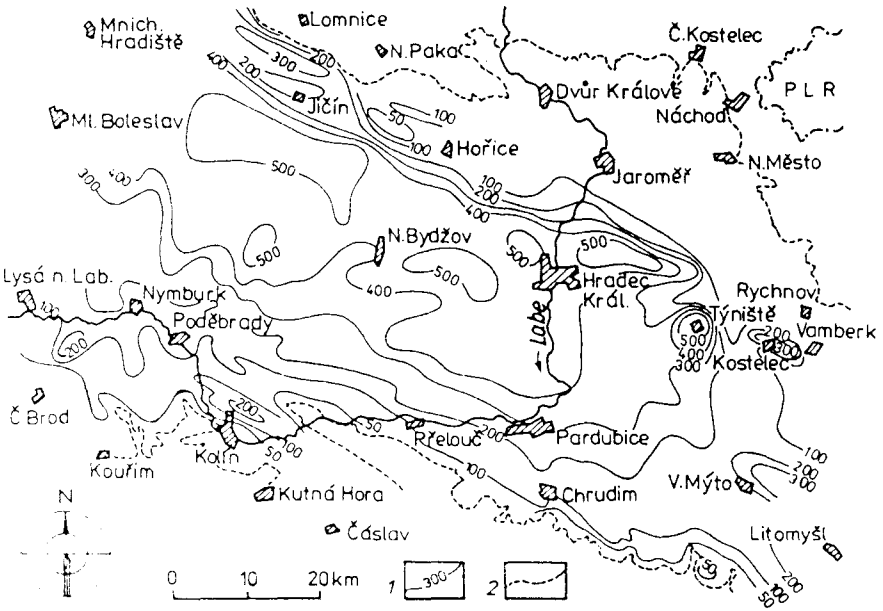

Figure 4.13 Map showing the depth to the basement of the Cretaceous sediments in the Bohemian Cretaceous Basin based on VES. With regard to the small density of points, the map provides an atectonic picture (Karous, 1972). *1* — isolines of the depths to the basement surface (m), *2* — margin of the Cretaceous Basin.

Hydrogeologically significant tectonic structures in relatively conductive sediments can be assessed only indirectly, because of the small difference between the resistivity of fracture fillings and adjacent sediments. The *location of faults* can be established indirectly, only where a block moved downwards. In this case, the fault is shown by a sudden change in the interpreted parameters (e.g., thickness, conductivity S, resistivity for a given spacing - Fig. 4.15a). Faults may also occur where the character of the sounding curves changes. The changes may be assessed quantitatively using the association coefficients A_{ij} (Habberjam, 1970), whose maxima locate the sites of marked changes in resistivity conditions (Fig. 4.15b).

The magnetometric method is used to locate hidden outcrops of volcanic sediments, to determine changes in basement rock types, and to map the extent

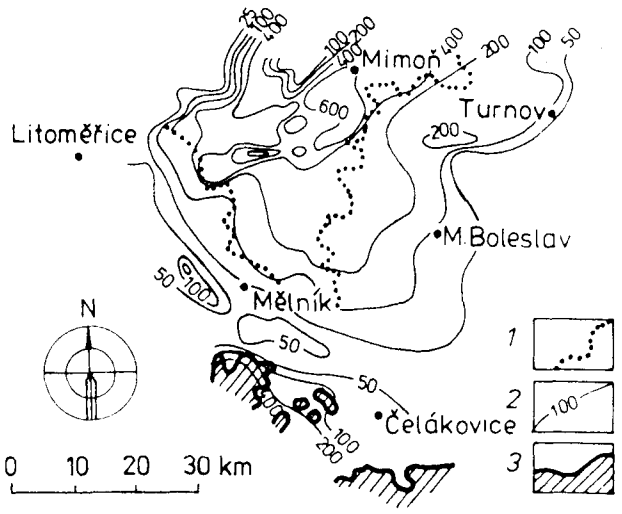

Figure 4.14 Map showing apparent resistivities for spacing AB/2 = 100 m, in the Middle Turonian sandstone facies in the Bohemian Cretaceous Basin. *1* — delineation of the middle Turonian sandstone facies based on the geological map 1:200,000, *2* — isoline of apparent resistivity ρ_a (Ω m) according to VES's for an AB/2 spacing of 100 m, *3* — margin of the Bohemian Cretaceous Basin.

of magnetic basement rocks. Additionally, it serves for mapping neovolcanic intrusions and buried vents associated with tectonic lines. In this way, a magnetometric survey can assist in refining the picture of the tectonic structure of a sedimentary basin.

To determine depths to shallow water tables, the seismic method is employed in a similar way as in Quaternary sediments. For determining the *direction of ground-water flow*, the method of spontaneous polarization is appropriate, and the hydrogeological variant of the mise-a-la-masse method is suitable for determining the direction and velocity of ground-water flow (Figs. 4.16 and 4.17).

4.1.4 Neovolcanic Areas

Until recently, neovolcanic rocks were not regarded as prospective ground-water resources. Investigations have now shown that young volcanics contain large

ground-water reserves (e.g., in the area of central Slovakia). Geophysical surveys are concentrated on the following tasks: to delineate medium-to-coarse-grained pyroclastics, to distinguish between permeable and impermeable

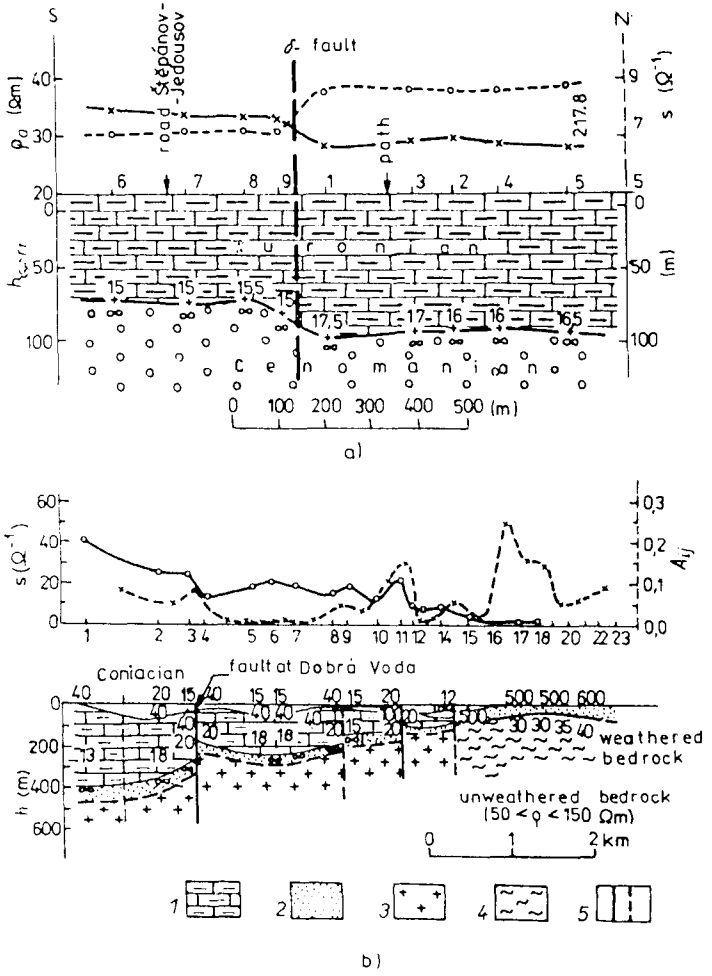

Figure 4.15 Examples of indirect location of faults, using geoelectrical methods, in conductive sedimentary basins. (a) Location of a fault based on the parameters S and ρ_a at Štěpánov near Přelouč, at the margin of the Bohemian Cretaceous Basin. (b) Application of Habberjam's coefficients (A_{ij}) to assess dislocations on the profile 17b across the Jflovice fault (Karous, 1972). *1* — Turonian sediments, *2* — Cenomanian, *3* — crystalline basement, *4* — Permo-Carboniferous basement, *5* — dislocations based on geoelectrical measurements.

volcanic structures, and to assess the tuffite layers, permeable lava flows which often overlie impermeable clayey rocks, pelitic beds and other potential water-bearing materials. Of particular hydrogeological importance are *water-bearing fault* lines in solid volcanic rocks. Geophysical surveys of neovolcanic areas will

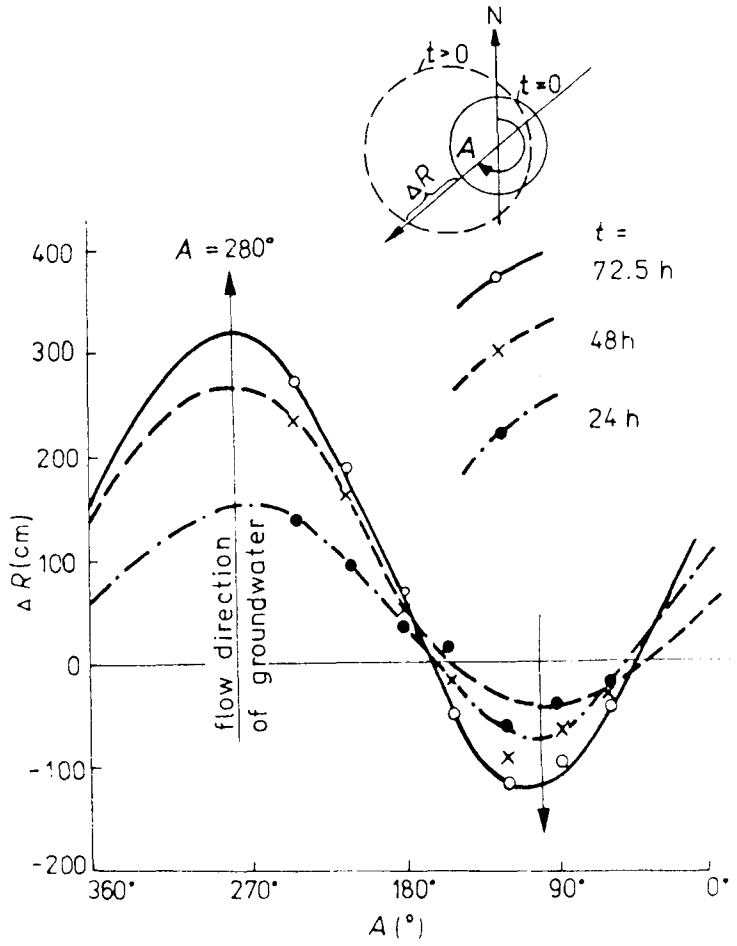

Figure 4.16 Dependence of the shift of equipotential lines (ΔR), on the azimuth of radial profiles (A), using the mise-a-la-masse method. Data gathered at borehole HMÚ near Srbská Kamenice in the Cretaceous of Bohemia (modified according to Kolinger, 1976). The parameter studied was the ground-water flow in the Turonian horizon. (The water table was at a depth of 10 m, and the direction of flow is given by the direction of the profile, with the maximum shift being ΔR, and velocity equal to $v_{\Delta x} \approx \Delta R_{max}/\Delta t$).

be illustrated using the results from hydrogeological investigations of the neovolcanic area of central Slovakia. The hydrogeological structures are due to deep tectonic systems, which separate a volcanic complex from impermeable horizons. They are particularly effective in capturing surface water. These structures can be detected by gravity, magnetic, and geoelectrical methods. One such hydrogeological structure proved to be a fault zone that separates the Žiar depression from the Handlová ridge; it was well-defined on the maps of total Bouguer anomalies and horizontal gravity gradients (Fig. 4.18). On the western side of the fault, large quantities of ground water collect in neovolcanic lava flows and pyroclastics. These are expressed on the aeromagnetic map by pronounced ΔT anomalies, in contrast with the steady magnetic field over the rocks of the Žiar intravolcanic depression (Fig. 4.18).

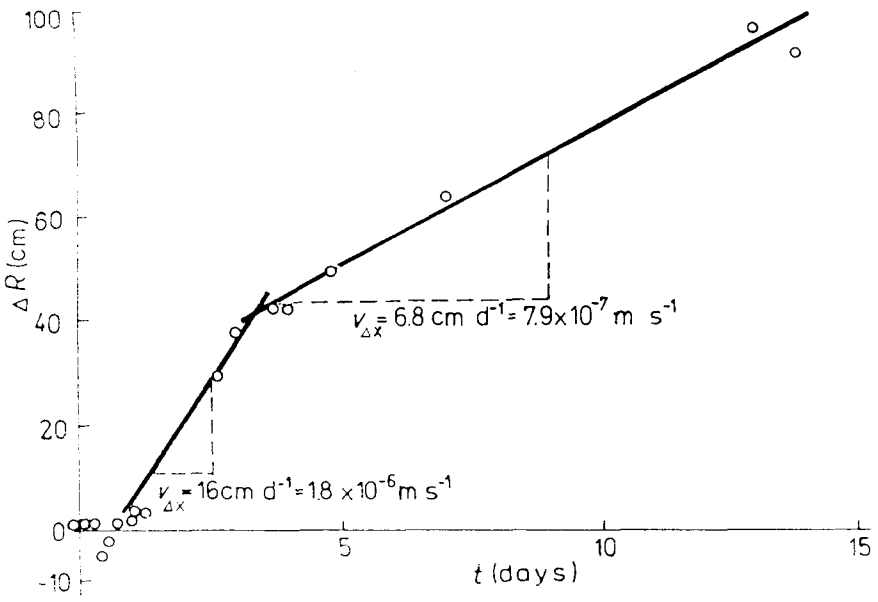

Figure 4.17 Determination of the ground-water flow velocity ($v_{\Delta x}$) in a borehole (IKS-1) near Srbská Kamenice, Cretaceous of Bohemia. Relation between maximum shift of equipotential lines (ΔR) and the time of measurement (t) (Kolinger, 1976). The flow was traced in a Turonian horizon at a depth of about 25 m, with an optimum distance of the stable electrode from the borehole being R_M = 50 m.

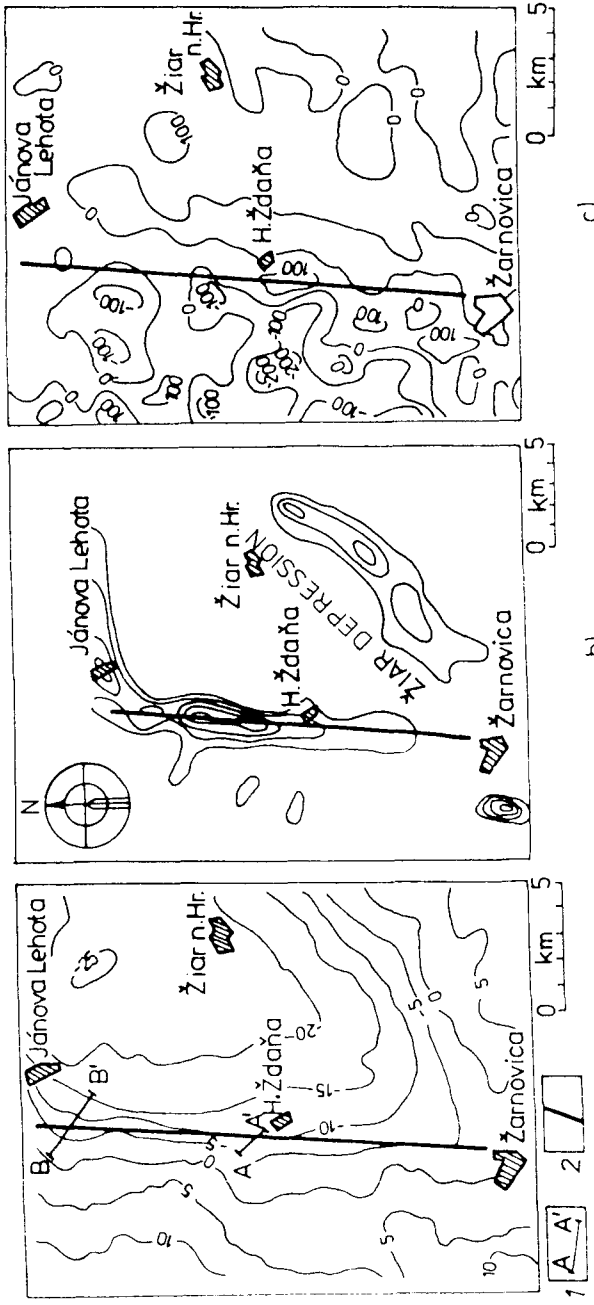

Figure 4.18 Geophysical maps showing the extent of the Žiar depression, Czechoslovakia (Zbořil et al., in Sborník, 1972). (a) Simplified map of total Bouguer anomalies. (b) Map of horizontal gravity gradients. (c) Simplified aeromagnetic map (Šalanský, 1970). *1* — location of profiles shown in Fig. 4.19, *2* — major fault bordering the Žiar depression.

VES profiles across the interpreted fault more accurately define the contact between the neovolcanics of the Vtáčnik Mountains and the sedimentary rocks of the Žiar depression (Fig. 4.19). Gravimetric methods combined with aerial and surface magnetic surveys, and VES and resistivity profiling have been successfully used to resolve hydrogeological problems in other neovolcanic areas, e.g., in the České středohoří and the Slánské pohorie Mountains.

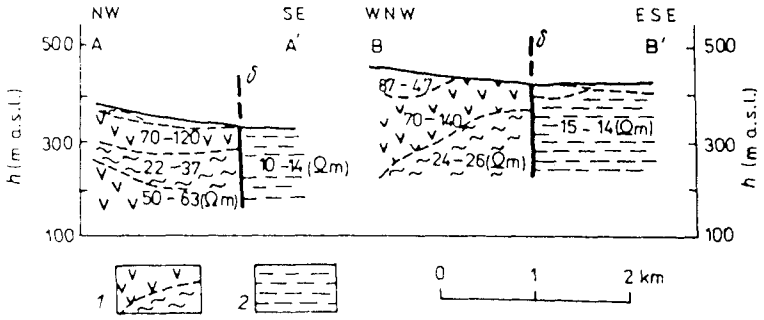

Figure 4.19 Geoelectrical sections determined from VES results along profiles A-A′ and B-B′ across the contact separating sediments of the Žiar depression from neovolcanic rocks of the Vtáčnik Mountains (Májovský, 1970). For the locations of profiles see Fig. 4.18. *1* — volcanic complex of the Vtáčnik Mountains, *2* — sediments of the Žiar depression.

4.1.5 Crystalline, Igneous, and Metamorphic Rocks

Locating good sites for wells in crystalline areas is among the most difficult tasks for geophysical surveys. Crystalline regions (except for karst areas formed of crystalline limestones) are characterized by the presence of essentially impermeable igneous and crystalline rocks. Unweathered rocks typically have total porosities of less than 3%; accumulations of ground water are thus restricted to tectonically affected zones or partially weathered rock complexes.

The following methods are used in *explorations of tectonic zones*: geoelectrical methods using direct current SRP, VES and alternating electromagnetic fields (VLF), spontaneous polarization, temperature, gasometric, gravity, magnetometric and radiometric surveys. It is advisable to conduct geophysical investigations in two phases. In the first phase the survey is directed at

establishing promising rock types; those with a higher porosity or jointing and, locations of more intensive disturbance. The second phase involves a detailed investigation of the promising localities and fractures zones, and a study of the physical and hydrogeological characteristics of these zones. In places where weathered surficial deposits and the zone of weathering reach a greater thickness, vertical electrical soundings and shallow refraction seismics are utilized. Radial (circular, polar) resistivity measurements, in both the profile and sounding variants, are used for characterizing general tectonic conditions. Based on the principle of anisotropy, the principal direction of rock fracturing coincides with the direction along which the highest values of apparent resistivity are measured. The radial sounding variant also allows the depth and degree of fracturing to be established.

The location of a fault and its geometrical and physical properties can be accurately and efficiently determined by asymmetric resistivity profiling with two or more current electrode spacings. A fault, as a conductive zone, is determinable only if the contrast in resistivities is at least three times as great as the realizable accuracy of measurement. Water-bearing, strongly mylonitized faults are signified by resistivities of 1 to 10 Ω m, whereas in contrast, sound rocks resistivities are of the order of hundreds to thousands of Ω m. In crystalline systems, the condition of a sufficient resistivity contrast is, in most cases, easily satisfied.

For rapid and economical mapping of water-bearing faults, portable electromagnetic methods (Slingram and VLF) are usually used. An example of an investigation for a tectonic contact between limestones and Culm shales is provided in Fig. 4.20.

4.1.6 Karst Areas

In karst areas, geophysical surveys are centered on the assessment of karstified permeable zones, verification of the structural-tectonic position of limestones with respect to their basement, and determination of the spatial distribution of

carbonate rock complexes. Zones of intensive karstification are associated with regional tectonic lines, and especially with intersections of tectonics systems. Therefore, it is necessary to first locate the tectonic lines and fault zones on the basis of regional and (aero) magnetic maps, or maps plotted from remote sensing images. Regional gravity and geomagnetic maps are also useful for studying the relief of impermeable basement rocks, whose dips control the general directions of ground-water flow in a limestone block.

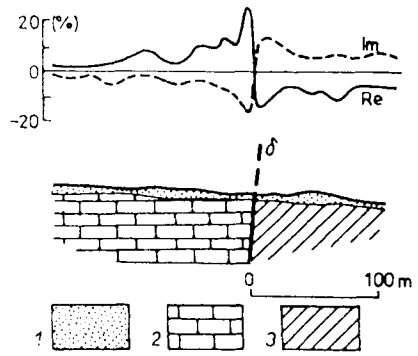

Figure 4.20 Water-bearing fault, indicated by the very low frequency method, which separates the Devonian limestones and the Culm shales at a location near Holštejn (Moravian Karst) (Bláha, 1975). *Im* — imaginary part, *Re* — real part (VLF measured values); *1* — Quaternary cover, *2* — limestones, *3* — shales.

Karst formations, both the surface (sinkholes, depressions) and underground forms (caverns, ground-water conduits, underground streams), appear as conductive zones relative to adjacent undisturbed limestones with resistivities of the order of thousands to tens of thousands of Ω m. Karstified zones are investigated using geoelectrical methods.

An indication of the intensity of karstification in a vertical section can be obtained from the results of vertical electrical sounding in profiles, arranged in a regular (square or rectangular) or an irregular network. In a karst area, four principal layers can typically be differentiated in a vertical section: near-surface (clayey) loam, dry karstified limestone, water-bearing karstified limestone and

solid unkarstified limestone (Fig. 4.21). Quantitative interpretation of VES curves (and other geophysical measurements in karst areas) is a most difficult problem because of the considerable variability found in all of the physical properties and parameters. As the results of quantitative interpretation are usually ambiguous, some form of qualitative interpretation (e.g., construction of an isoohmic section) is used in the final analysis.

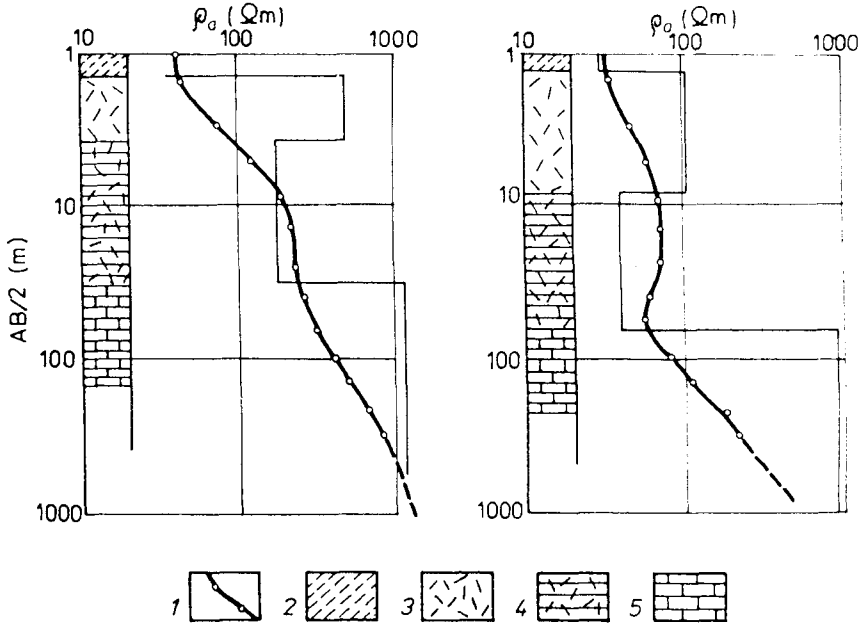

Figure 4.21 Typical VES curves in karst areas: example from the northern part of the Moravian Karst (Daněk and Blížkovský, 1968, modified). *1* — measured values and interpreted VES curve, *2* — soil layer (tens Ω m), *3* — dry karstified limestone (many hundreds Ω m), *4* — water-bearing karstified limestone (a few hundreds Ω m), *5* — solid limestone (thousands and more Ω m).

Fractures and *karstified zones* are also investigated by seismic and gravimetric methods. Precise gravity measurements, corrected for regional anomalies, can locate karstified zones by their minima which also cause minima on resistivity maps or profiles. A set of resistivity methods combined with detailed gravity measurements can thus provide more reliable results (Fig. 4.22). Large

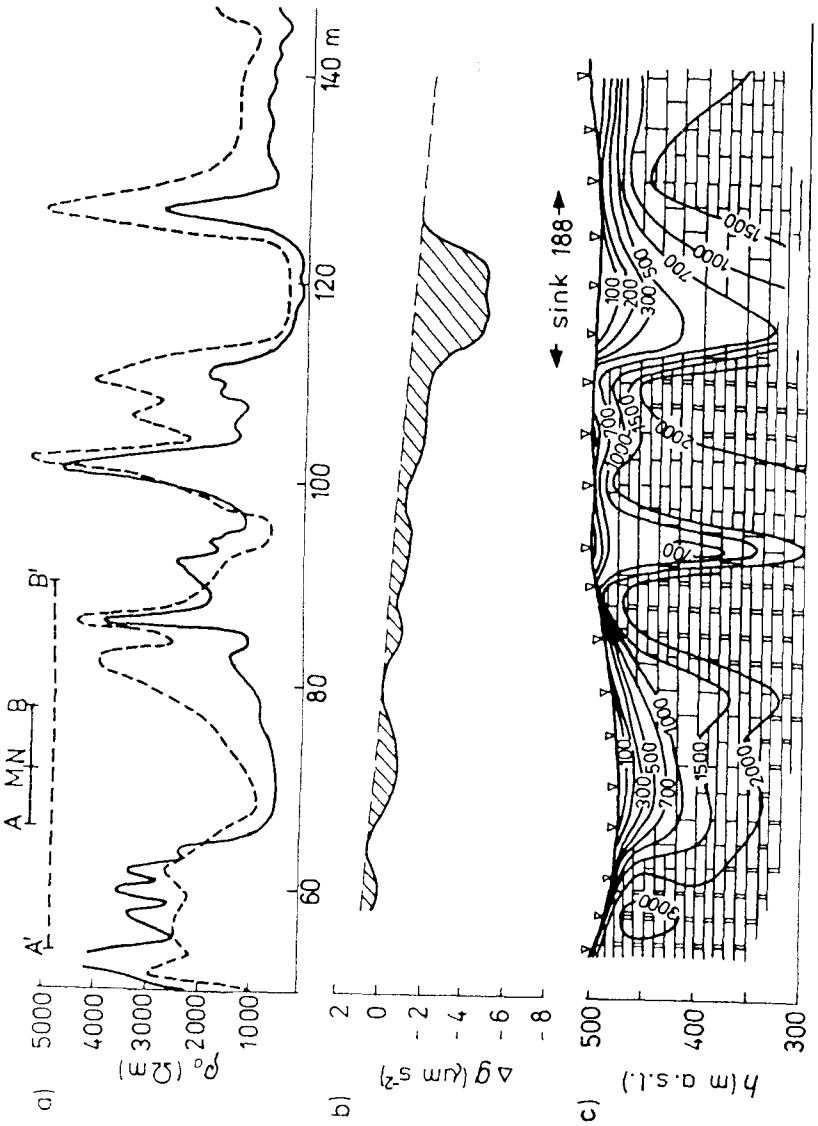

Figure 4.22 Geophysical measurements on profile 16 in the northern part of the Moravian Karst, 2 km south of Sloup near Blansko (Daňko and Bližkovský, 1968). (a) Resistivity profiling with two current electrode spacings. (b) Gravity measurements. (c) Isoohmic section based on VES.

variations in resistivity curves are caused by decreases in resistivity at sites with karst phenomena, and by variations in thickness and resistivity of the overburden. To distinguish between these two causes, profiling with two or more current electrode spacings is utilized.

The application of the mise-a-la-masse method to determine the *direction of ground-water flow* is demonstrated in Fig. 4.23.

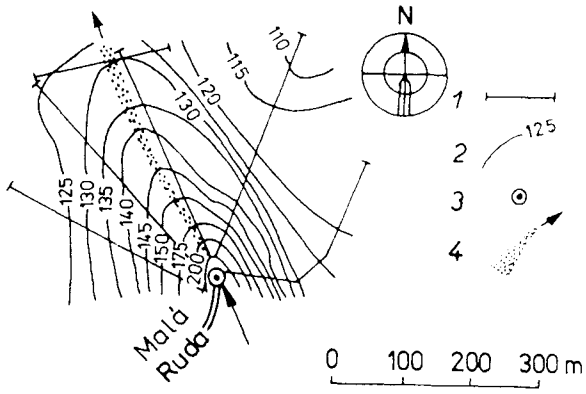

Figure 4.23 Tracing ground-water flow in karst with the mise-a-la-masse method in the Jugoslavian Karst (Kovacevic and Krulo, 1967). *1* — geophysical profile, *2* — isolines of ΔV potential (mV) of the charged body, *3* — earthing of current electrode, 4 — direction of ground-water flow.

A special task for geophysics in karst areas is locating and tracing *cavities* (channels and caves). Where the cavities are connected by conduits with flowing water, we may use methods appropriate for tracing ground-water flow (e.g., the seismic or mise-a-la-masse method). Microgravimetry is used for locating isolated and closed cavities (Fig. 4.24).

The direction of karst water flow can also be traced with thermal methods and the method of spontaneous polarization.

Vertical electrical soundings, spontaneous polarization measurements, or induced polarization soundings provide information about the overburden deposits, which control the infiltration of surface water into limestones and thus also the karstification process.

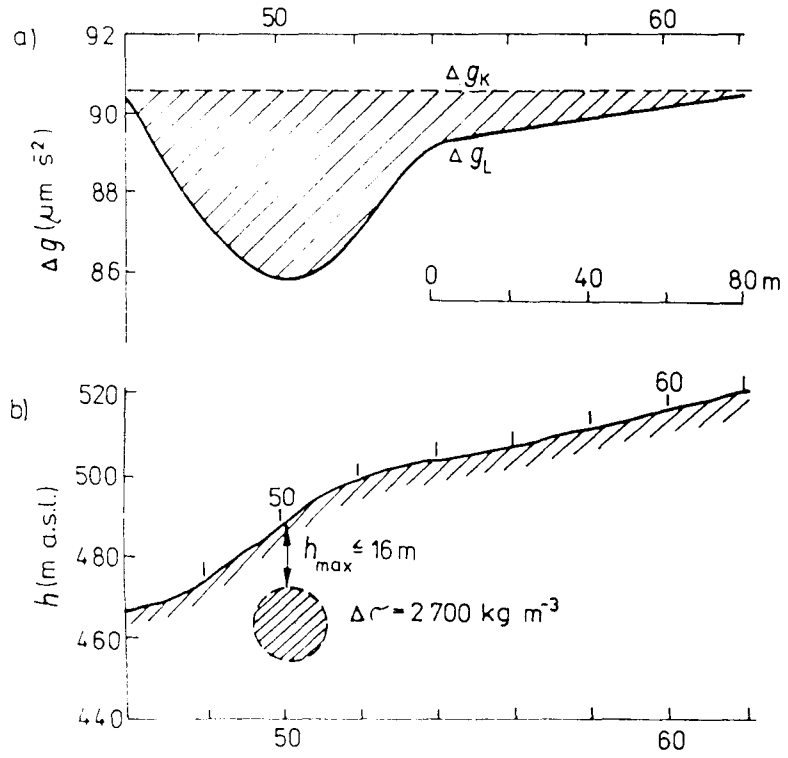

Figure 4.24 Interpretation of a detailed gravity survey above the Kulna cave in the Moravian Karst (Daňko and Blížkovský, 1968). (a) Profile of gravity anomaly. (b) Interpretation.

4.2 Special Hydrogeological Surveys

The methods, techniques and layout of geophysical measurements in practical hydrogeological surveys are aimed at studying two problems; these are determination of the geometrical shape of the hydrogeological structure, and assessment of the hydrogeological characteristics needed in investigations of:

- Thermal, hypothermal, and mineral waters
- Contamination and protection of ground-water resources
- Soil improvement

4.2.1 Thermal, Hypothermal and Mineral Waters

In connection with world-wide energy problems, substantial resources have been expended in searching and prospecting for geothermal resources (vapor, thermal and hypothermal water, high thermal conductivity rocks, and tectonic zones). At the same time, investigation of mineral and low-temperature waters are increasing, because the known resources are not sufficient to meet the ever-growing demands of the balneological institutions.

Location and investigation of hypothermal and mineral water resources involve a specific regimen of observations, general geological studies, geophysical, geochemical, and hydrogeological and boring investigations; geophysical methods play an important part in all stages of exploration, development and protection of these waters.

Appropriate direct geophysical methods are selected based on the physical properties of the waters and the specific character of the area studied. The high temperature of thermal and hypothermal waters, usually with high dissolved solids contents, favors the application of regional and shallow geothermal surveys, remote sensing and logging methods. The high content of dissolved solids, usually an elevated CO_2 content, temperature and radioactivity provide suitable conditions for the use of geoelectrical methods, measurements of CO_2 in soil gas, shallow thermal surveys, and radiometric and logging methods (Table 4.1).

The Čačín area (Husák, in Sborník, 1972) is a typical example of the use of thermo- and gasometric techniques in the investigation of seepage of low-temperature calcium-bicarbonate waters (temperature ϑ = 10 to 15 degrees C) located at the intersection of two perpendicular systems (Fig. 4.25). Similarly, a comprehensive survey in the area of the Karlovy Vary hot spring contributed to the establishment of its geological position (Fig. 4.26).

Figure 4.27 illustrates a successful location of water-bearing tectonic lines using thermometry in an area where no other geophysical methods could be

Table 4.1 Geophysical methods applied to investigation of geothermal and mineral water resources (Marušiak, in Sborník, 1976; Melkanovitski et al., 1978; Škuthan et al., in Sborník, 1976; Ward and Wright, in *Proceedings*, 1989, modified)

Geophysical methods	Note	Purpose and type of measurement
Indirect		
Magnetometric	3A	In the first investigative stage airborne variant used to identify rocks demagnetized by hydrothermal alterations and intrusive bodies associated with tectonic systems
Gravimetric	3A	Used in the first investigative stage to assess essential structures favorable for accumulation or discharge of (hyper)thermal and mineral waters
Geoelectrical	3B	VES, method of telluric currents, magnetotelluric profiling and sounding for assessing fundamental structural elements and appraise water-bearing characteristics of rocks at a regional scale
Seismic	3B	The methods of refracted and reflected waves and deep seismic sounding are suitable for studying global geology of the area, for the survey of deep sectors and where great accuracy is needed (usually performed after gravimetric and magnetometric surveys are made)
Direct		
Gravimetric	3B	Predominantly on a detailed and micro-scale to establish external hydrogeological characteristics of the structure and locate dislocation zones
Magnetometric	3A	On detailed and microscale to assess detailed structural-tectonic setting
Radiometric (enamometry)	2B	Principal method in investigation of radioactive water, for tracing warm-spring lines; radiometric methods with radioactive tracers may be used to assess the direction and velocity of ground-water flow
Atmogeochemical	2A	Determination chiefly of CO_2 concentrations, rarely of halogenes, SO_2, etc., in soil air in order to locate warm- and hot-spring lines (Chapter 7) (gasometry) and concentration of metal element molecules in soil air or atmosphere and in natural or artificial sorbents
Geothermal in boreholes	1A	Principal method for investigating distribution of earth's heat and geothermal zoning based on temperature measurement in boreholes (Čermák in Sborník, 1976)
Geothermal ground measurements	3A	Detection of temperature anomalies caused by disturbance of temperature field by heat sources located at depth, by the rising thermal waters along tectonic lines or by a change in the thermal conductivity of fault zone fillings
Geoelectrical	2A	A large set of geoelectrical methods for assessment of geometrical and some hydrogeological parameters (Sections 3.1, 3.2); their applicability is mostly favorably affected by the high dissolved solids content of mineral and thermal waters
Seismic	3A	Method of refracted and reflected waves to assess geometrical parameters of a structure or aquifer, to locate fault zones and water-bearing tectonic lines; tracing of microseisms and earth's noise (Ward, 1972)
Remote sensing	3B	Multispectral scanning in infrared range to appraise temperature (Malik, in Sborník, 1976; see also Chapter 7); in microwave variation to establish moisture content in connection with location of mineral-spring lines
Logging	3A	A broad complex of logging methods used in conjunction with test holes (or in production stages) to make the geological profile more accurate and obtain detailed data on the dynamics of water in boreholes and on some other hydrogeological parameters (see Sections 3.2 and 4.5)

Explanation:
1 - Geophysical methods applied chiefly to exploration of resources of geothermal energy
2 - To exploration of mineral and low-thermal water
3 - In both types of exploration
A - Frequently used
B - Less used

employed (a densely built up area, electrical utilities, and the low resistivity of the Turonian claystones). Positive temperature anomalies indicate water-bearing tectonic lines adequate for locating wells.

4.2.2 Pollution of Ground Waters and Delineation of Protection Zones

In essence, two principal purposes of an investigation may be distinguished. In the first case, investigations may be directed at the *protection of ground water* or to the prevention of its pollution. The objectives of such investigations are, for example, mapping of protection zones for ground-water resources and recognition of the danger zone around sources of pollution and establishment of appropriate protection measures. The methods employed usually are the same methods used for defining ground-water resources. Combined with classical hydrogeological methods, they make it possible to construct predictive maps of

Figure 4.25 Thermometric and gasometric studies of calcium-bicarbonate water near Čačín (according to Husák, in Sborník, 1972). *1* — temperature at a depth of 2 m, *2* — CO_2 content (%) in soil air, *3* — low-temperature spring of calcium bicarbonate water.

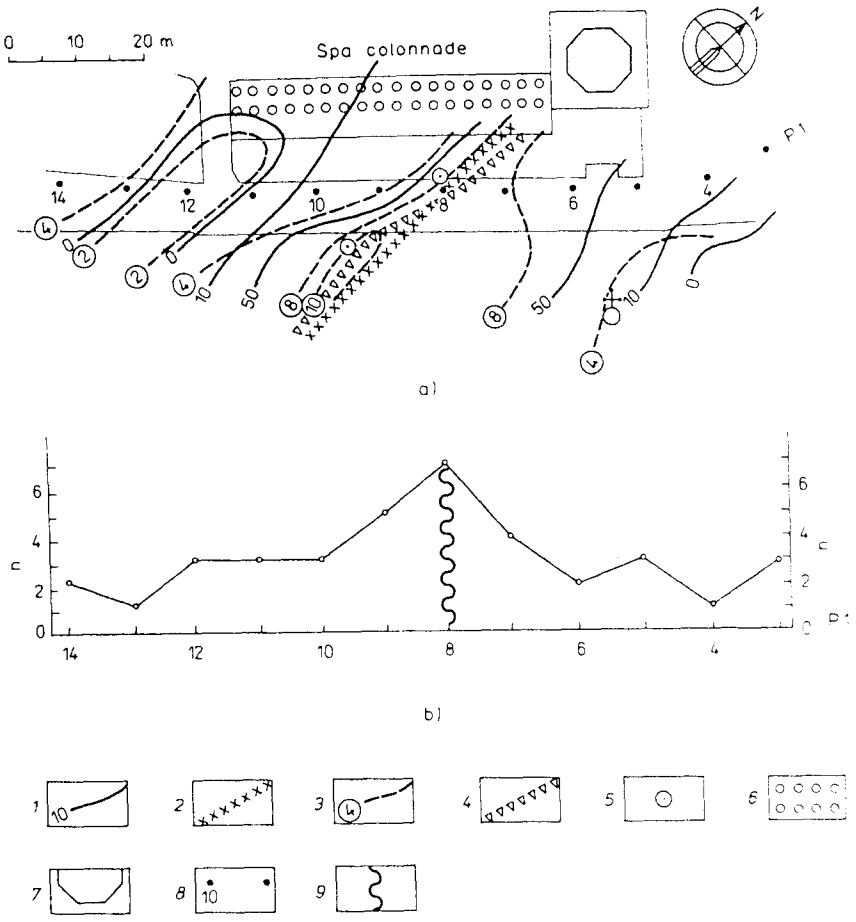

Figure 4.26 Geophysical survey of the structure around the Karlovy Vary hot spring (according to Škuthan and Eremiášová, in Mazáč et al., 1986). (a) Gasometric, emanometric and temperature measurements. (b) Number of indicated anomalous Zn, Mg and Fe concentrations (on November 11 and December 12, 1981) in atmospheric air from the total number (n) of measurements at one point (n = 8). *1* — CO_2 (%) concentration; *2* — axis of anomalies in CO_2 concentration; *3* — isoanomalies of radon content in soil air (in emans); *4* — axis of anomalous radon content; *5* — centers of abnormally elevated temperature up to ϑ = 23 degrees C at a depth of 1 m below the ground surface at a normal background temperature (ϑ = 12 degrees C); *6* — colonnade; *7* — Karlovy Vary hot spring; *8* — points on profile P1, sites of recurrent measurement of Zn, Mg and Fe concentrations in atmospheric air 1 m above the ground surface; *9* — presumed tectonic zone.

pollution (Fig. 4.28) and assess the migration and filtration parameters needed for these calculations.

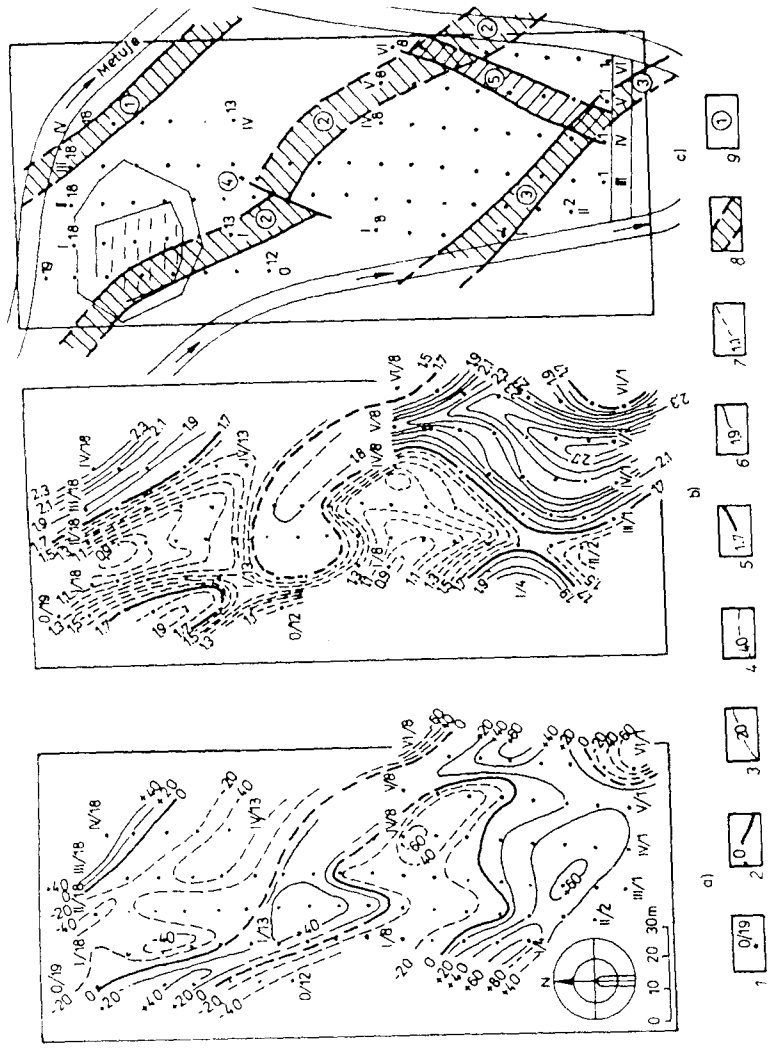

Figure 4.27 Determination of water-bearing tectonic lines using temperature measurement at Teplice nad Metují. (a) Isoanomalies of temperatures $\Delta\vartheta$ at a depth 1 m below the ground surface (°C/10). (b) Isoanomalies of temperature measured at the earth/snow boundary (°C). (c) Location of water-bearing tectonic lines. *1* — measurement point, *2* — isoanomaly $\Delta\vartheta = \vartheta_m - \vartheta_n$ (ϑ_m — temperature observed, ϑ_n — normal temperature); *3* — isoanomaly for $\Delta\vartheta > 0$; *4* — isoanomaly for $\Delta\vartheta < 0$; *5* — isoline of normal temperature $\vartheta_n = 1.7$°C; *6* — isoline for $\vartheta_m > \vartheta_n$; *7* — isoline for $\vartheta_m < \vartheta_n$; *8* — delimitation of zones of positive temperature anomalies (tectonic zones); *9* — number of the anomaly.

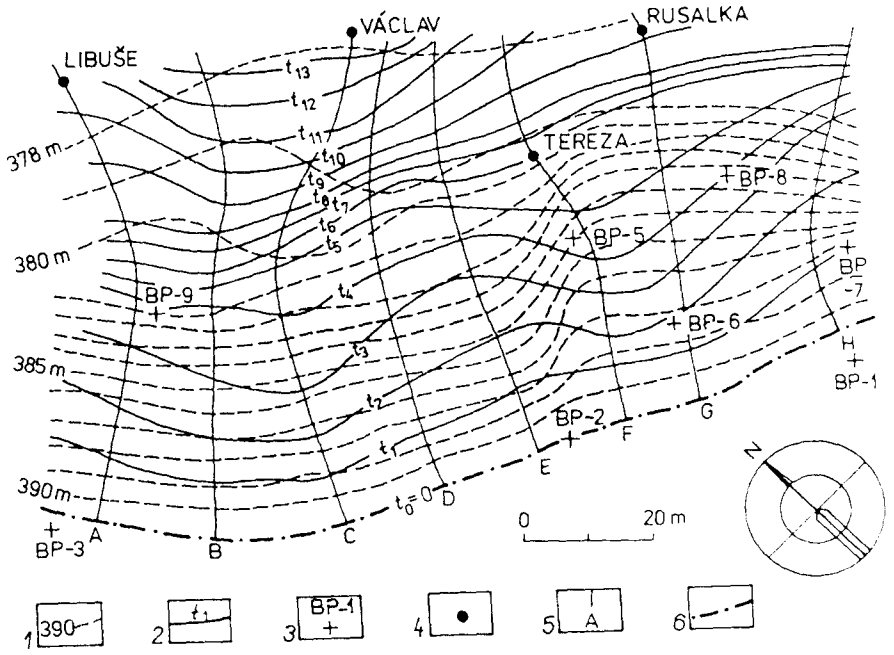

Figure 4.28 Predictive map of pollution in an area of minor thermal springs near Karlovy Vary (according to Škuthan et al., 1978). *1* — water table contours constructed from the results of shallow boring (max. 10 m) and geophysical measurements; *2* — boundary of pollution zone at time t_i, constructed from a set of hydrodynamic tests and geophysical measurements (dipole profiling, thermometry, gasometry, radiometry, spontaneous polarization and the mise-a-la-masse method); *3* — borehole; *4* — spring; *5* — calculated flow line; *6* — line $t_0 = 0$ corresponding to the provisional boundary of the protection zone, which in calculations was considered as a line of constant pollution ($\Delta t = \Delta t_{(i+1)} - t_i = 15$ min.).

Investigations are also conducted to determine the *extent and causes of existing pollution* and to plan remediation. The choice of geophysical methods and their interpretation depend on the physicochemical properties of the pollutant and on the hydrogeological conditions. In addition, the organization of the geophysical investigation is motivated by the following considerations (Švoma, in Mazáč et al., 1987):

- The site of the investigation is controlled by the location of the source and by pollution processes; geophysical measurements are often impeded, and even prevented, by the presence of multiple disturbing factors

such as underground electric utilities, pipelines, and high building densities in locations where measurements are required or most needed.

- Time is very important because the timeliness of remedial activities depends on the time required for the assessment of the pollution. Generally, the use of geophysical methods can be expected to shorten this time relative to the time needed for a traditional investigation with test borings.

The application of one or several geophysical methods depends on the purpose of the investigation. The methods are listed in Table 4.2, but a few words of explanation should be added.

The effectiveness of *resistivity methods* for the assessment of oil or chemical pollution requires that the character of the geoelectrical field before pollution be known and that the conditions under which pollution is detectable be established (Fig. 4.29).

Atmogeochemical methods are employed for assessing petroleum products in soil gas using detection tubes (Doležal et al., in Sborník, 1976) or analyzers which work on the flame ionization principle. Logging methods can be used to determine the proportion of petroleum products in a borehole by measuring the oil-water ratio (using the difference in permittivity of the two liquids); chemical solutions showing an electrolytic character are detectable by resistivity surveys. Three *remote sensing methods* are utilized in various spectral ranges: the UV range for detection of oil films on water surface; the visible infrared and microwave range of the spectrum for the same task and for assessing the health and temperature state of vegetation, which depends on the presence of oil products in soil and ground water.

Pollution of ground water by pathogenic organisms can only be established indirectly by logging methods using fluid resistivity and photometry logs.

Radioactive contamination of ground water is detectable from emanation aureoles of soaked-in radioactive solutions and by measurement of the radioactivity in ground-water samples.

Table 4.2 Application of geophysical methods in investigation of ground-water pollution and in establishing protection zones for water resources (according to Švoma, in Sborník, 1976; Mazáč et al., 1981; Greenhouse et al., in *Proceedings*, 1989, modified)

Purposes	Geophysical Methods										
	Ground Survey										
	Gravimetric	Magnetometric	Radiometric (emanometry)	Geothermal	Atmogeochemical	Geoelectrical resistivity	Electromagnetic	Seismic	Geoacoustic	Logging borehole	Remote airborne sensing
Establishment of zones of ground-water sources protection, construction of prognostic maps of pollution (Fig. 4.28), prevention of pollution	B	B	B	A	A	A	B	A		A	B
Determination of oil or chemical pollution					A					A	B
Determination of pollution by pathogenic organisms										A	
Determination of radioactive contamination			A							A	
Determination of thermal pollution				A						A	
Tracing of underground pipelines and sites of leakage		B			B	A			B		

A - More used
B - Less used

In investigating *thermal pollution* with geothermal methods we must take into consideration that a slight heating of ground water can also be produced by the process of seepage through a porous medium (Fig. 4.30).

Pipeline leaks are most easily detected and located using electromagnetic methods. Acoustic methods, which record the noise caused by an escaping

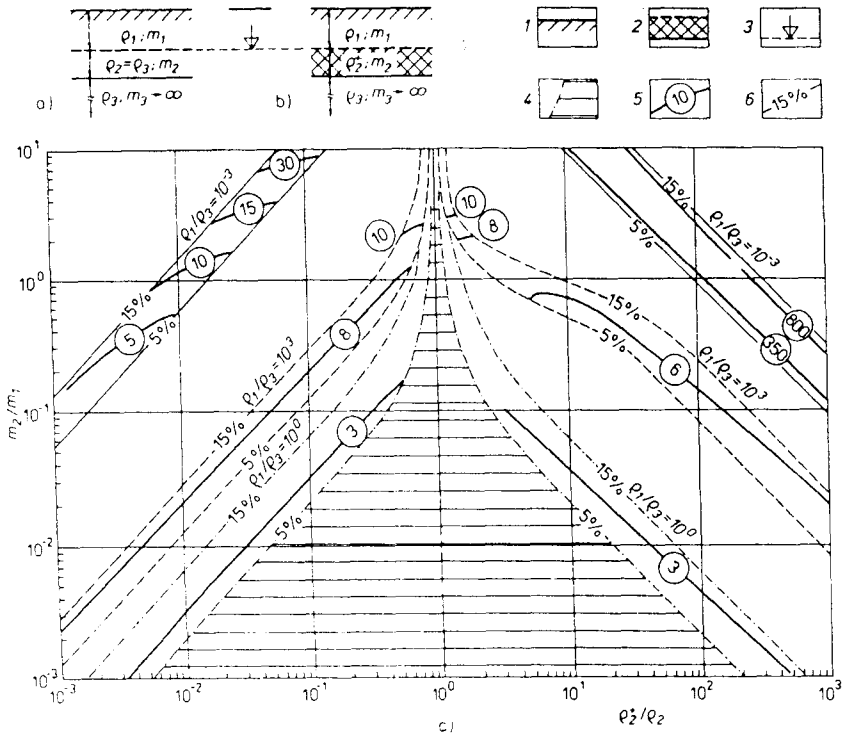

Figure 4.29 Conditions of the detectability of ground-water pollution using resistivity methods: (a) geoelectrical model with unconfined ground water before pollution, (b) same conditions but after pollution: the polluted layer is characterized by resistivity ρ_2^+, (c) graph delimiting the conditions under which the polluted medium is undetectable by resistivity methods. *1* — earth's surface; *2* — contaminated layer; *3* — water table; *4* — area representing combination of factors (ρ_2^+/ρ_2, m_2/m_1) under which the polluted layer (ρ_2^+, m_2) is undetectable; *5* — $AB/2m_1$, where AB is the spacing of current electrodes at which the divergence of the VES curves (before and after pollution) for the given detectability limit (η) was maximum; *6* — detectability limit (η) equal to common mean measuring error (5%) and its three-fold value (15%).

product, are less effective (Eliáš in Sborník, 1976). In special cases the atmogeochemical methods are also useful.

4.2.3 Land-Improvement Surveys

An optimum proposal of land improvement measures requires a detailed knowledge of:

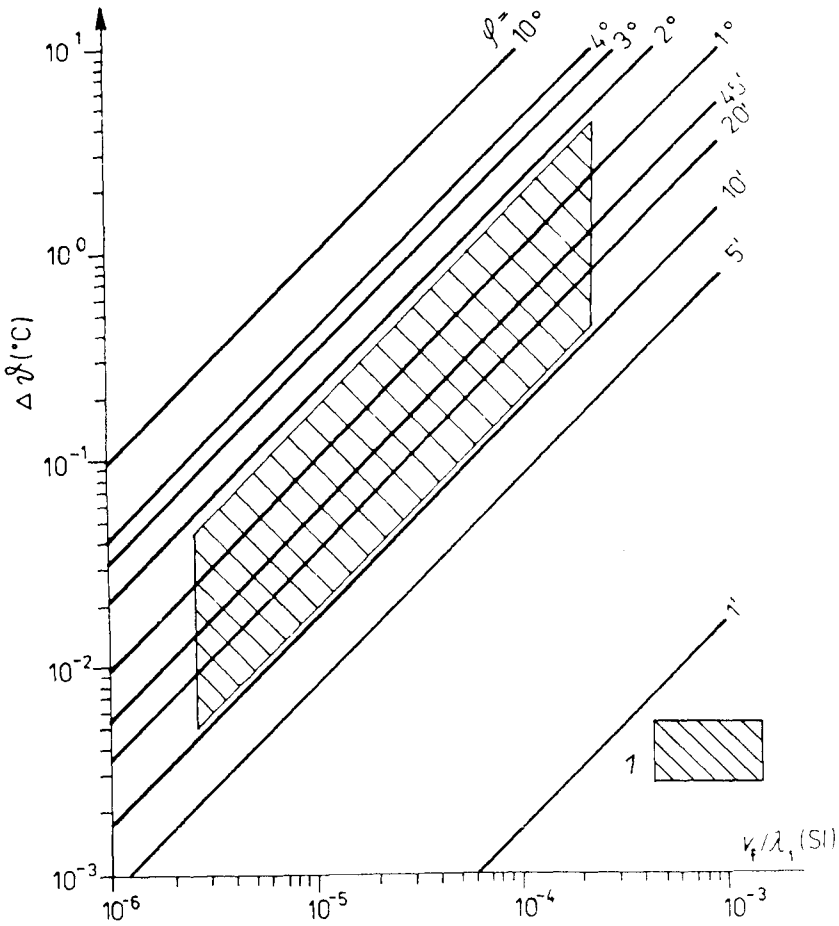

Figure 4.30 Increase in ground-water temperature (degrees C) in relation to the filtration velocity v_f (m s^{-1}) and thermal conductivity λ_1 (Wm^{-1}K^{-1}) with bulk density of the aquifer being σ = 2000 kg m^{-3} and specific heat equal to c_M = 800 J kg^{-1} K^{-1}. φ — slope of water table. *1* — range of validity of the nomogram for Quaternary gravel and sand in the Labe River floodplain.

- Physico-pedological conditions of the soil profile (geological and geomorphological structure, differentiation of lithologicogenetic structures in the area investigated)
- Hydrogeological characteristics of the zone of aeration (moisture content, connected porosity, clay and salt content, etc.), and of the zone

of saturation (effective porosity, hydraulic conductivity and transmissivity, dissolved solids content)
- Relationship between surface, soil and ground water
- Physical state of soils, ecological characteristics of the landscape units and the presence of preferential paths in soil and beneath the soil profile.

The application of geophysical methods (Table 4.3) can substantially increase the cost effectiveness of an investigation. For example, the number of borings and field tests may be reduced in comparison to the requirements of a traditional investigations (over areas of the order of hundreds of square kilometers at least) by 30 to 50% with the required accuracy, information content and reliability of the results still being obtained. Cost benefits for smaller areas (of the order of 0.01 to 0.1 km^2) are not the same, and the effectiveness of geophysical methods and their use must be considered separately for each locality.

The geophysical methods commonly used in this field are in essence identical with the methods applied in hydrogeological surveys. However, it must be considered that the object of investigation is a soil medium at shallow depth with considerable physical and hydrogeological variability.

In Figure 4.31 the use of vertical electrical sounding and seismic methods in a study of the causes of soil waterlogging is shown (see paragraph 5 in Table 4.3). Waterlogging is caused by ground-water discharge along a tectonic line. The water-bearing parts of the crystalline complex are indicated by decreased resistivities, and the tectonic line is manifested in the geoelectrical profile as well as in the lower velocity of compressional waves v_p below the limit of 1000 m s^{-1}.

4.3 Hydrogeology of Mineral Deposits

The hydrogeology of mineral deposits has a specific character due principally to the fact that the development of a mineral deposit means a serious, often very

serious, interference with the natural hydrogeological conditions. The task for the hydrogeologist is to recognize the changes which may result from this interference and to propose measures to prevent the damage which could occur from inflow of ground water into the mining work. In many cases it is necessary to decide between conflicting interests of a mining organization and water-management, agricultural, health and spa institutions.

The tasks of a hydrogeological survey in the different stages of exploration

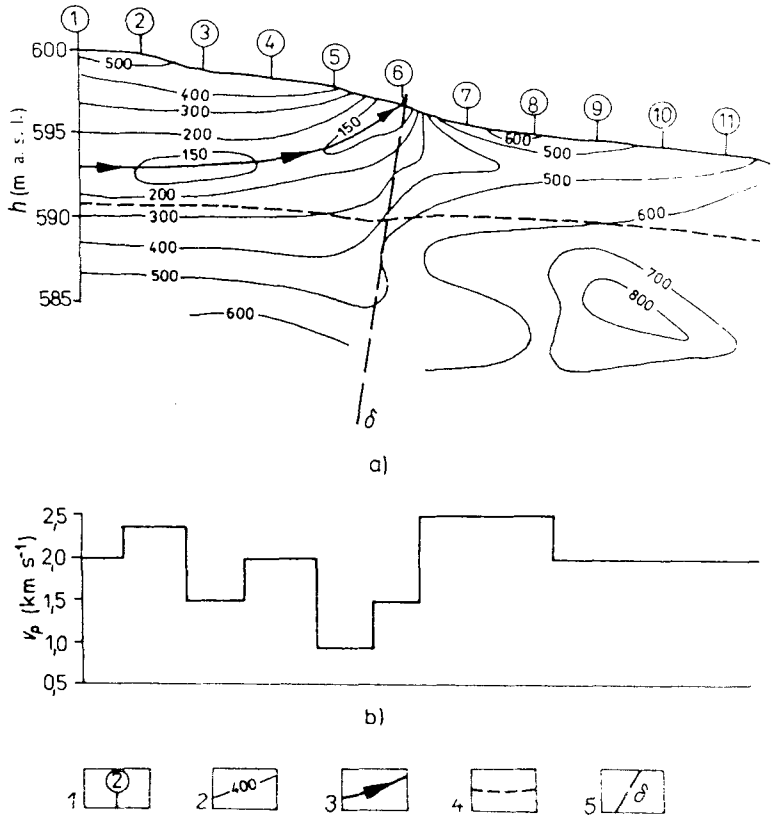

Figure 4.31 Geophysical investigation of the causes of waterlogging at Šediviny in the Orlické hory Mountains. (a) Geoelectrical profile. (b) Velocity of longitudinal seismic waves (v_p) beneath the weathered layer. 1 — location of vertical electrical soundings, 2 — isoline of apparent resistivity (Ω m); 3 — direction of ground-water flow, 4 — seismic interface (weathered layer - sound rock), 5 — vertical resistivity bo dary (tectonic line).

Table 4.3 Application of geophysical methods in soil improvement investigation (Wolgemuth, 1978, modified)

Tasks of investigation	Geophysical methods													
	Gravimetric	Magnetometric	Radiometric, nuclear geophysics	Gasometry	Geothermal	Geoelectrical	Radio-wave profiling	Radar	Seismic	Ultrasonic	Logging	Cone penetrometers and logging	Remote sensing	Systems of stable sensors
1. Assessment of physical-pedological state of soil														
Assessment of physical properties of soil *in situ*			B		B	A	B	B	B	B	B	B	B	B
Determination of physical units of soil environment						A	B	B	A		B		B	
Differentiation of soil layers						B	B	B	B	B	A	B		
Assessment of natural and artificial failures	B	A	B	A	A	A	B	B	B	B				
2. Assessment of hydrogeological parameters of aeration and saturation zones														
Depth of water table	B					B		B	A		A			
Total solids content, coefficients of permeability and transmissivity, porosity of aquifers			B			A			B		A			
Moisture content in soil and zone of aeration			B			A	B	B			A		B	B
Ground-water flow and flow of water in soil			A			A			B		A			
Lithology of aquifers and their shaliness						A	B	B	A	B	A	B		
Salt content in formations of aeration zone						A								
Jointing in bedrock		B		B		A			B		A			
Resources of subsurface water	B	B	B	B	A	A	B	B	B				B	
3. Assessment of relationship between surface, soil and ground waters	B	B	B	B	B	A	B	B	B	B	B		A	
4. Assessment of mechanical state of built-up and cultivated soils			B			B			B	A		A		
5. Appraisal of factors concerning soil-improvement and ecology of regional units														
Presence of water in agricultural lands and causes of waterlogging					B	A	B	B	B		B		A	B
Presence and state of plants on lands													A	
Function of soil improvement					B								B	A
Effects of soil improvement on ecology and development of regional units					B								A	B
6. Search for engineering systems in and beneath soil profile														
Routes of nonmetallic network and dewatering pipes						B	B	B						
Metallic pipes and cable systems		A		B		A	B	B						

Explanation:
A - More used
B - Less used

of a deposit are multiple and demanding, usually depending on the hydrogeological conditions of the deposit. For example, Homola-Klír (1975) distinguished eight types of hydrogeologic conditions encountered in mining solid minerals alone. This suggests why it is so difficult to present a concise overview of the hydrogeological problems that may be resolved using applied geophysical methods. We will therefore emphasize only some principles that should be observed in all cases.

The complex of geophysical methods, which are more or less utilized in prospecting for mineral deposits, should involve those which provide information needed by the hydrogeologist.

Geophysical prospecting should be done in *stages* corresponding to those of a hydrogeological survey (Table 4.4). In the prospecting and preliminary exploration stages, the geophysical methods are the same as those of routine hydrogeological surveys. In the mine development and exploitation stages, the geophysical methods should be selected with regard to the specific tasks to be performed, and after thorough consultation with a hydrogeologist.

A good example of a complex of geophysical methods used in prospecting and preliminary exploration of a mineral deposit is illustrated by the set of logging methods used in investigating bituminous coal deposits in the Slaný area of the Central Bohemian Carboniferous region. The objective of the logging was to establish the occurrence and thickness of the coal seam; for this purpose the density variant of gamma-gamma logging and caliper logging were used. The second task; i.e., to obtain as much information as possible on the hydrogeological structure (mainly number and thickness of water-bearing zones, their porosity, and the total dissolved solids content of ground water) was accomplished by a complex of logging methods including resistivity, SP, gamma-ray, neutron-gamma and fluid-resistivity logging (Fig. 4.32).

Table 4.4 Hydrogeological surveys in economic geology and suitable geophysical methods

Tasks of hydrogeological survey	Suitable geophysical method(s)	For details see section
In the prospecting stage		
To obtain general information on the hydrogeological structure	Gravimetry, magnetometry VES, resistivity profiling, geothermal (vehicle-borne) survey, borehole logging	3.1
In the reconnaissance investigation stage		
Number of water-bearing aquifers and their thickness	VES, refraction seismics	3.1
Permeability (hydraulic conductivity and transmissivity) of aquifers	VES, logging methods	3.2.4
Porosity of aquifers	Logging methods	3.2.2
Depth to water table	Refraction seismics, logging	3.2.5
Physical properties of ground water, total dissolved solids content and chemistry	Logging methods (RL, TL, PHL)	3.2.6
Gas content, agressivity of water	Water sampling at depth	
Effects of ground water on the rocks of the deposit and those around it (slaking, swelling, washing)	Logging methods (CL, AL)	
Approximate appraisal of the possibility of deposit drainage (effect of drainage on hydrogeological structure)	Gravimetry, geoelectrical, geothermal survey	
In the detailed investigation stage		
More precise determination of parameters (denser network of exploration works, changes of parameters studied in time)	Detailed resistivity survey, refraction seismics, logging	3.1 3.2
Location and extent of the area of natural recharge	Geoelectrical methods	3.1
Ground-water reserves (static, dynamic) in the affected part of hydrogeological structure	VES, logging methods	3.2
Quantity of underground outflow	Observation of ground-water dynamics in boreholes, based on logging	4.5

Table 4.4, continued

Tasks of hydrogeological survey	Suitable geophysical method(s)	For details see Section
Expected inflow into mining field at different phases of mine opening and working	Observation of ground-water dynamics in boreholes, based on logging	4.5
Model of drainage and its course in time		
Changes in water regimen caused by drainage	Observation of changes in the ground-water level - refraction seismics and borehole logging	3.2.5
Treatment and removal of water pumped from the deposit		
In the mine opening and working stage		
Registration of sites and amounts of ground-water inflows	Repeated logging of hydrogeological boreholes in and near the deposit	4.5
Changes in the regimen of ground water and characteristics of water bodies in and around the deposit with time	Repeated resistivity measurements (VES, profiling)	
Comparison with predictions and reworking of drainage design if needed		
Influence on the natural conditions and living environment	Remote sensing	

4.4 Special Hydrogeology

This grouping comprises geophysical methods that are employed to detect and trace *leakage and seepage of fluids from reservoirs*, settling ponds, and other storage facilities. The problem can be most satisfactorily demonstrated for dams and reservoirs constructed for hydropower generation, drinking-water supply, irrigation, navigation, flood protection and recreation. Leakage is a frequent but undesirable phenomenon which endangers the function and sometimes even the existence of these structures and may unfavorably impact the natural environment. Therefore they are monitored thoroughly and in cases where the leakage exceeds acceptable limits, appropriate preventative measures are undertaken. In

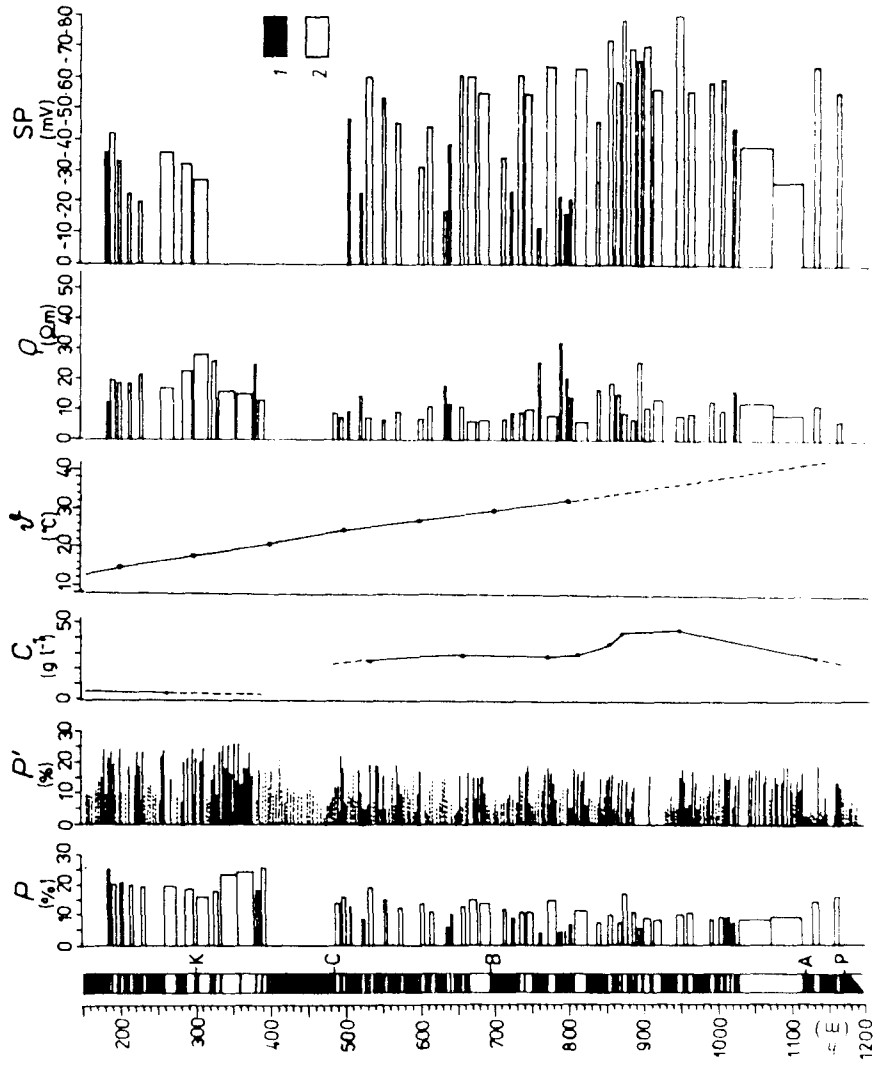

Figure 4.32 Complex evaluation of logs from prospecting boreholes (borehole Bř-2) in the Slaný area of the Central Bohemian Carboniferous. *1* — permeable beds, according to logging; *2* — impermeable beds ($\mu \leq 10^{-4}$ μ m^2); *P* — porosity of permeable beds, according to logging. *P'* — porosity of psammitic (____) and pelitic (. . .) rocks, according to laboratory measurements; *C* — total dissolved solids content of ground water; ϑ — temperature as a function of depth, for a steady thermal regime; ρ — resistivity of permeable beds; SP — anomaly of static or pseudostatic self potentials; P — base of the Carboniferous; A — base of the Nýřany Member; B — base of Týnec Formation; C — base of Malešice Member; K — Kounov coal seam.

addition to the commonly used procedures, geophysical methods can also provide information on the location and extent of leakage.

Geophysical methods used to identify leakage and seepage paths may be utilized inside reservoirs (including the upstream face of a dam and its immediate proximity) and in boreholes (observation, piezometric, grouting) located in and close to a dam (Škuthan, in Sborník, 1972). The methods, type of measurement, and density of the measuring network (regular network, radial or contour profiles) depend on the supposed character of the seepage (through, around or under the dam), see Table 4.5.

For continuous monitoring of seepage, a special system (Fig. 4.33) is used consisting of an electrode system located below the sealing element in a thin bed of sand, the connecting cables and detecting system, and a readout or recording device to which the apparatus is connected. Tests of PVC liners on dams which have been purposely punctured have demonstrated that locations of leakage can be determined reliably by measuring the transition resistance of inlaid stable electrodes (Fig. 4.35) or by measuring the changes in the potential of a line source located under the liner (Fig. 4.34).

The volume of leakage can be assessed from changes in geophysical parameters (apparent resistivity, natural potentials and temperature) only in the case of newly constructed dams; new construction allows the increase in leakage due to reservoir filling to be compared with changes in the geophysical fields.

4.5 Logging of Hydrogeological Wells

The field methods, the extent and number of logging methods, and the evaluation of logs depend to a large extent on the type of aquifer examined (interstitial, fracture, karstic); the type of hydrogeological structure is not determining. Logging methods are discussed in a separate chapter, because, in contrast to surface geophysical methods, the complex of logging procedures and the manner of evaluation is in essence identical, or at least very similar, for shallow

Table 4.5 Geophysical methods used for assessing seepage from reservoirs (after Škuthan, in Sborník, 1972; and Bogoslavski and Ogilvi, 1970, modified)

Parameter explored	Appropriate physical methods, mode of application	The most common disturbing factors
Water level in dam, location of phreatic surface	Refraction seismics and VES in earth dam	Inhomogeneity of velocity and resistivity of dam, low resistivity of dam material, effect of capillary fringe
Discrimination between gravity and capillary water	Refraction seismics, VES, IP (η_a in aeration zone is 1.5 to 3 times higher than in the saturation zone)	Metal elements in the dam body, electrical fields
Location of seepage into dam body or reservoir bottom	SP and thermometry on the reservoir bottom, on the dam, MAM method in the basin near the presumed site of leakage, radiometry using open radioactive tracers in the reservoir	Stray currents, disturbance of thermal field by insertion of measuring probes, conductive elements of larger volume in the dam
Approximate depth of water inlet into the sealing element	Measurement of temperature gradient in reservoir and temperature of outflowing water	Water seepage at several depths, great length of the flow path and small velocity of water flows
Path of seepage	SP method, resistivity profiling and thermometry on the dam, MAM method (charging of outflowing water)	Stray currents, low resistivity of the medium, inhomogeneous resistivities
Locations of seepage	SP method, thermometry, radiometry (after application of open radioactive tracers in the reservoir) on the downstream side of the dam and in its vicinity	Stray currents, inhomogeneity of thermal conductivity in the dam, changes in vegetation and sunlight
Filtration velocity, velocity and direction of flowing water in dam and in the vicinity of the reservoir	Dilution technique, MAM method in observation wells in and beyond the dam	Low resistivity of medium near the charged body and metal casing (MAM method)
Quality of liner sealing	Measurement of potential and potential gradient of geoelectrical field excited by electrode system under the liner	Stray currents

sedimentary structures, delta areas, littoral and coastal areas made up of clastic sediments, sedimentary basins and some neovolcanic regions, where pyroclastics alternating with normal clastic sedimentary types predominate in hydrogeological

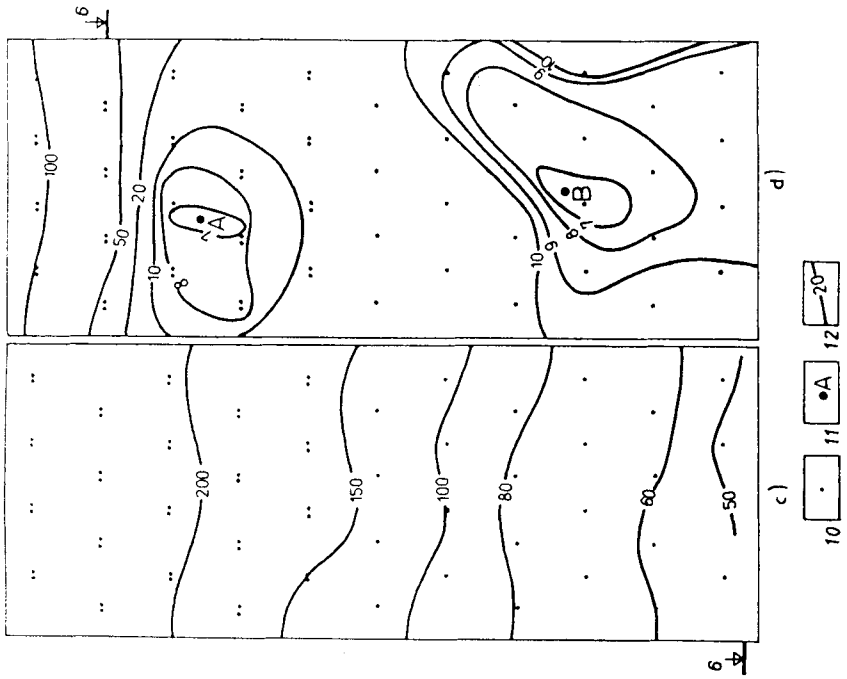

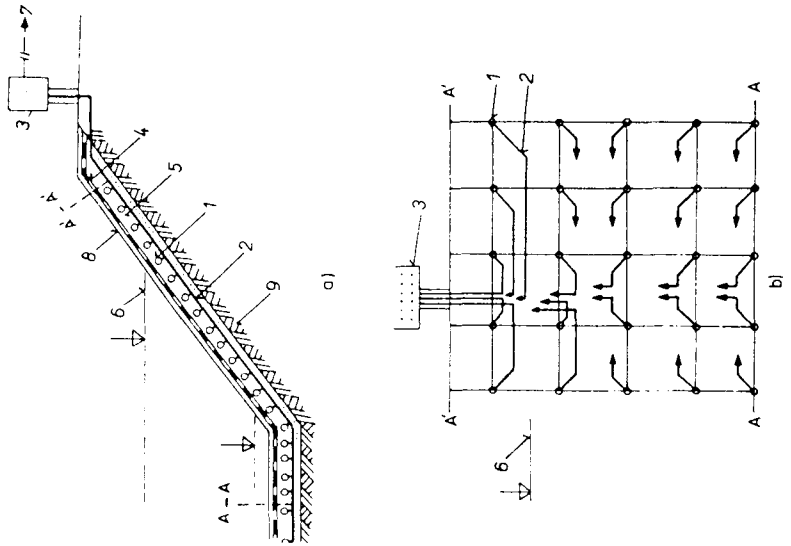

Figure 4.33 Facing page. Location of leakage from the Liptovská Mara dam at the foot of the Vysoké Tatry Mountains, Czechoslovakia (according to Mazáč et al., 1990). (a) Vertical section of the stable electrode system placed on the upstream face of the dam. (b) Schematic view of the electrode network from above. (c) Normal field of contact resistances. (d) Map showing contact resistances after artificially puncturing the liner and filling the reservoir. *1* — electrodes, *2* — connecting cables, *3* — measuring center, *4* — sealing foil, *5* — sand, *6* — water level in the reservoir before and after filling, *7* — evaluating device, *8* — infiltration layer, *9* — gravel, *10* — control electrode system plotted in the map, *11* — sites of artificial perforation of insulating foil, *12* — isolines of contact resistances (10^2 Ω); abnormally low contact resistances indicate sites of leakage.

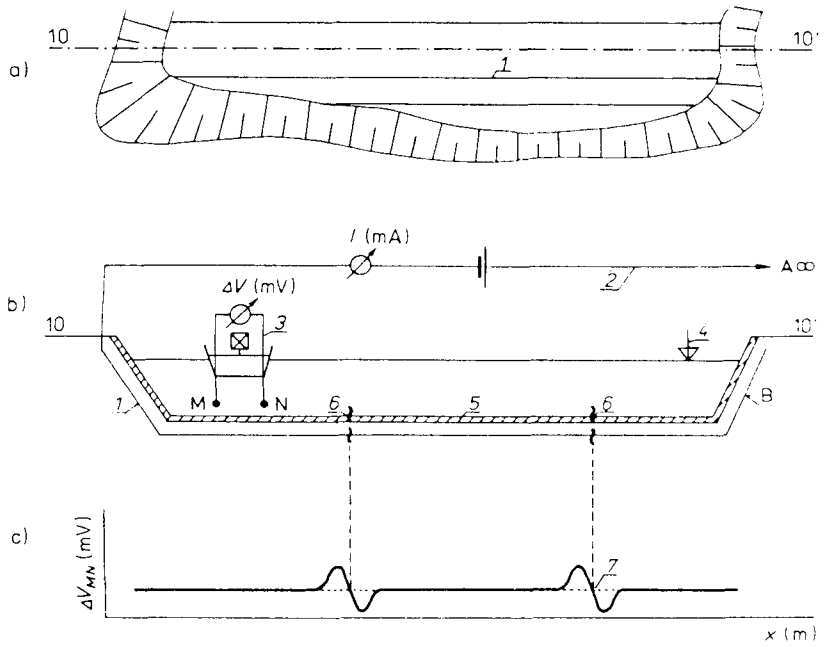

Figure 4.34 Location of seepage areas in a fly-ash settling pond 30 km north of Prague, Czechoslovakia. (a) Schematic plan of the settling pond. (b) Vertical section of the settling pond along profile 10 - 10′. (c) Potential gradient ΔV_{MN} along profile 10 - 10′. *1* — system of line electrodes grounded in the bottom of the settling pond under the liner (electrode B); *2* — current circuit A, B; *3* — movable carrier for potential electrodes M and N, with measuring equipment and the locating target (movement of carrier by mechanical means or wireless control); *4* — water level in the reservoir; *5* — intact liner; *6* — punctured liner; *7* — indication of perforated liner on the curve ΔV_{MN}.

structures. In all these cases, hydrogeological structures with interstitial aquifers or aquifers with combined interstitial and fracture permeability are the concern.

On the other hand, aquifers with fracture or karstic permeability require a substantially different set of logging methods and methods of data processing.

The number of methods and the extent to which logging methods are used is largely dependent on the amount of information required. Table 4.6 lists the logging possibilities using commonly available equipment. Information in groups (a) to (c) are obtained from logs of individual boreholes; information in group (d) is obtained, in most cases, only after borings are made; i.e., on the basis of an integrated interpretation of logging results for the entire hydrogeological region under study. Recognizing that the hydrogeologist will not require all available information in all cases and that logging equipment is not everywhere the same, it is recommended that a logging program be established by a mutual agreement between the responsible hydrogeologist and a geophysicist after a thorough study of the hydrogeology.

The organization of field investigations has also to be adapted to the type of drilling fluid employed. Where water is used for drilling, logging is not impeded and the entire logging program can be completed at the same time. However, it is recommended that measurements only be made after a well is developed and performance pumping tests have been made as the results are then more representative. Where drilling mud is used, logging must be done in two phases; logging in the mud-filled hole provides information on groups (a) and (c). These measurements usually make it possible to determine the depths of aquifers and the hydrogeologist can immediately propose a design for well completion; specifically, the intervals to be screened. The additional logging measurements needed to obtain the information in group (b) are done after the well has been cased and developed so that drilling mud is removed, and after a pumping test has been carried out.

The assessment of *lithology, shaliness, porosity, jointing,* and the *delineation of permeable layers* (information from group (a), Table 4.6) has been discussed in detail in Section 3.2. An example of the automated processing of results from a suite of borehole logging methods (Bohemian Cretaceous Basin, contact of

Cenomanian sandstones with overlying lower Turonian marlstones) is presented in Fig. 4.35. The procedures used to obtain the other data listed in Table 4.6 (groups (b) to (d)) are dealt with later in the text.

4.5.1 Dynamics of Water in a Borehole

Movement of water in a borehole may occur either across the borehole (Sec. 3.2.7) or along the borehole axis. Movement along the borehole axis occurs wherever the borehole or well taps a confined water body with a positive piezometric level or where two or more water bodies with different piezometric levels are penetrated. This flow is caused by disturbing the natural conditions, which allows equalization of piezometric pressures between the water bodies. Vertical flow in a borehole can also be induced by pumping or injecting water into the borehole.

Vertical movement of water in a borehole can be characterized both quantitatively and qualitatively. Qualitative data include information on the locations of inflow or losses and on the intervals of vertical water flow, while quantitative data involves vertical velocities v (m s^{-1}) and vertical flow rates Q' (m^3 s^{-1}).

Locations of *inflow, water loss, and intervals of vertical flow* are usually very conspicuous on high resolution temperature logging TL records, and appear even more distinctly on gradient or *differential temperature logs* TL_d (Fig. 4.37). This is because the temperature of water, which is near the rock temperature at the site of inflow, is generally given by the value of the local geothermal gradient. The depth intervals in which there is natural flow along the borehole axis is then shown on the temperature log by a constant or almost constant temperature, even at low vertical flow rates of the order of 10^{-4} m^3 s^{-1}. Where the individual inflows differ in dissolved solids contents, and thus also in resistivity, the locations of inflow are also indicated on fluid resistivity logs RL; they also often are evident on photometric logs PHL if the borehole was not completely purged of the drilling fluid.

Table 4.6 Logging methods according to the information desired

Group Parameters measured	Optimum set of logging methods Interstitial aquifers	 Fractured aquifers	For details see section
a. Lithology, reservoir properties of aquifers			
Basic lithological type	Ra, SP, GR, GGL-D, NNL	GR, GGL-D, NNL, MSL, GR	3.2.1
Delineation of permeable beds	Ra_{mn}, Ra_{ml}, LES, SP	SP, CL, GR, after application of ORT	3.2.4
Shaliness	Ra, SP, GR, GGL-D, NNL		3.2.1
Porosity	NNL, GGL-D, Ra, SP, GR	NNL, GGL-D, AL	3.2.2
Total dissolved solids in ground water	RL, SP, Ra_{LL}, Ra_{ML}, water sampling at selected depth	RL, water sampling at selected depth	3.2.6
b. Flow dynamics, hydraulic and filtration parameters of aquifers			
Sites of water inflow into and water losses from boreholes, intervals with vertical flow	TL, RL, PHL, GR after treatment of water with appropriate tracer	See interstitial aquifers	4.5.1
Vertical velocity, vertical flow rate, water yield, infiltration	Well flowmeters, RL, PHL, GR after water treatment	See interstitial aquifers	4.5.1
Hydraulic conductivity, transmissivity	Same, at constant injection or pumping rate		3.2.4
Coefficient of protective capacity	High-resolution temperature logging		3.2.4
Water level in borehole	RL, TL, PHL, resistivity measurements	See interstitial aquifers	3.2.5
Piezometric water level	RL, PHL, TL at recurrent water injection or pumping at various water levels in borehole	See interstitial aquifers	3.2.4
Filtration velocity	Dilution method (RL, PHL, GR)		3.2.7
Direction (azimuth) of ground-water flow	GR after application of ORT, special (photographic, photometric) direction meters	See interstitial aquifers	3.2.7
Physical properties of borehole fluids (density, resistivity, temp., transparency)	Densitometers, RL, TL, PHL	See interstitial aquifers	

Table 4.6, continued

Group Parameters measured	Optimum set of logging methods Interstitial aquifers	 Fractured aquifers	For details see section
c. Technical characteristics and condition of borehole			
True borehole diameter	CL		4.5.2
Trend of borehole in space	IM		
Bottom of casing	Ra_I		
Perforated casing	Ra_I (PVC casing), cement-bond log (steel casing)		4.5.2
Casing collars	Location of casing collars (steel casings), resistivity log and sensitive CL (PVC and wood casings)		
Lost casing, tools	Ra, MSL		
Deflection of the bit from the original hole	IM, CL, in borehole with overflow also high-resolution TL		
Top of cement behind casing	TL until 24 hrs, after cementation, GGL-D, GR after application of ORT		
Quality of cementation	Cement-bond log		
Tightness of casing	TL, RL, PHL, GR after treatment of water with appropriate tracer		
Effect of casing on the yield of aquifers	Repeated yield assessment of water inflows before and after the borehole has been cased		4.5.1
Communication between two adjacent boreholes	Tracer tests using RL, CL, GR		
d. Spatial changes in hydrogeological structure			
Correlation of beds, location of faults	Ra, GR, dipmeter survey		4.5.3
Facies changes, maps of sand and clay content	SP, GR, Ra		
Spatial changes in total dissolved solids	Maps of ρ_w (input data from RL, SP, Ra)		
Characteristics of temperature field	Maps of temperature for a given elevation, map of temperature gradients		
Spatial changes in hydraulic parameters of the aquifer	Maps of hydraulic conductivity and transmissivity after logging data		
Spatial changes in filtration velocity	Maps of filtration velocity		

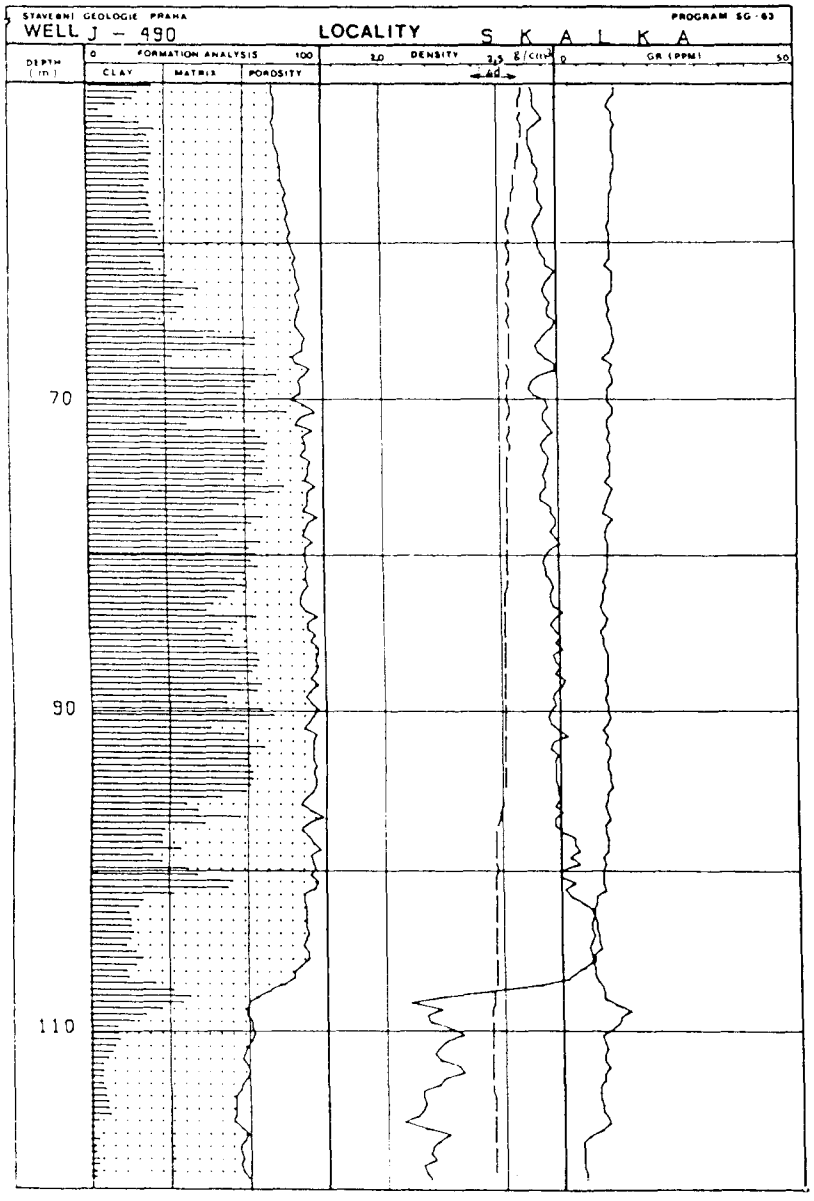

Figure 4.35 Results of computer processed logs from a borehole in the Bohemian Cretaceous Basin (according to Křesťan and Mareš, 1977). The following logging methods were used: GR, GGL-D, NNL, Ra and CL.

Indications of water inflow and loss may be enhanced by using NaCl to lower water resistivity in the borehole. Sites of inflow are then revealed on RL records by an abrupt change in fluid resistivity since the fresh ground water has a resistivity much higher than the salt-treated water; i.e., within a range ρ_w = 30 to 100 Ω m (Figs. 3.21 and 4.37).

The *vertical velocity* is determined using a propeller flowmeter (where $v > 10^{-2}$ m s^{-1}), or for low velocities of flow ($v < 10^{-2}$ m s^{-1}) using a thermal-pulse flowmeter (Hess and Paillet, 1990) and a time series of fluid resistivity, photometric and temperature logs, after the water in the borehole is first treated with respect to the parameter to be measured. Vertical velocity is then determined from the vertical shift of characteristic points on two subsequent records (minimum on PHL log after a colored mark has been made, mean temperature on TL logs, fluid resistivity $\bar{\rho}_m$ corresponding to the mean salt concentration in the treated and untreated water - Fig. 4.36).

The *vertical volumetric flow* rate Q' (m^3 s^{-1}) is the initial parameter for determination of the yield Q_i of individual inflows and for assessing the hydraulic parameters of individual aquifer layers as well (Section 3.2.4). It may be calculated indirectly from the vertical velocity v (m s^{-1}) and the borehole radius r ($Q' = \pi r^2 v$).

The vertical volumetric flow rate can also be established from high resolution temperature measurements if a water body with a positive piezometric level has been tapped by the well and from fluid resistivity logging under stabilized pumping of water from the well (Mareš, 1976), or by combining several approaches (Fig. 4.37).

4.5.2 Control of Technical Conditions and Casing of Boreholes

In an uncased borehole, only two parameters are observed: the diameter (existence of voids) and drift (azimuth and inclination) of the borehole.

Borehole casing may be of various materials (steel, PVC, etc.), and may be either solid or perforated. T' logging methods allow assessment of the casing

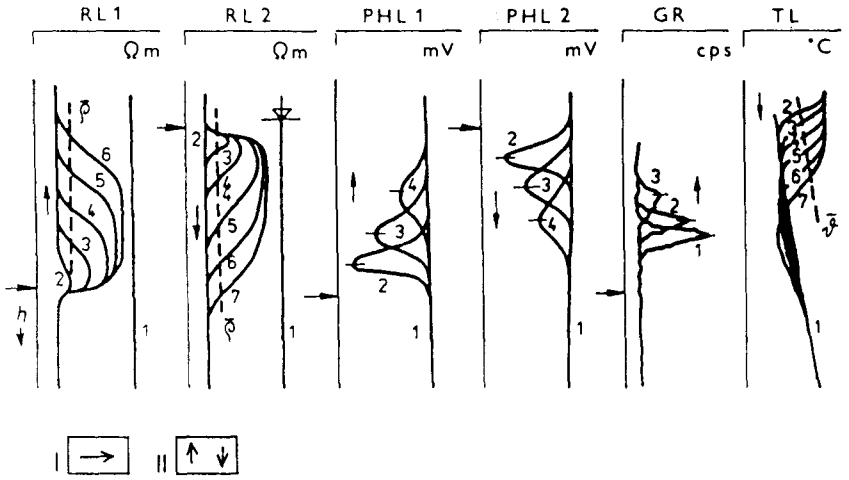

Figure 4.36 Character of a chronological series of RL logs after treatment of a well with NaCl. PHL logs after introduction of nigrosin using a deep electromagnetic pump. GR logs after tracing with an open radioactive tracer and TM logs on injecting warmer water into the borehole. All series can be used for computing vertical velocity (v). The chronological sequence of logs is denoted by ordinal numbers. I — water inflow; II — direction of water flow in the borehole. $\bar{\rho}$ — line of fluid resistivity corresponding to average equivalent NaCl concentration in water before and after water treatment. $\bar{\vartheta}$ — line of mean water temperatures in borehole and of water injected.

Figure 4.37 **Facing page.** Determination of vertical volumetric flow rate (Q') and yield (Q_i) of water inflows from the middle Turonian aquifer (well Žsj-P4 Dolní Bukovina, Cretaceous at Bohemia after Zbořil and Mareš, 1972) by high resolution temperature measurements and photometry, after treating the water with nigrosin at depths of 132, 146, 150, 160 and 166 m. GR — gamma ray log; Ra_n 0.3, Ra_n 0.6 — resistivity logs measured with normal probes of spacings AM = 0.3 and 0.6 m; CL — caliper log; RL — fluid resistivity log under natural conditions; TL 1 — temperature log measured with standard thermometer (record 15 — with thermometer run in the well, 16 — run out of the well); TL 2 — high resolution temperature measurement with thermometer run in the well; TL 3 — high resolution temperature measurement with thermometer run out of the well. TL_d 1 and TL_d 2 — differential temperature measurement with thermistor spacing L = 1.5 m; 1 — with thermometer run in the well, 2 — run out of the well); PHL 1 — photometry, with the tool running in the well; PHL 2 — photometry, with the tool running out of the well (record 1) under natural conditions, (records 2 to 7) after treating the water with nigrosin, using a deep electromagnetic pump); Q_i — yields of separate inflows, Q'_i — graph of vertical volumetric flow rate; a — Lithological profile according to logging results. I — sandstone, II — silty sandstone, III — siltstone, IV — casing, V — water inflows.

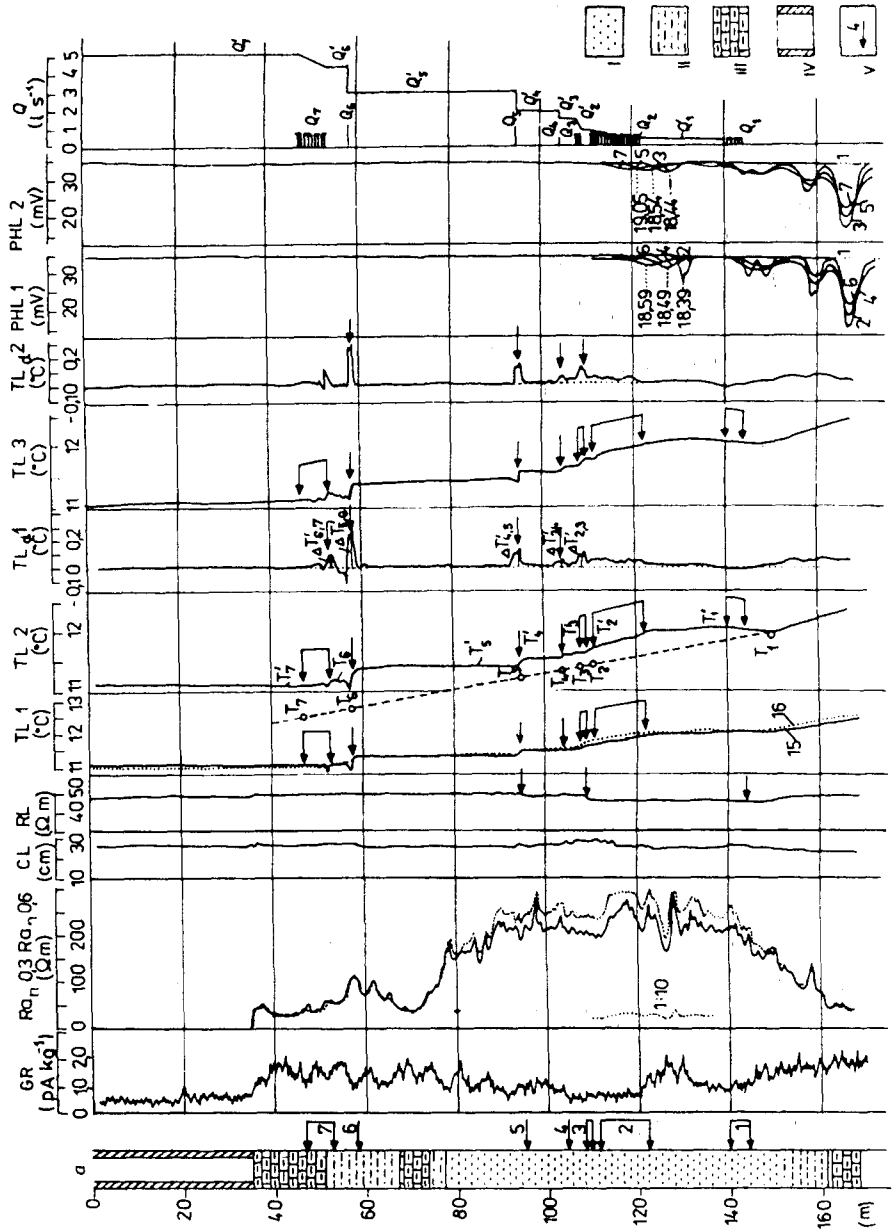

material (chiefly distinguish steel from PVC and wood), the condition of joints, the location of screened intervals (Fig. 4.38), the location of the top of the grout behind the casing, the condition of the grout, and to assist in many specialized problems (broken drill collar or casing, deviation from the original opening, the negative effects of well completion on the yield of the well, etc. (Table 4.6 (c)).

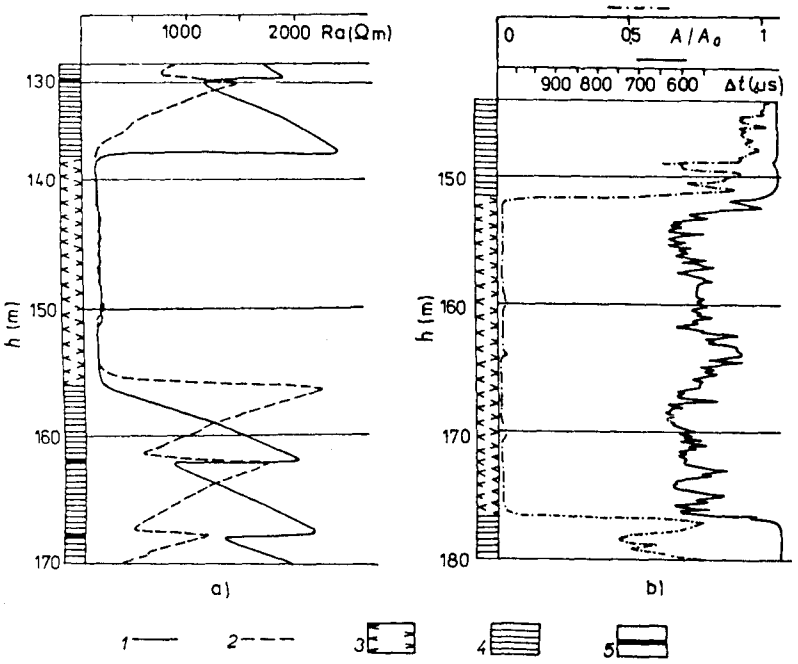

Figure 4.38 Character of logs in screened sections of casings (according to Havelka and Těžký, 1979). (a) Ra 0.55 logs measured by combined lateral probes in PVC casing. (b) Cement-bond log in steel casing. A/A_0 — relative amplitude, Δt — interval transit time. *1* and *2* — the curves measured, *3* — screened interval, *4* — massive casing, *5* — leaky weld of PVC casing.

Figure 4.39 **Facing page.** Application of logging methods as seen in studies of spatial changes in a hydrogeological structure. (a) Correlation of borehole profiles in the Cretaceous Litomyšl basin according to apparent resistivity curves measured by a normal probe. *A* to *P* — correlation horizons, *E* — base of middle Turonian, *E* to *H* — lower Turonian sandstone, *P* — base of the Cretaceous; *1* — sandstone, *2* — crystalline complex, *3* — water inflows into borehole; (b) Spatial variations of resistivity (Ω m), based on trend surface analysis (4th degree polynomial) in the middle Turonian complex, in the Bohemian Cretaceous Basin, also indicate facies changes. In areas with $\rho_t > 100$ Ω m, the Middle Turonian is formed of sandstones (a source of water supply), with $\rho_t < 40$ Ω m, of siltstones. *4* — location of well, resistivity value indicated.

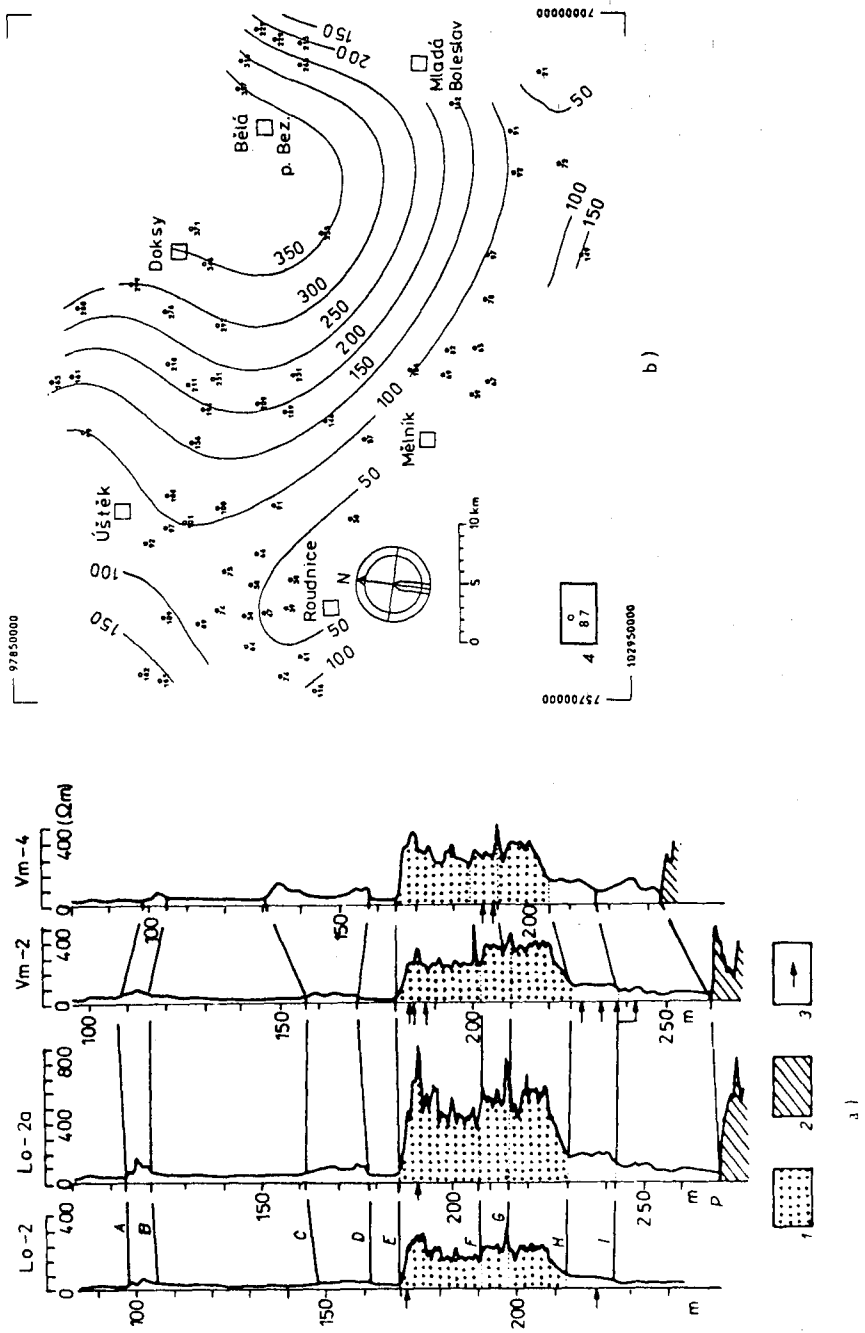

4.5.3 Integrated Evaluation of Logging Results in a Hydrogeological Structure

We have so far only considered the logging of individual boreholes. Where a hydrogeological structure is investigated with a large number of boreholes, it is appropriate to prepare an integrated evaluation of all logging data obtained over the entire area. This technique often provides a fresh view of many relationships and sometimes even worthwhile new information about the hydrogeological structure, particularly when there is collaboration between a hydrogeologist and a geophysicist.

Integrated data processing should always involve construction of *correlation sections or correlation charts* along a profile, using the most clearly differentiated logging curves (Fig. 4.39). The profiles selected should correspond with geological profiles; the evaluation of correlation sections may assist in refining the geology of the area and in locating faults, facies changes, and other hydrogeological features. It is also possible to construct maps of some geophysical parameters (e.g., ρ_t, Q_{eU}, V_{sh}) of an aquifer or an entire complex, the thickness of aquifers, resistivities and temperature of ground water, hydraulic conductivities and filtration velocities. Regrettably, integrated evaluation of logging data is not yet firmly established; however, it is an absolute prerequisite if the information that logging can provide is to be completely utilized.

Chapter 5

Geophysical Surveys for Engineering-Geological Purposes

Geophysical methods are used to study the physical fields and parameters which allow us to define the physical and stress-strain state of a rock massif, some properties and parameters of rock materials and their changes in time.

5.1 Physical State of Rock and its Evaluation Using Geophysical Methods

The physical state of a rock massif is controlled by a set of physical parameters and other properties which characterize the physical conditions at the time of study. The physical state of a rock massif depends on its mineralogy and petrology and stage of petrogenesis, the structural tectonic system, climatic, geomorphological and hydrogeological conditions, biological factors and human activity. As a result of changes in natural and anthropogenic factors, the physical state changes constantly so that the *physical state* may be regarded *as a dynamic system*. It should be recognized, however, that since a geophysical survey is carried out within a certain limited time period, the physical state of a rock massif is evaluated as a static system; i.e., the state at a certain time. The evaluation of the physical state of a massif as a dynamic system is possible with *repeated measurements* at different times, preferably at accurately known fixed points.

In evaluating the physical state of a rock it is of particular importance to choose an appropriate scale for the survey relative to the size of the body. The physical state of a massif, as a whole differing in genesis and petrography from